UNIVERSIDADE DA CORUÑA

Programa regulado por el RD 1393/2007: Programa oficial de doctorado interuniversitario en Física Aplicada

Tesis doctoral

Nanocompuestos conductores basados en nanotubos de carbono y poliamidas: Estudio de sus propiedades eléctricas, reológicas y su morfología

Autora: Laura Arboleda Clemente

Marzo 2017

Directoras:

Dra. María José Abad López, Dra. Ana Isabel Ares Pernas

Departamento de Física

Página intencionadamente en blanco

UNIVERSIDADE DA CORUÑA

LABORATORIO DE PLÁSTICOS

Centro de Investigaciones Tecnológicas

Campus de Esteiro, s/n Ferrol

Las doctoras **María José Abad López y Ana Isabel Ares Pernas**, ambas Profesoras Titulares del Departamento de Física de la Universidad de A Coruña, **AUTORIZAN** a Laura Arboleda Clemente a presentar la memoria titulada "**Nanocompuestos conductores basados en nanotubos de carbono y poliamidas: Estudio de sus propiedades eléctricas, reológicas y su morfología"**, realizada bajo su dirección en el Laboratorio de Plásticos del Centro de Investigaciones Tecnológicas para optar al grado de Doctora por la Universidad de A Coruña.

Y para que así conste a los efectos oportunos firman la presente en Ferrol, a 8 de Marzo de 2017.

Fdo: Dra. Mª José Abad López Fdo: Dra. Ana Isabel Ares Pernas

Página intencionadamente en blanco

Agradecimientos

Este trabajo no hubiera sido posible sin la ayuda de todos aquellos que han estado a mi lado, de un modo u otro, durante este tiempo. Por ello, en esta memoria no puede faltar mi más sincero agradecimiento a todos ellos:

En primer lugar, a mis directoras de tesis, la Dra. Mª José Abad López y la Dra. Ana Isabel Ares Pernas, por la confianza depositada en mí y por su constante apoyo y asesoramiento para la realización de este trabajo.

Al Departamento de Física de la Universidad de A Coruña y a sus directores durante estos años; Mª Carmen Ramírez y Joaquín López por su trabajo y dedicación. Al Grupo de Polímeros y en especial a su director Luis Barral Losada por su apoyo y su acogida en el grupo y al director del Centro de Investigaciones Tecnológicas José Manuel Vilariño por el apoyo recibido durante todo mi trabajo de tesis realizado en el centro.

A la Dra. Ana Isabel Ares Pernas, que además de mi directora de tesis, es una gran amiga que siempre ha estado ahí en los buenos momentos y en los no tan buenos. Muchas gracias, Ana, por todo.

Al Dr. Senentxu Lanceros-Méndez, de la Universidade do Minho, por permitirme realizar una estancia en Guimaraes que me ha aportado el conocimiento de técnicas complementarias para el estudio de las propiedades eléctricas. Le agradezco mucho el tiempo dedicado en mi aprendizaje tanto a él como a los componentes de su grupo de investigación, en especial, a Víctor, Caterina, Paulo, Cristina, Renato, Pedro y, sobre todo, a Armando, por su inmensa paciencia conmigo y su buen humor tan necesario durante el trabajo diario en el laboratorio.

A los compañeros del departamento de Física por los momentos compartidos en todos estos años. Quiero incluir un cariñoso recuerdo a Natalia que me enseñó a utilizar casi todos los equipos del laboratorio y me transmitió los valiosos trucos aprendidos con la experiencia, a Xoán por los momentos inolvidables a lo largo de la cantidad de horas que

hemos compartido peleándonos con la extrusora y la granceadora, a Sonia por ser una enorme científica y una magnífica compañera de trabajo dispuesta siempre tanto a compartir sus conocimientos como a aportar valiosos razonamientos para intentar entender el complejo mundo de los polímeros y, finalmente, a Paula por su valiosa ayuda con los últimos ensayos necesarios para culminar esta tesis.

Una mención aparte se merecen mis dos grandes compañeras y amigas: Belén y Rosa. Mi agradecimiento a vosotras dos sería casi tan largo como esta tesis y además sabéis perfectamente lo que me cuesta resumir, pero haré un esfuerzo. Con vosotras aprendí qué eran los polímeros al llegar al laboratorio de Serantes, aprendí a utilizar los equipos y a pelearme con ellos pero, lo más importante de todo ha sido conoceros, compartir los momentos buenos y malos del día a día que algunas veces nos han hecho soltar alguna lagrimilla, pero en la inmensa mayoría de las ocasiones habéis conseguido hacerme ver el lado positivo de las cosas y que al final hayamos podido reírnos con amplias carcajadas, como a mí me gusta, de casi todo.

Para casi finalizar quiero expresar mi más profundo y sincero agradecimiento a mi padre y a mi hermano, cuyo esfuerzo y sacrificio han hecho posible que yo haya llegado hasta aquí. A mis sobrinos, Hugo y Míkel, que aunque ellos probablemente no lo sepan me han dado la alegría necesaria para continuar con esta tesis. A mi familia de Huelva, por recibirme siempre cada verano con esa alegría y sentido del humor que a mí me aportan el mejor descanso posible en vacaciones. A mi mejor amiga Marta, juntas e inseparables desde los cuatro años de edad, sigue siendo la persona que mejor me conoce, que sólo con mirarme sabe lo que me preocupa y que, a pesar de la distancia, siempre está cuando la necesito. A mi novio, Diego, que ha estado siempre a mi lado en los buenos, pero, sobre todo, en los más necesarios e ingratos malos momentos, aguantando en esas ocasiones mi mal humor y mi pesimismo. Sin lugar a dudas, sin su apoyo y su cariño no habría podido acabar esta tesis.

En este momento de alegría quiero tener un recuerdo muy especial para aquellas personas que me han apoyado y querido mucho en mi vida y que, aunque ya no están físicamente conmigo, siguen vivos porque su

recuerdo siempre va en mi corazón. A mis abuelos y mi tía abuela que siempre me animaron a estudiar y creyeron en mi capacidad. A mi primito Jorge, un ángel que el cielo nos prestó muy pocos años, por ser el niño más especial que he conocido nunca.

Finalmente, quiero dedicar esta tesis a la persona más importante y que más he querido en mi vida, a mi madre. Desde pequeña siempre creyó en mí, en mi valía y en mi capacidad de esfuerzo y sin sus enseñanzas de vida no habría llegado nunca a ser la persona que hoy soy. Sé que desde el cielo me estará viendo el día de la lectura de esta tesis con una gran sonrisa de madre orgullosa. Gracias, mamá.

Página intencionadamente en blanco

A mi madre

Página intencionadamente en blanco

Índice

Página intencionadamente en blanco

Resumen

El trabajo de esta tesis tiene como objetivo el diseño y posterior caracterización de nuevos materiales compuestos poliméricos conductores utilizando mezclas de diferentes poliamidas como matriz y nanotubos de carbono de pared múltiple como nanorelleno conductor. Se han utilizado dos mezclas distintas de poliamidas (PA), una de ellas parcialmente miscible y la otra inmiscible para estudiar la influencia de esta variable en las propiedades eléctricas de los compuestos obtenidos.

Durante el desarrollo de la tesis se hizo especial hincapié en evaluar las relaciones entre procesado, morfología y propiedades macroscópicas de los diferentes nanocomposites, buscando siempre maximizar las propiedades obtenidas con la menor cantidad de nanotubos de carbono. Dado que el estado de dispersión de los nanotubos influye directamente en las propiedades de la red conductora formada y, por tanto, en las propiedades macroscópicas finales, se estudió cualitativa y cuantitativamente, este aspecto en función del tipo de poliamida, proporción y grado de miscibilidad entre las poliamidas utilizadas como matriz y tipo de predispersión usada para preparar los compuestos poliméricos conductores. Utilizando una mezcla inmiscible de poliamidas, se obtuvo una morfología con una red conductora segregada que permite optimizar las propiedades eléctricas de los nanocompuestos.

Página intencionadamente en blanco

Resumo

O traballo de tese tivo como obxetivo o deseño e caracterización de novos materiais compostos poliméricos condutores empregando mixturas de diferentes poliamidas como matriz e nanotubos de carbono de parede múltiple como nanorecheo condutor. Empregáronse duas mixturas distintas de poliamidas (PA), unha delas parcialmente miscible e a outra inmiscible, para estudar a influenza desta variable nas propiedades eléctricas dos compostos obtidos.

Durante o desenvolvemento da tese fíxose especial enfase en avaliar as relacións entre procesado, morfoloxía e propiedades macroscópicas dos diferentes nanocompostos, buscando sempre maximizar as propiedades obtidas coa menor cantidade de nanotubos de carbono. Dado que o estado de dispersión dos nanotubos inflúe directamente nas propiedades da rede condutora formada, e por tanto, nas propiedades macroscópicas finais, estudouse cualitativa e cuantitativamente, este aspecto en función do tipo de poliamida, proporción e grao de miscibilidade entre as poliamidas usadas como matriz, e tipo de predispersión usada para preparar os compostos poliméricos condutores. Coa mixtura inmiscible de poliamidas, optimizáronse as propiedades eléctricas do nanocomposto debido á formación dunha rede condutora segregada.

Página intencionadamente en blanco

Abstract

The main target of this Doctoral thesis was the design and characterization of new conductive polymer composites using blends of different polyamides, as matrix, and multiple wall carbon nanotubes, as conducting nanofillers. In order to analyse the influence of polyamide miscibility on the electrical properties of nanocomposites, two different blends were selected: a partially miscible polyamide blend and an immiscible polyamide blend.

During the development of this work, particular emphasis has been placed on assessing the relationships between processing, morphology and macroscopic properties of the different nanocomposites. The ultimate purpose was to maximize the properties achieved with the minimum amount of carbon nanotubes. As the dispersion state of carbon nanotubes directly influences the properties of the conductive network and, therefore, the final macroscopic properties, this aspect was studied from a qualitative and quantitative point of view. The effects of the type of polyamide, polyamide ratio, degree of miscibility between polyamides selected as matrix and type of predispersion, used to prepare the conductive polymer composites, were evaluated. Using an immiscible polyamide blend, a segregated conductive network was obtained. This structure allowed the optimization of the nanocomposites electrical properties.

Página intencionadamente en blanco

Capítulo 1

Introducción

Página intencionadamente en blanco

1.1 Materiales nanocompuestos con matriz polimérica

Muchas de las aplicaciones industriales actuales exigen materiales con baja densidad y buenas propiedades macroscópicas, fundamentalmente mecánicas (elevada rigidez y resistencia). Esta combinación de propiedades es difícil de obtener con materiales convencionales como los metales, los polímeros o los materiales cerámicos. Sin embargo, el desarrollo de los materiales compuestos ha permitido superar muchas de las limitaciones observadas en los materiales tradicionales.

Un material compuesto puede definirse como aquél en el que dos o más materiales, de distinta naturaleza química, se combinan en una estructura multifásica separados por una interfase fácil de distinguir, para dar lugar a un nuevo material, con propiedades macroscópicas distintas a los materiales de partida [1].

En lo que respecta a los compuestos con matriz polimérica, la selección del tipo de relleno a utilizar dependerá de las características físico-químicas que se necesiten para el material compuesto. Comercialmente, los rellenos pueden clasificarse en función del tamaño de sus partículas (micro-refuerzos o nano-refuerzos) y de su morfología tal y como aparece en la tabla 1 [2].

Inicialmente el desarrollo de los compuestos de matriz polimérica se basó en el empleo de rellenos con un tamaño micrométrico, dando lugar a micro-compuestos de matriz polimérica. Éstos presentaban aumentos significativos en el módulo, resistencia a la tracción y mayor resistencia a la fractura que las matrices poliméricas [3, 4].

Sin embargo, el uso de este tipo de rellenos presenta dificultades a la hora de optimizar otras características del compuesto final. El incremento deseado en las propiedades, se obtiene con contenidos de relleno entre el 10% y el 70% en peso, lo que aumenta la densidad del material, dificulta su procesabilidad, disminuye su resistencia mecánica y elasticidad (sobre todo si la matriz y las partículas de refuerzo no son compatibles) y a veces, eleva mucho el coste del material final [5]. En muchas ocasiones, si las interacciones en la interfase matriz-relleno son débiles, el aumento de la resistencia mecánica y otras propiedades macroscópicas del compuesto es modesto [6].

Morfología	Ejemplos	Usos
Tridimensional	Partículas metálicas (sílica, aluminio)	Mejora de la conductividad térmica y/o eléctrica, refuerzo mecánico
	Partículas minerales inorgánicas (carbonato cálcico, dolomita, etc…)	Como pigmento en filmes
	Esferas de vidrio o cerámicas, negro de carbono, etc	Refuerzo mecánico, aumento de la resistencia térmica
Bidimensional (en forma de lámina)	Arcillas	Mejora del aislamiento térmica, la resistencia al fuego y refuerzo mecánico
	Mica	Refuerzo mecánico; mejora las propiedades dieléctricas, térmicas y mecánicas. Bajo coste
	Talco	Refuerzo mecánico, aumento de la rigidez y resistencia a la tracción
	Grafeno	Refuerzo mecánico, mejora de la conductividad eléctrica
Unidimensional (en forma de fibra)	Whiskers alúmina, fibras naturales, etc…	Refuerzo mecánico, mejora de la conductividad térmica
	Fibras de carbono / grafito / Nanotubos de carbono	Refuerzo mecánico: alto módulo y gran resistencia mecánica. Baja densidad. Mejora de la conductividad eléctrica.
	Fibras de vidrio	Refuerzo mecánico, mejora la resistencia mecánica, térmica y química. Aumento de la estabilidad dimensional

Tabla 1 Clasificación de los rellenos en función de su morfología

La utilización de nanorellenos en el desarrollo de materiales compuestos (nanocompuestos) puede, en algunos casos, mejorar las prestaciones de los microcompuestos con un contenido de relleno mucho menor.

Los nanocompuestos son materiales formados por dos o más fases, donde al menos una de ellas tiene una de sus tres dimensiones en la escala nanométrica [7]. Debido al tamaño nanométrico, las interacciones entre la matriz y el nanorefuerzo aumentan en la interfase y, por ello, los nanocompuestos pueden presentar mejores propiedades macroscópicas con cantidades de carga mucho menores [8, 9]. Estas propiedades dependen tanto de la naturaleza de sus componentes iniciales, como de la morfología obtenida y de las características de la interfase [10]. A su vez, la morfología de los nanocompuestos depende del método de mezclado utilizado, que también influye en gran medida, en el grado de dispersión del nanorelleno en la matriz.

Así pues, los mayores retos en el diseño de nuevos nanocompuestos de matriz polimérica, son definir adecuadamente las relaciones entre morfología-procesado-propiedades, para optimizar las propiedades finales del material, [11] y el desarrollo de técnicas innovadoras que faciliten la incorporación, dispersión y distribución de estos nanorefuerzos en la matriz polimérica.

Respecto a los tipos de nanorefuerzo, las nanoarcillas, en las últimas dos décadas, los nanotubos de carbono y las nanopartículas metálicas son los más comúnmente empleados para fabricar una gran variedad de nanocomposites de altas prestaciones [12-18].

Las nanoarcillas, como la montmorillonita (MMT), poseen excelente resistencia mecánica, son baratas y pueden ser pretratadas y dispersadas en disolventes comunes e incluso en medio acuoso [12, 13].

Las nanopartículas metálicas muestran excepcionales propiedades como refuerzo mecánico y además pueden añadir conductividad eléctrica y térmica a los polímeros aislantes [18-20]. Sin embargo, estas nanopartículas no son fácilmente dispersables en matrices poliméricas debido a su hidrofobicidad [21-23].

Otro nanorelleno frecuente usado son las nanopartículas de óxidos metálicos, las cuales dan lugar a compuestos con una buena procesabilidad y alta resistencia mecánica, si se comparan con los correspondientes de las nanopartículas metálicas, pero su integración en matrices poliméricas es bastante compleja [24-26].

El negro de carbono es el nanomaterial más comúnmente usado en la industria como refuerzo mecánico y para la mejora de las propiedades térmicas y eléctricas de los materiales poliméricos [27, 28]. Tiene la ventaja de que se puede funcionalizar fácilmente, es abundante y barato. Entre sus principales inconvenientes se encuentra su pequeña relación de aspecto (cociente entre su longitud (L) y su diámetro (D)), lo que ocasiona que las propiedades mecánicas y eléctricas en el compuesto final no sean comparables con las obtenidas con otras nanocargas.

En la actualidad, los nanotubos y nanofibras de carbono son considerados como los nanorellenos más prometedores debido, principalmente, a su baja densidad y a su extremadamente alta relación de aspecto. Sus extraordinarias propiedades mecánicas, térmicas y eléctricas permiten desarrollar nanocompuestos de matriz polimérica que cumplen distintas exigencias de conductividad eléctrica para disipación electrostática (ESD) y apantallamiento electromagnético (EMI) [14-16, 29-31].

Entre los principales escollos que hay que superar para optimizar las propiedades de estos nanocompuestos, se encuentran una excesiva agregación de los nanotubos en las matrices, alto coste y escasa interacción interfacial con los polímeros [32-36].

Finalmente, el grafeno ha emergido como una nueva clase de nanorelleno interesante para nanocompuestos avanzados. El grafeno y sus derivados (como los óxidos de grafeno) muestran un gran potencial para mejorar las propiedades mecánicas, eléctricas, térmicas y químicas de materiales poliméricos relevantes para aplicaciones con gran demanda en la actualidad [37-44] como el almacenamiento de energía (baterías más duraderas, celdas más eficaces) [37, 38] o aplicaciones electrónicas (pantallas flexibles, biosensores, etc) [39, 42].

1.1.1 Nanocompuestos de nanotubos de carbono y matriz polimérica

Esta tesis está enfocada al desarrollo de nuevos nanocompuestos de matriz polimérica, usando nanotubos de carbono como nanorelleno.

Los nanotubos de carbono (CNT) son alótropos de carbono que se asemejan a un cable cuántico unidimensional (1D). Tienen una estructura tubular hecha de capas de átomos de carbono

(láminas grafénicas), enrolladas entre sí [45], con un radio de unos pocos nanómetros, de 3 a 30 nm, y una longitud del orden de los micrómetros [46-48], aunque pueden llegar hasta los 20 cm de longitud. Las paredes de los nanotubos de carbono se componen de una red hexagonal, análoga a la de los planos atómicos del grafito, cuya punta, en sus extremos puede ser abierta o cerrada por una tapa semi-hemisférica con forma de fullereno [49].

La síntesis y estudio de los nanotubos de carbono comenzó a partir de los años 50 [50-52]. En esta década, Radushkevich y Lukyanovich publicaron imágenes de tubos de carbono con un diámetro de 50 nm [50]Posteriormente, en 1976, Oberlin, Endo y Koyama sintetizaron fibras de carbono huecas con diámetros menores de 10 nm, mediante la descomposición de hidrocarburos en presencia de partículas catalizadoras metálicas [52, 53]. En 1979, John Abrahamson describió los nanotubos de carbono como fibras de carbono producidas mediante descarga de arco [54].

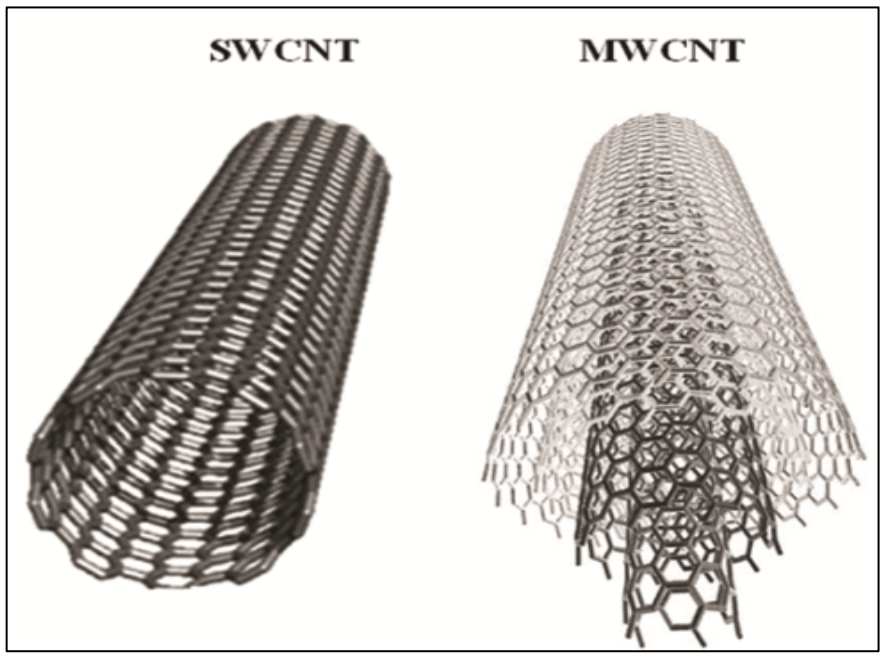

Figura 1 Esquema de los dos grupos de nanotubos de carbono

Sin embargo, no fue hasta 1991, cuando Ijima describió la estructura de los nanotubos como una disposición concéntrica de hojas de grafeno, su disposición helicoidal y quiralidad. A partir de

entonces, el número de estudios sobre este tipo de nanopartículas creció exponencialmente [45].

Los nanotubos de carbono se pueden dividir en dos grandes grupos cuyo esquema puede verse en la Figura 1:

- Nanotubos de carbono de una sola pared (SWCNT single walled carbon nanotubes por sus siglas en inglés): Un SWCNT es una única hoja de grafeno enrollada en sí misma, con un diámetro típico de alrededor de 1.4 nm [45, 55-57].
- Nanotubos de carbono de pared múltiple (MWCNT multi-walled carbon nanotubes por sus siglas en inglés): Se componen de varios (dos o más) tubos concéntricos de capas grafíticas con una separación de 0.34 nm entre capas; pueden alcanzar diámetros de hasta 100 nm [45, 58, 59]. El ejemplo más simple son los nanotubos de carbono de doble pared (DWCNT) compuestos por sólo dos cilindros concéntricos [60].

En la literatura se han propuesto dos tipos de estructuras para las capas de los MWCNT que se pueden ver en la Figura 2: i) estructura en espiral ”Swiss-roll”, en donde los nanotubos están compuestos de rollos de hojas de grafeno en espiral [49, 59]; ii) estructura "Russian doll", la estructura más habitual, compuesta por cilindros huecos concéntricos de carbono.

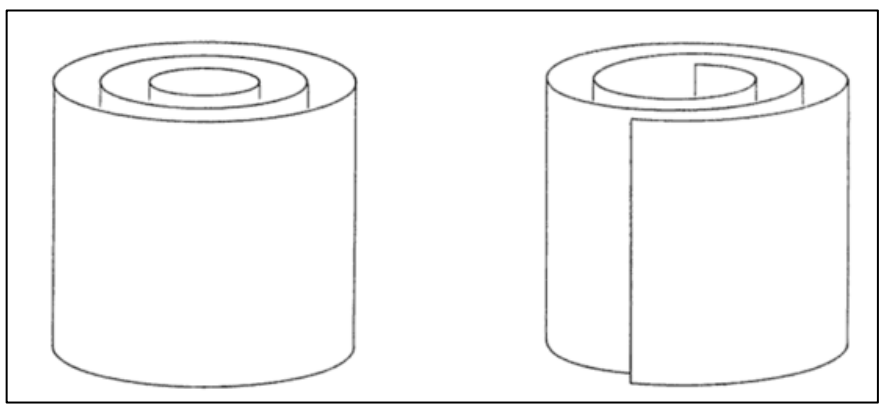

Figura 2 Esquema de las configuraciones “Russian doll” y “Swiss roll” [49]

Los nanotubos de carbono cuentan con propiedades únicas como: alta conductividad eléctrica, del mismo orden que el cobre y

la plata [32], alta relación de aspecto y elevada conductividad térmica [61]. En cuanto a sus propiedades mecánicas, los nanotubos de carbono son muy rígidos y tenaces, propiedades muy deseables para su uso como nanorefuerzos en materiales compuestos [62].

Los compuestos CNT/polímeros combinan altas prestaciones con una buena procesabilidad, ya que pueden ser preparados utilizando las técnicas convencionales en el moldeo de materiales poliméricos. Esto, junto con la reducción de los costes en la síntesis de los CNTs obtenida en los últimos años, representa una gran ventaja de cara a implementar estos materiales en nuevas aplicaciones industriales [63].

Sin embargo, la obtención de buenas propiedades mecánicas, un buen balance con otras propiedades deseadas en el compuesto y una óptima calidad superficial depende en buena medida del grado de dispersión alcanzado por los CNTs dentro de la matriz (debido a su alta tendencia a aglomerarse), así, la selección del método más adecuado para incorporar el relleno conductor en la matriz polimérica es crucial. Se debe evitar la presencia de los aglomerados iniciales o primarios (normalmente con un tamaño > 1 μm) para conseguir el máximo refuerzo mecánico.

No obstante, la completa dispersión de los CNT en un polímero puede ser contraproducente para obtener altos valores de conductividad eléctrica. Está demostrado que cierto grado de aglomeración en los nanotubos, es necesario para la formación de la red conductora, a pesar de que los aglomerados iniciales, que permanecen sin dispersar, reducen la cantidad disponible de CNTs individuales para formar caminos conductores [64].

Así pues, el grado de dispersión de los CNT en la matriz polimérica o, lo que es lo mismo, la morfología del nanocompuesto, va a determinar el balance entre las propiedades eléctricas y mecánicas de los materiales obtenidos. Claramente el método de preparación de los nanocompuestos, va a influenciar en gran medida la morfología obtenida y, por ende, las propiedades macroscópicas del material. Se pueden citar tres métodos de preparación de los nanocompuestos de CNT y matriz polimérica como los más habitualmente utilizados: mezclado en disolución, polimerización in situ y mezclado en fundido.

El mezclado en disolución [65-67] consta de tres pasos. Primero se dispersan los CNTs en un disolvente adecuado, mediante agitación mecánica, magnética o ultrasonidos. A continuación, se mezclan los CNTs dispersos con la matriz

polimérica, mezclado que puede realizarse a temperatura ambiente o a temperaturas elevadas según el caso concreto. El nanocompuesto final se obtiene mediante precipitación o vertiendo la mezcla en un molde, y dejando evaporar el disolvente, obteniendo composites en forma de film (film-casting). El problema de esta técnica es que los CNTs son insolubles en disolventes orgánicos comunes lo que dificulta su dispersión [68-70]. Por otra parte, la duración del proceso de formación del film-casting (en ocasiones más de 24 horas), favorece la reagregación de los nanotubos [35].

La polimerización in situ logra dispersar los CNT uniformemente en matrices termoestables. Con este método, se mezclan los CNTs con los monómeros, en presencia o en ausencia de disolvente y, a continuación, los monómeros polimerizan en presencia de un endurecedor o agente de curado [63]. Una de las principales ventajas, es que se pueden forman enlaces covalentes entre los CNTs, previamente funcionalizados, y la matriz polimérica, lo que permite mejorar las propiedades mecánicas del compuesto. Este método es utilizado mayoritariamente para fabricar nanocomposites conductores con resinas epoxi [71-74].

El mezclado en fundido es el método más habitual para fabricar nanocompuestos de nanotubos de carbono con polímeros termoplásticos [35, 70, 75-78]. El relleno se dispersa directamente en la matriz y no se requieren disolventes. El método es fácilmente escalable a nivel industrial utilizando las técnicas habituales de moldeo de termoplásticos, como la extrusión o la inyección, capaces de generar altos esfuerzos de cizalla a altas temperaturas. Sin embargo, se obtiene menor grado de dispersión de los CNTs en la matriz. La eficacia del método, así como las propiedades finales del nanocompuesto, dependen de los parámetros experimentales utilizados durante el procesado [65], del tiempo de mezclado [79], del tiempo de residencia, del diseño del husillo [80], de la velocidad de husillos [81, 82], etc.

Las interacciones entre el relleno y la matriz polimérica son otro factor importante a tener en cuenta, ya que influyen en la dispersión de los nanotubos durante el proceso de mezclado en fundido. Los CNTs forman aglomerados grandes en matrices apolares como el polipropileno (PP) [83-85]. Sin embargo, se dispersan más fácilmente en una matriz polar como la poliamida 6 (PA6), debido a la fuerte interacción entre las cadenas de PA6 y los CNTs [86]. Para mejorar las interacciones entre relleno y matriz apolar, se pueden utilizar compatibilizantes o surfactantes que se

añaden durante el procesado en fundido del compuesto [85, 87-89].

Otra forma eficaz para mejorar la dispersión de los nanotubos en la matriz, es la utilización de masterbatchs de CNTs [90]. Es un procesado en dos pasos donde primero se prepara la masterbatch, con un alto contenido de nanotubos (típicamente entre el 10-20% en peso), utilizando altas cizallas para favorecer la dispersión. Posteriormente, se funde la masterbatch y se mezcla con el polímero virgen para su dilución hasta la concentración deseada [91]. Para realizar este proceso se suelen escoger matrices poliméricas de baja viscosidad y, de este modo, conseguir una mejor infiltración de las cadenas moleculares en los aglomerados primarios formados por los nanotubos. La mejor dispersión y distribución se encuentra cuando se usa para la dilución el mismo polímero que está presente en la masterbatch o, al menos, uno que tenga un comportamiento reológico similar [92]. En la mayoría de los casos, después de un procesado en dos etapas, se obtiene una mejor dispersión de la carga en la matriz, si se compara con una incorporación directa (o en una sola etapa), lo que se puede atribuir tanto al efecto de las altas fuerzas de cizalla como del mayor tiempo de mezclado. Además, presenta ventajas de cara al procesado industrial y desde el punto de vista de la seguridad durante la manipulación de los nanotubos. Por la contra, puede causar una disminución en la longitud del nanotubo, que puede afectar negativamente tanto a las propiedades eléctricas del compuesto, como al refuerzo en propiedades mecánicas que se busca [64, 85].

1.1.1.1 Nanocompuestos de CNT y Poliamidas

Las poliamidas (PA) son polímeros termoplásticos semicristalinos particularmente interesantes debido a su versatilidad y facilidad de procesado [82]. Constan de macromoléculas que contienen unidades amida (N-H-C=O). Una de las más conocidas, la poliamida 66 (PA66) fue sintetizada por primera vez por DuPont en 1935, mediante la reacción de un ácido adípico con hexametilendiamina. Al contrario que la PA66, la poliamida 6 (PA6) y la poliamida 12 (PA12) se sintetizan a partir de un solo tipo de monómero. La poliamida 6 (PA6) procede de la policondensación de la caprolactama mientras que la poliamida 12 (PA12) es el resultado de la polimerización de la laurolactama

Las poliamidas se encuentran entre las familias de polímeros con más aplicaciones en la industria. Sus propiedades varían desde la dura y tenaz PA66, hasta la blanda y flexible PA12.

Además de la síntesis que es diferente en cada uno de los casos, la diferencia que existe entre la PA6 y la PA66 es estructural. La diferencia más importante está indicada en la propia nomenclatura de las poliamidas, ya que el número que aparece en el nombre indica el número de carbonos que aparecen entre los grupos amida, tal y como puede verse en la Figura 3 donde los puntos rojos son átomos de oxígeno, los azules de nitrógeno y los amarillos hidrógeno. La dirección de los enlaces amida es diferente en el caso de la PA6 y PA66, mientras que en el caso de la PA12, la menor concentración de grupos amida en su cadena (mayor número de átomos de carbono), la hace más flexible. Debido a su naturaleza higroscópica, las PA absorben humedad, lo cual puede afectar negativamente a sus propiedades macroscópicas y su proceso de moldeo [93, 94].

Figura 3 a) Poliamida 66 (PA66); b) Poliamida 12 (PA12); c) Poliamida 6 (PA6)

La combinación de poliamidas y nanotubos de carbono para obtener nanocompuestos conductores, permiten su utilización en aplicaciones en el sector de la electrónica y la industria del automóvil, que demandan materiales con características

disipativas de la electricidad estática (aplicaciones ESD) o cierto grado de conductividad eléctrica (aplicaciones de apantallamiento electromagnético, EMI, pintado electrostático, etc). En la industria naval, los compuestos CNT/poliamida también permiten construir barcos ultraligeros [95] utilizados para competiciones deportivas.

1.2 Desarrollo de compuestos poliméricos conductores (CPCs)

Exceptuando el pequeño grupo de polímeros intrínsecamente conductores (como la polianilina, poli(3,4-etilendioxitiofeno) y el polipirrol), la gran mayoría de los polímeros son buenos aislantes eléctricos, por lo que no son aptos para algunas aplicaciones, como en la fabricación de limitadores de corriente, dispositivos de disipación electrostática (ESD) o carcasas para apantallamiento de interferencias electromagnéticas (EMI) donde se requieren altas conductividades eléctricas. Los materiales metálicos, con alta conductividad, presentan dos importantes inconvenientes: su precio y su peso. Por otra parte, los polímeros intrínsecamente conductores son difíciles de procesar, caros y no aptos para el moldeo de productos con formas complejas. A mayores, suelen ser quebradizos y poco estables a la temperatura y la humedad [96]. Por todas estas razones, la estrategia más habitual para obtener polímeros con buena conductividad eléctrica, es añadir rellenos conductores a la matriz aislante. Este tipo de materiales se conoce como compuestos poliméricos conductores (CPCs).

Los rellenos conductores más habituales en este tipo de compuestos son partículas de tamaño micrométrico como cargas metálicas o materiales de carbono (negro de carbono (CB), grafito exfoliado o fibras de carbono). Para conseguir buena conductividad eléctrica utilizando este tipo de rellenos, es necesario incorporar a la matriz entre un 10 y el 50% en peso lo que, en general y tal como se comentó previamente, causa que el compuesto tenga alta densidad y pobres propiedades mecánicas [97-99].

La utilización de nanotubos de carbono (CNTs) ofrece una alternativa que, a priori, permitiría superar estos inconvenientes. Comparados con los rellenos conductores tradicionales, los CNTs presentan, entre otras ventajas, una alta relación de aspecto (típicamente >1000) y una conductividad eléctrica excelente (del mismo orden que el cobre y la plata). Estas características pueden facilitar la formación de redes conductoras dentro de la matriz

polimérica con contenidos a menudo por debajo del 1% en peso [100, 101].

1.2.1 Concepto de percolación. Diferencias entre percolación eléctrica y reológica

La teoría de percolación, aplicada a materiales compuestos conductores, predice que, a partir de una concentración umbral, debe existir al menos un camino conductor a lo largo de la matriz aislante, formado por partículas o agregados de partículas interconectados entre sí. Es decir, considera que para la conducción eléctrica se necesita contacto físico entre las partículas del relleno conductor. La concentración umbral ("threshold" en inglés), habitualmente definida como pc (contenido en volumen de partículas conductoras), es la concentración a partir de la cual, se produce un incremento exponencial de varios órdenes de magnitud, de la conductividad eléctrica. Así pues, el valor de la concentración umbral podría ser determinado gráficamente, representando los valores de conductividad en corriente continua (DC) de los distintos nanocompuestos, o la conductividad en la zona de bajas frecuencias para las medidas en corriente alterna (AC) (Figura 4), en función de la concentración de nanotubos. Sin embargo, éste es un método bastante subjetivo, por lo que es preferible utilizar el ajuste matemático de los datos de conductividad eléctrica, aplicando el modelo de la ley de la potencia, según la ecuación 1:

$$propiedad \approx \left(p - p_C\right)^{\beta} \qquad (1)$$

La conductividad eléctrica depende de la concentración de relleno en el material compuesto según la ecuación 1. El valor de β define teóricamente la dimensionalidad de la red conductora formada, con un valor entre 1.1-1.3 para una red 2D y un valor entre 1.6-2.0 para una red 3D [102]. Estos valores son correctos sólo en el caso ideal que el relleno sea infinitamente conductor y la matriz infinitamente aislante.

Otro método para determinar la concentración umbral consiste en observar las propiedades reológicas de los compuestos, por ejemplo, la evolución de la viscosidad compleja con la frecuencia en la zona de frecuencias bajas. De este modo, se puede determinar también gráficamente la concentración umbral donde se produce el cambio de material aislante a conductor. El composite tiene un comportamiento newtoniano, en las

concentraciones por debajo de la umbral, y un comportamiento dependiente de la frecuencia después de dicho punto. Este fenómeno es conocido con el nombre de percolación reológica.

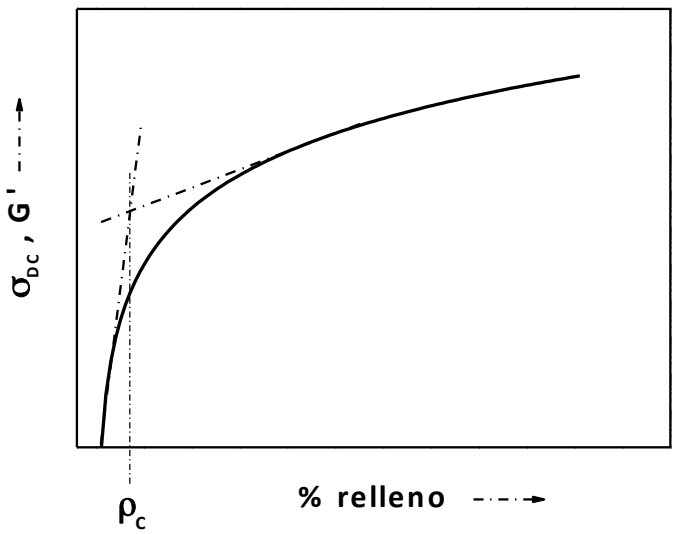

Figura 4 Determinación de la concentración umbral a partir de la representación de datos eléctricos o reológicos

En los experimentos reológicos, se puede determinar matemáticamente la concentración umbral, mediante el ajuste de los datos del módulo elástico G' o la viscosidad compleja de los compuestos a la ecuación 2, ya que son dos propiedades que cambian de forma drástica en torno al umbral de percolación (Figura 4). Lo habitual es utilizar para el ajuste los valores obtenidos a frecuencias bajas porque el comportamiento como sólido del material es más evidente en esa región.

$$G'(p) \propto (p - p_{c,G'})^{t_{c,G'}} \qquad (2)$$

Los datos publicados en la bibliografía muestran que el umbral de percolación eléctrica y el de percolación reológica para un mismo composite, no coinciden. En la gran mayoría de los casos, la percolación reológica ocurre a concentraciones más bajas que la percolación eléctrica [103-105], aunque también se pueden encontrar referencias bibliográficas del comportamiento contrario

[39, 106, 107]. La diferencia entre ambos umbrales de percolación está relacionada con la distancia mínima entre nanotubos para formar la red. Para la formación de la red conductora eléctrica, se necesita que los nanotubos se encuentren mucho más cerca unos de otros (del orden de los 3 nm o menor), no necesariamente en contacto físico entre ellos, pero sí lo suficientemente cerca para permitir los procesos de conducción por efecto túnel. En el caso de la percolación reológica, es suficiente con que la distancia entre nanotubos sea aproximadamente el radio de giro de una molécula del polímero, claramente mayor de 3 nm en la mayoría de las macromoléculas [32].

Además la percolación reológica se origina a partir de una red combinada que incluye tanto la red polímero-polímero, la red entre nanotubos de carbono y la red polímero-nanotubos de carbono [108], mientras que la percolación eléctrica se relaciona sólo con la red formada por los nanotubos.

Otra diferencia a destacar, es que para el estudio de la percolación reológica los experimentos se realizan sobre el material en estado fundido, mientras que el análisis de las propiedades eléctricas de los compuestos, se realiza con el material sólido. El estado de agregación de los nanotubos puede ser distinto y, por tanto, la red formada. Además, el valor de concentración umbral para la percolación reológica depende de la temperatura del ensayo y disminuye al aumentar ésta [109, 110]. Los datos publicados indican que, durante el ensayo, el material sufre cambios estructurales debido a la reaglomeración de los nanotubos dentro de la matriz fundida. Así pues, aunque a menudo en la bibliografía se equiparan los fenómenos de percolación eléctrica y reológica, no es del todo correcto a menos que se compruebe que la morfología del material (el grado de dispersión de los nanotubos) es la misma antes y después del proceso de fundido del ensayo de reología.

Para la mayoría de las matrices poliméricas, la transición de aislante a conductor se produce con un contenido de CNTs inferior al 5% en peso, aunque para un mismo sistema polímero/CNTs las diferencias en los valores de concentración umbral, existentes en bibliografía, son considerables. Esto se puede atribuir a los distintos tipos y métodos de fabricación de los CNTs utilizados, su relación de aspecto [98], pero sobre todo al tipo y condiciones de procesado, al estado de dispersión y a las características superficiales de los CNTs, en el caso de haber sido funcionalizados [35]. La gran mayoría de los nanotubos utilizados en aplicaciones industriales y estudios científicos, son nanotubos

de carbono multipared (MWCNTs) producidos por deposición catalítica en fase de vapor (CVD). Estos nanotubos de carbono tienen tendencia a formar grandes aglomerados con tamaños del orden de varias micras. Las fuertes interacciones de Van der Waals dificultan su completa dispersión en la matriz polimérica durante el proceso de mezclado y por esta razón, la concentración umbral de percolación eléctrica obtenida en la mayoría de los casos [35, 80, 82,111-113] es mayor que el valor teórico esperado.

Comparando con otros rellenos conductores como el negro de carbono, la mayor relación de aspecto de los nanotubos de carbono (L/D ≈102 -106 frente a L/D ≈ 1 del negro de carbono) permite obtener umbrales de percolación eléctrica más bajos [114]. Por ejemplo, Sumfleth y sus colaboradores [100] midieron un valor de pc de 0.025% en peso para el sistema epoxi/MWCNT, mientras que, con negro de carbono, dicha concentración es de 0.085% en peso. En otro estudio usando como matriz resina epoxi, se obtiene el cambio al estado conductor con un contenido entre 0.1 y 0.5% en peso de nanofibras de carbono, mientras que con nanotubos de carbono esta transición se observa a concentraciones menores de 0.1% en peso [101].

El hecho de tener que añadir sólo pequeñas cantidades de CNTs para alcanzar la transición aislante-conductor hace que sea más fácil mantener ductilidad de la matriz polimérica [64]. En el caso contrario, la adición de grandes cantidades de relleno (como el negro de carbono) perjudica las propiedades mecánicas del compuesto final y también su procesabilidad.

1.2.2 Influencia del estado de dispersión de los CNTs sobre las propiedades eléctricas de los CPCs

Tal y como ya se comentó, el método de procesado utilizado y sus parámetros experimentales cambian la distribución de los nanotubos dentro de la matriz polimérica, o, lo que es lo mismo, la morfología de la red conductora y por tanto, las propiedades eléctricas obtenidas [80, 82, 111, 115]. Los estudios publicados no muestran una coincidencia unánime sobre, si es mejor una distribución uniforme de nanotubos en la matriz, para obtener mejores propiedades eléctricas [98, 116] o, por el contrario [117-119], se obtiene una mejor conductividad eléctrica cuando los nanotubos muestran cierto grado de agregación. Lo cierto es, que las relaciones entre procesado, morfología obtenida y propiedades eléctricas son complejas y para cada sistema, nanotubo-matriz

polimérica, es necesario realizar un estudio en profundidad para conocer dichas relaciones, optimizar todos los parámetros experimentales y con ello, maximizar las propiedades eléctricas.

El estado de dispersión de los nanotubos en una matriz polimérica se puede caracterizar cualitativamente o semi-cuantitativamente mediante análisis morfológico utilizando diferentes técnicas: microscopía óptica (OM), microscopia electrónica de barrido (SEM), microscopía electrónica de transmisión (TEM) y microscopía de fuerza atómica (AFM) [120]. Con la microscopía óptica sólo se pueden observar aglomerados muy grandes de nanotubos; la microscopía electrónica de barrido (SEM) o la microscopía de fuerza atómica (AFM), sólo permiten observar la superficie o un corte transversal del compuesto. Con la microscopía electrónica por transmisión (TEM), resulta difícil extraer conclusiones sobre morfología global del compuesto a partir de imágenes de secciones de muestra de poco espesor (en torno a 100 nm). Así pues, se hace necesario combinar la información obtenida mediante varias de estas técnicas, para conocer en detalle la disposición de los CNT en la matriz y la morfología de la red formada.

Algunos trabajos publicados han demostrado que aquellos compuestos donde los nanotubos muestran mejor dispersión, tanto en la nanoescala (observada mediante TEM) como en la microescala (observada mediante SEM), pueden presentar, sin embargo, grandes agregados macroscópicos (solo visibles mediante microscopía óptica, OM) y unas propiedades eléctricas pobres. Sin embargo, un compuesto con peor dispersión, según los análisis realizados en TEM y SEM, a pesar de la existencia de aglomerados, su óptima distribución en la red conductora lleva a mejores propiedades eléctricas [121-123]. Esta mayor conductividad de los materiales con menor grado de dispersión, se justifica por el mayor número de contactos nanotubo-nanotubo existentes después de haberse formado la red conductora, lo que facilita el transporte electrónico.

Además, en el caso de los polímeros semicristalinos, el estado cristalino es otra variable a tener en cuenta. La presencia de nanopartículas, como los nanotubos de carbono, afectan tanto a la estructura cristalina (por la creación de nuevos sitios de nucleación) como a la velocidad de crecimiento de los cristales. El aumento de cristalinidad, en principio, mejora la dispersión de los CNTs en la microescala y en la nanoescala, porque los cristales evitan en cierta medida la formación de aglomerados [98, 124-126].

Por último, es necesario comentar la influencia de las propiedades reológicas de la matriz polimérica en el estado de dispersión de los nanotubos y, como consecuencia, en las propiedades eléctricas del compuesto.

Para comprender la importancia que tienen las propiedades reológicas de la matriz, hay que tener en cuenta qué ocurre durante el procesado en fundido de los compuestos. Primero, el polímero fundido se infiltra, en mayor o menor medida, en los aglomerados primarios de nanotubos, posteriormente las fuerzas de cizalla generadas durante el mezclado actúan dispersando los CNT individuales y los aglomerados primarios remanentes. También puede darse un proceso de reaglomeración de los nanotubos individuales, generándose aglomerados secundarios de CNTs dentro de la matriz. Todo ello, nanotubos individuales, aglomerados primarios y secundarios, definen las propiedades de la red conductora y, por tanto, las propiedades eléctricas del nanocompuesto. Además, se debe evitar que durante el procesado se reduzca la longitud de los nanotubos, lo que disminuiría la conductividad del material.

El primer paso es la infiltración del polímero diluyente en los aglomerados primarios [127]. Esta infiltración es más rápida y más completa (aunque depende del tamaño de los aglomerados) en el caso de polímeros fluidos, con lo que se consigue una disminución de la resistencia de los nanotubos para ser dispersados. En estos polímeros de baja viscosidad, las fuerzas de cizalla generadas durante el procesado en fundido son menores que en el caso de los polímeros más viscosos, pero en estos últimos, esta cizalla puede hacer que los nanotubos de carbono se rompan y disminuyan su longitud.

Para que tenga lugar la transición de aislante a conductor se necesita la formación de una red conductora, y para facilitar este proceso, la movilidad de los nanotubos no debería estar restringida en los aglomerados primarios. La red conductora puede establecerse entre aglomerados conectados por nanotubos separados o a través de estructuras de aglomerados [128], formadas mediante aglomeración secundaria [126, 129].

Ha y Kim [130] observaron una disminución de la dispersión de MWCNT en polipropileno (PP) y policarbonato (PC), ambos de alto peso molecular y por tanto de mayor viscosidad, aún aplicando mayores esfuerzos de cizalla, comparando con muestras equivalentes realizadas con PP y PC de bajo peso molecular y por tanto más fluidos. Este resultado fue explicado en base a una

menor movilidad de los MWCNTs cuando se procesan con polímeros de alta viscosidad. En este estudio, el umbral de percolación eléctrica fue menor para los composites de baja viscosidad.

En otros dos estudios se discutió el efecto causado por el uso de varios policarbonatos (PC), con diferentes pesos moleculares y por tanto, diferentes viscosidades en fundido [127, 131]. La mejor dispersión de aglomerados de MWCNTs se encontró para el compuesto con el PC más viscoso [127]. Sin embargo, para un contenido fijo de un 1% en peso de CNTs y utilizando las mismas condiciones de mezclado, las muestras con valores de conductividad más altas son aquellas preparadas con el PC de menor viscosidad.

Hay que tener en cuenta el hecho de que la resistividad eléctrica (inversa de la conductividad eléctrica), no sólo depende de la dispersión obtenida después de la incorporación de los CNTs, ya que la mayor o menor aglomeración secundaria que tenga lugar, por ejemplo, durante un procesado por moldeo por comprensión, influye en la resistividad eléctrica final del compuesto.

Un artículo muy detallado sobre la influencia de la viscosidad en la morfología y las propiedades eléctricas de los nanocompuestos con CNTs es el de Socher y sus colaboradores [132]. Prepararon nanocompuestos con MWCNTs en cinco polímeros distintos (PA12, polibutilentereftalato (PBT), PC, poliéter éter cetona (PEEK) y polietileno de baja densidad (LDPE)) cada uno de ellos, con tres grados de viscosidad distinta (baja, media y alta). Para todos los polímeros, la transición de aislante a conductor ocurre con menor contenido de nanotubos en las matrices de baja viscosidad. Al analizar conjuntamente la morfología y las propiedades eléctricas, los autores concluyen que los nanotubos presentan mejor dispersión en aquellos compuestos cuyas matrices poliméricas son las más viscosas, pero también son los que tiene un umbral de percolación eléctrico mayor.

1.3 Modificación de la conductividad térmica de las matrices poliméricas

El transporte del calor en sólidos puede ser electrónico (causado por portadores de carga, electrones o huecos) o fonónico. En el caso de los materiales aislantes y

semiconductores, la mayor contribución a la conductividad térmica del material la realizan los fonones, mientras que en el caso de los metales la contribución principal es la electrónica [133]. Por tanto, para la mayoría de los polímeros la conducción térmica se produce a través de los fonones [134]. En la actualidad, una buena disipación térmica es crítica para el buen funcionamiento, la fiabilidad y el aumento de la vida útil de los aparatos electrónicos [135]. Para muchas de estas aplicaciones la conductividad térmica de la mayoría de los polímeros (en el rango de 0.1-0.5 W/(m.K)) no es suficiente [136]. Sin embargo, las ventajas de los polímeros respecto a otro tipo de materiales (su buena procesabilidad, bajo peso, resistencia a la corrosión, su precio, etc.) hace potencialmente muy interesante el desarrollo de compuestos poliméricos, con alta conductividad térmica, que puedan ser utilizados en estas aplicaciones.

La estrategia más habitual para conseguir que el polímero aislante sea buen conductor térmico, es la de añadir rellenos con buena conductividad térmica. Los más habituales son: óxido de aluminio, nitruro de boro, nitruro de aluminio, nitruro de silicio, diamante, grafito, partículas metálicas y nanotubos de carbono. Para aplicaciones que requieren alta conductividad térmica, pero que el material siga siendo aislante eléctrico, se utilizan rellenos conductores cerámicos, como el óxido de aluminio, nitruro de boro y nitruro de aluminio. Por el contrario, se utiliza el grafito, el grafeno, las partículas metálicas y los nanotubos de carbono para aquellas aplicaciones que no requieren que el material sea aislante eléctrico. Los rellenos de carbono, sin embargo, son los más prometedores de este grupo porque combinan alta conductividad térmica y bajo peso. Dentro de este grupo se encuentran el grafito, la fibra de carbono, el negro de carbono, los nanotubos de carbono y el grafeno.

El grafito tiene alta conductividad térmica (entre 100 y 400 W/m.K), bajo coste y una fácil dispersión en los polímeros [137-139]. La fibra de carbono también incrementa la conductividad térmica de la matriz polimérica aunque hay grandes diferencias en función de la orientación de la fibra [140, 141].

Las partículas de negro de carbono tienen baja conductividad térmica [142] con lo que al ser añadidos a los polímeros contribuyen en mayor medida a la conductividad eléctrica que a la térmica [143].

Los nanotubos de carbono tienen una alta conductividad térmica con valores de entre 2800-6000 W/(m.K), medidos en

nanotubos individuales a temperatura ambiente [144, 145], comparable a la del diamante y mayor que la del grafito y las fibras de carbono. Sin embargo, la conductividad térmica de los compuestos poliméricos con CNTs, muestran valores mucho más bajos que los estimados a partir de la conductividad intrínseca de los CNTs y la regla de las mezclas [146, 147]. En la bibliografía se pueden encontrar resultados muy dispares: desde incrementos de más de un 125% en la conductividad térmica tras añadir un 1% de CNTs [148], hasta disminuciones en la conductividad térmica del material con el incremento de nanotubos de carbono [149, 150].

Por último, el grafeno es un material de carbono en dos dimensiones, con una estructura de una única capa que facilita el transporte de calor [151]. Aunque tiene mayor conductividad térmica que la de los CNTs, su mayor área superficial dificulta su incorporación en grandes cantidades, en las matrices poliméricas, lo que unido a su alto precio limita sus aplicaciones.

1.3.1 Factores determinantes en la conductividad térmica de los compuestos de matriz polimérica

La conductividad térmica de los materiales compuestos con matriz polimérica depende, al igual que en el caso de la conductividad eléctrica, del contenido, la forma y orientación del relleno, su relación de aspecto, las interacciones interfaciales relleno-polímero y la dispersión del relleno. Para alcanzar el nivel apropiado de conductividad térmica, para su uso en las aplicaciones anteriormente comentadas, se necesitan altos contenidos de relleno (por encima del 30% en volumen) que producen un aumento considerable de la viscosidad, lo que dificulta en gran medida el procesado del material compuesto mediante extrusión o inyección [152]. Además, la adición de altas cantidades de rellenos inorgánicos empeora la resistencia mecánica del material compuesto y aumenta su densidad. Hoy en día, mediante estos procesos de moldeo (inyección o extrusión) es difícil obtener compuestos con conductividades térmicas mayores de 4 W/(m.K).

Con el descubrimiento de los CNTs y sus propiedades, se generaron grandes expectativas para mejorar las propiedades térmicas de los polímeros utilizando menores contenidos de relleno [150]. Sin embargo, los datos de conductividad térmica obtenidos en estos compuestos muestran sólo pequeños incrementos en esta propiedad, comparando con el aumento de la conductividad

eléctrica que se produce para un mismo contenido de nanotubos. Está claro que los mecanismos de transporte de la carga eléctrica y la energía térmica son diferentes [65].

Por otra parte, muchos de los rellenos conductores (fibras de carbono, nanotubos de carbono, láminas de grafeno) presentan una dirección preferencial, con lo que son orientados debido a los esfuerzos de cizalla aplicados durante el procesado (extrusión o inyección fundamentalmente), obteniéndose compuestos con propiedades térmicas anisotrópicas [153-156]. En la mayoría de los casos, los rellenos conductores se orientan en la dirección del flujo produciendo una conductividad térmica elevada en el plano y más baja, en la dirección perpendicular al plano. Este fenómeno, observado por ejemplo en compuestos con nanotubos de carbono [157, 158], fibras de carbono [154, 159], grafito [160, 161] y grafeno [162], puede ser deseable en algunas aplicaciones, pero en otras es preferible que la conductividad térmica sea una propiedad isotrópica.

Otro aspecto a tener en cuenta, es que mantener la relación de aspecto de los nanotubos después del procesado del composite, es crucial [163].

La interacción del relleno con la matriz polimérica también es importante [164, 165]. Si la interacción entre los nanotubos y la matriz polimérica es pobre, aumenta la resistencia interfacial y disminuye la conductividad térmica [136].

Para finalizar, es necesario hablar de la influencia de la dispersión de los nanotubos en la conductividad térmica de los polímeros. Al igual que en el caso de la conductividad eléctrica, éste es uno de los factores críticos durante el procesado de compuestos CNT/polímeros debido a que los nanotubos tienden a formar aglomerados [166-168]. Sin embargo, no es sencillo establecer una relación clara entre la dispersión de los nanotubos y la conductividad térmica de los nanocompuestos, debido a que la dispersión depende tanto de las técnicas experimentales utilizadas, como de la interpretación de los autores y, en bibliografía, se suelen encontrar pocos parámetros cuantitativos que permitan hacer comparaciones objetivas entre los distintos datos.

1.4. Concepto de red segregada: influencia de la morfología en las propiedades de los composites poliméricos conductores.

Como se ha explicado en los capítulos anteriores, la morfología del nanocompuesto y el estado de dispersión de las cargas conductoras obtenido durante el proceso de mezclado con la matriz polimérica, influyen directamente en las propiedades macroscópicas de los compuestos poliméricos conductores (CPCs). Optimizar dichos parámetros para disminuir la concentración mínima de refuerzo (threshold) necesaria para lograr la transición de aislante a conductor eléctrico, es de gran relevancia en la fabricación de CPCs. Para alcanzar este objetivo existen dos estrategias: o bien crear estructuras con doble percolación o formar redes segregadas.

Al añadir un relleno conductor a una mezcla de polímeros inmiscibles, se puede producir la llamada doble percolación, cuando al menos una de las fases poliméricas es continua y el relleno conductor se localiza en esa fase continua [169]. La concentración umbral de percolación de estos CPCs, disminuye de forma significativa con respecto a aquellos cuya matriz es un único polímero, debido a la localización selectiva del relleno conductor. Esta depende del balance entre energías interfaciales del relleno y de los polímeros, y se puede predecir calculando el parámetro de mojado (wetting parameter), ωAB, que se define según la siguiente ecuación:

$$\omega_{AB} = \frac{\sigma_{CNT-B} - \sigma_{CNT-A}}{\sigma_{A-B}} \qquad (3)$$

En la ecuación 3, σ_{CNT-X} es la energía interfacial entre el relleno y los polímeros A y B, y en el denominador se encuentra la energía interfacial entre los dos polímeros de la mezcla. El relleno conductor tiende a localizarse en el polímero B, si el coeficiente de mojado es menor de -1 y, por el contrario, tiende a localizarse en el polímero A, si el coeficiente es mayor de 1 (Figura 5 a,c).

En el caso en que dicho coeficiente tenga un valor entre -1 y 1, el relleno se localizará en la interfase entre los dos polímeros (Figura 5b), y se formará lo que se conoce como una red segregada dentro de la matriz polimérica. Esta morfología todavía reduce más el umbral de percolación (en comparación con la anterior). Así pues, este coeficiente se puede utilizar como

indicador de la tendencia termodinámica de las partículas de relleno para situarse en una matriz u otra, minimizando las energías interfaciales.

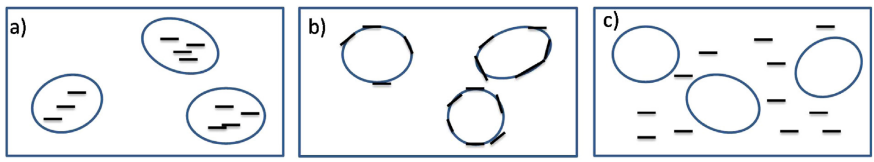

Figura 5 Esquema de la morfología obtenida en función del valor del parámetro de mojado [170, 171]. El polímero A es la fase dispersa, y el polímero B es la fase continua.

En la literatura científica existen varios ejemplos de cómo la selección de las matrices poliméricas [169, 172, 173], influye en la distribución del relleno. Debido a las diferentes interacciones entre esos polímeros y las cargas conductoras, éstas tienden a localizarse en la fase polimérica con la que tienen una mayor interacción y por tanto, menor energía interfacial.

Por ejemplo, en los CPCs formados por nanotubos de carbono y cuya matriz es una mezcla de policarbonato y estireno-acrilo-nitrilo (PC/SAN), se puede observar que las nanopartículas se localizan de forma selectiva en el PC, de acuerdo con los cálculos del coeficiente de mojado. Al mezclar en fundido los componentes juntos, la fase de SAN reblandece antes por lo que inicialmente los CNTs quedan embebidos en ella. Sin embargo, cuando se produce el reblandecimiento del PC, los nanotubos de carbono se transfieren al PC. Incluso en el caso de que los CNTs estén predispersos en SAN, se produce una rápida transferencia desde el SAN al PC [174, 175].

Otro ejemplo es el publicado por Abbasi y sus colaboradores [176] que descubrieron que, al añadir CNTs a mezclas inmiscibles PA6/PP, se producía la localización selectiva de los nanotubos de carbono en la PA6. De esta forma, la concentración efectiva de relleno en la poliamida es mayor, lo que explica que el nanocompuesto con un 3% en peso de CNTs, tenga una conductividad varios órdenes de magnitud mayor que los compuestos conductores con una matriz de PA6 y un 3% en peso de CNTs. De esta manera, se pueden obtener bajos umbrales de percolación y, por tanto, materiales con los mismos niveles de conductividad, pero utilizando concentraciones de nanotubos mucho menores.

La preferencia termodinámica de los nanotubos de carbono por localizarse en un polímero u otro puede modificarse de distintas formas. Por ejemplo, Gültner y sus colaboradores [177] añadieron un compuesto reactivo miscible con el copolímero de acrilonitrilo-estireno, para mejorar la interacción entre el SAN y los MWCNTs en una matriz de PC/SAN. Los autores observaron la transferencia de los MWCNTs desde la fase de PC a la fase de SAN después de la adición del aditivo, debido a la mejora de la interacción entre el SAN y los nanotubos. Otra posibilidad es la funcionalización de los CNTs que, por ejemplo, con dióxido de titanio, permite su localización en la fase de SAN en lugar de situarse en la poliamida 66, como cabría esperar según los cálculos de la energía interfacial, en mezclas de SAN/PA66 [178].

Las condiciones del mezclado de los nanotubos y las matrices, también influyen en la localización del relleno conductor en una u otra fase polimérica. Dashan M y sus colaboradores [179] demostraron que, variando la energía aplicada durante el mezclado en fundido, se produce un cambio en la morfología de la mezcla poliamida 6/polietileno de alta densidad. Los MWCNTs, inicialmente predispersos en HDPE y con una pobre transferencia hacia la PA6, completan su transferencia de una fase a la otra utilizando los parámetros adecuados.

Como se comentó previamente, otra de las estrategias que se puede seguir para disminuir el umbral de percolación eléctrica en CPCs, consiste en formar redes segregadas [180, 181], donde las partículas del relleno conductor (en este caso los nanotubos de carbono), se distribuyen en un volumen restringido de la matriz en lugar de disponerse de forma aleatoria por todo el material. Esto causa un aumento sustancial de la densidad efectiva de los caminos conductores, para una concentración determinada de relleno. Esta estructura facilita la formación de una red conductora, donde existe un mayor contacto entre las partículas conductoras, con la mínima cantidad de relleno y, consecuentemente, se reduce de forma importante el valor de la concentración umbral de percolación (muchos autores hablan de umbrales de percolación "ultra-bajos") con respecto a los compuestos conductores convencionales [182].

Existen tres métodos referenciados para la formación de redes segregadas: por compresión directa, mediante la tecnología látex y utilizando el mezclado en fundido de las cargas conductoras y como matriz, una mezcla de polímeros inmiscibles. El primero consiste en realizar la compresión directa de la mezcla física o en disolución, del polímero y el relleno conductor para formar la red

conductora segregada [183-185]. Este método necesita polímeros viscosos, que preserven las redes segregadas conductoras durante el moldeo por compresión. El principal inconveniente es que no se pueden añadir grandes cantidades de relleno (menos del 10% en peso). Como ejemplo se puede comentar el trabajo de Gupta y sus colaboradores [186] que obtuvieron una red segregada de negro de carbono en acrilonitrilo-butadieno-estireno (ABS) con un valor umbral de percolación muy pequeño (aproximadamente un 0.0054% en volumen), concretamente el valor más pequeño encontrado hasta la fecha para materiales CPCs en la bibliografía.

El segundo método consiste en dispersar las partículas conductoras en una disolución acuosa de látex. Una vez evaporado el solvente, las partículas conductoras quedan retenidas dentro del espacio intersticial entre las partículas de látex [187]. Esta técnica es barata, ecológica, al sólo usarse agua destilada como disolvente, permite una buena dispersión de los rellenos conductores y se pueden añadir cantidades de relleno sin limitación, ya que en este caso no existen los problemas de las altas viscosidades presentes durante el mezclado en fundido [188, 189].

La tercera opción consiste en lograr la distribución selectiva de las partículas conductoras en la interfase de mezclas poliméricas inmiscibles durante el mezclado en fundido [190], tal y como se detalla a continuación, puesto que es el método utilizado en el trabajo de esta tesis.

1.4.1 Formación de redes segregadas mediante mezclado en fundido

El mezclado en fundido es el método más utilizado para la producción industrial de CPCs con redes segregadas, porque permite producir grandes cantidades, con costes reducidos. Sin embargo, la formación de redes segregadas con este método no es sencillo porque depende de muchos factores, tanto termodinámicos (la energía interfacial entre los polímeros y los rellenos conductores), como cinéticos (procedimiento y secuencia de mezclado, tiempo de mezclado y esfuerzo de cizalla) [191, 192]. Otros aspectos determinantes para la formación de la red, son la morfología de fases (directamente dependiente del ratio de viscosidad entre los polímeros inmiscibles), la secuencia de mezclado y la relación de aspecto del relleno conductor.

Existen dos formas de originar las redes segregadas conductoras mediante el mezclado en fundido. La primera requiere ajustar los parámetros termodinámicos (la energía interfacial relleno-polímero) y los cinéticos (la viscosidad en fundido y la secuencia de mezclado) de las mezclas poliméricas [188-190]. En este método, los rellenos conductores se predispersan en el polímero termodinámicamente desfavorable (polímero A), es decir, el que tiene una energía interfacial mayor y es menos viscoso que el otro, a la temperatura de procesado. A continuación, la masterbatch formada por el relleno conductor/polímero A se mezcla en fundido con el polímero termodinámicamente más favorable (polímero B), el más viscoso a la temperatura de procesado y con menor energía interfacial. Finalmente, las fuerzas termodinámicas aceleran la migración de las partículas conductoras desde el polímero A al polímero B, pero como el polímero B es muy viscoso, las partículas conductoras no son capaces de penetrar en esa fase y permanecen localizadas en la interfase de los dos polímeros.

En el trabajo realizado por Gubbels y sus colaboradores [194], se muestra una estructura segregada típica donde las partículas de negro de carbono (CB) se localizan principalmente en la interfase entre polietileno (PE) y poliestireno (PS). Gracias a esta morfología, se obtiene una concentración umbral de percolación eléctrica de sólo un 0.2% en volumen, de CB.

Baudouin y sus colaboradores [193] localizaron MWCNTs en la interfase de una mezcla inmiscible de poliamida 6 y un copolímero de etilén acrilato (EA). Observaron que cuando los MWCNTs se dispersan en PA6, la mayoría de ellos migran a la interfase, formando la red segregada. Lo mismo ocurre cuando las nanocargas, se predispersan en etilén acrilato o cuando se mezclan los tres polímeros juntos. Sin embargo, utilizando poliamida 12 (PA12), los nanotubos de carbono permanecen bien dispersos en esta matriz, en vez de localizarse en la interfase. En la misma línea está el trabajo de Zonder y sus colaboradores [195] que introdujeron CNTs en una mezcla de polietileno de alta densidad y poliamida 12 (HDPE/PA12), con morfología isla-mar, y obtuvieron una disminución de la resistividad eléctrica cuando los CNTs se encontraban en la interfase entre los dos polímeros.

La segunda posibilidad para construir una red segregada conductora es la introducción de un tercer polímero con alta afinidad hacia los rellenos conductores [190, 196]. Chen y sus colaboradores [190] utilizaron ABS grafteado con anhídrido maleico como compatibilizante, para mantener los CNTs en la

interfase de una mezcla de PC y ABS, con lo que se obtiene un largo canal conductor de CNTs entre las dos fases. Esta red conductora tiene un valor de pc de sólo un 0.03% en volumen.

Según los resultados publicados, los rellenos conductores con una menor relación de aspecto, son más fáciles de localizar en la interfase de mezclas poliméricas inmiscibles que los que presentan relaciones de aspecto grandes [197, 198]. Por esta razón, existen un gran número de trabajos sobre redes segregadas formadas por rellenos como el negro de carbono, pero pocos que utilicen otro tipo de partículas conductoras como nanoláminas de grafeno o nanotubos de carbono con una relación de aspecto mucho mayor [190, 193, 197].

Entre ellos, cabe citar el trabajo de Lim y sus colaboradores [198], que investigaron el efecto de rellenos conductores híbridos de MWCNTs y fibras de carbono recubiertas con níquel (NCCF), sobre la conductividad eléctrica y propiedades de apantallamiento electromagnético (EMI SE) en mezclas de PP y PA6 utilizando como compatibilizante un PP injertado con maleico. Por una parte, obtuvieron valores de conductividad eléctrica más altos en el compuesto ternario PP/PA6 /MWCNT que en los binarios, PP/MWCNT y PA6/MWCNT con contenidos para todos ellos de un 3% en peso con respecto al contenido del polímero (3 phr). Este resultado se debe a la localización selectiva de los MWCNT en la fase de PA6 que causa un aumento de la conductividad eléctrica.

1.5. Objetivos y estructura de la tesis

1.5.1 Objetivos

El principal objetivo de esta tesis es el diseño y caracterización de nuevos materiales compuestos poliméricos conductores utilizando mezclas de diferentes poliamidas como matriz y nanotubos de carbono de pared múltiple. En general, durante el desarrollo del trabajo de tesis se hizo especial hincapié en evaluar las relaciones entre procesado, morfología y propiedades macroscópicas de los diferentes nanocomposites desarrollados, buscando siempre maximizar las propiedades obtenidas con la menor cantidad de nanotubos de carbono. Con el propósito de que los materiales desarrollados pudiesen ser fácilmente producidos a escala industrial, y con el menor coste posible, se ha seleccionado el mezclado en fundido, mediante una extrusora, como la técnica de mezclado para la preparación de los diferentes compuestos.

Dado que el estado de dispersión de los nanotubos influye directamente en las propiedades de la red conductora formada y, por tanto, en las propiedades macroscópicas finales, se estudió cualitativa y cuantitativamente, este aspecto en función del tipo de poliamida, proporción y grado de miscibilidad entre las poliamidas utilizadas como matriz y tipo de predispersión usada para preparar el compuesto conductor.

De manera concreta los objetivos desarrollados en el trabajo de la tesis fueron:

- Estudio de la influencia del contenido de nanotubos de carbono, ratio entre poliamida 6 y poliamida 66 y tipo de predispersión utilizada, en las propiedades piezoeléctricas de los nanocompuestos.
- Evaluación del estado de dispersión de los nanotubos de carbono en función del ratio entre poliamida 6 y poliamida 66 y tipo de predispersión utilizada Influencia en las propiedades eléctricas y reológicas de los compuestos poliméricos conductores.
- Estudio de la formación de redes conductoras segregadas con nanotubos de carbono en una mezcla inmiscible de poliamida 6 y poliamida 12.
- Evaluación del contenido umbral de percolación eléctrica y reológica, correspondiente a una red segregada de nanotubos en una mezcla inmiscible de poliamida 6 y poliamida 12.
- Influencia de la formación de una red conductora segregada con nanotubos de carbono en el estado cristalino y en la absorción de agua de una mezcla inmiscible de poliamida 6 y poliamida 12.
- Análisis de la conductividad térmica de compuestos poliméricos conductores formados con nanotubos de carbono y una mezcla inmiscible de poliamida 6 y poliamida 12.

1.5.2 Relevancia de los objetivos propuestos

Los objetivos de este trabajo de tesis surgieron de la idea de combinar sinérgicamente, las excelentes propiedades de las poliamidas, con las características excepcionales de los nanotubos de carbono, para obtener nanocompuestos conductores.

Dichos nanocompuestos presentan un gran número de aplicaciones potenciales en sectores muy diferentes, se puede

destacar a modo de ejemplo, en la electrónica y en la industria del automóvil, que cada vez más, demandan materiales con características eléctricas que permitan la disipación de la electricidad estática (ESD) o un efectivo apantallamiento electromagnético (EMI), además de bajo peso y buen ratio entre coste y propiedades.

En el caso de la industria del automóvil, estos compuestos conductores pueden sustituir ciertas piezas metálicas y seguir utilizando técnicas de pintado electrostático. En el campo de la electrónica, actualmente los circuitos electrónicos se protegen de la radiación electromagnética mediante carcasas realizadas con aleaciones metálicas, que pueden ser sustituidas por otras más ligeras y fácilmente moldeables en formas complejas, fabricadas con compuestos poliméricos conductores con nanotubos de carbono.

La selección de la familia de poliamidas como matriz de los nanocompuestos conductores, se realizó considerando su versatilidad y el gran número de aplicaciones que tienen en la actualidad en la industria del automóvil. Ya que cada tipo de poliamida tiene propiedades útiles, pero diferentes entre ellas, la idea de utilizar mezclas de poliamidas se antojaba como una buena estrategia para combinar sinérgicamente las ventajas de cada una de ellas y superar, o al menos minimizar, sus desventajas.

Además, se escogieron como matrices poliméricas dos mezclas de poliamidas (PA), una mezcla de poliamidas parcialmente miscibles y otra de poliamidas inmiscibles, para poder estudiar la influencia de esta variable en las propiedades eléctricas de los compuestos obtenidos.

Las mezclas de poliamida 66 y poliamida 6, se utilizaron como matriz de los compuestos conductores al inicio del estudio. Se trata de dos poliamidas parcialmente miscibles, muy similares entre sí, con propiedades mecánicas similares y contenido de absorción de agua muy parecido. Sin embargo, tienen puntos de fusión diferentes.

Las mezclas de poliamida 6 y poliamida 12 son, en cambio, inmiscibles y se han seleccionado con el propósito de superar alguno de los conocidos inconvenientes de la PA6, como la alta sensibilidad a la propagación de grietas en solicitaciones de impacto a temperaturas por debajo de cero, alta absorción de humedad y su pobre estabilidad dimensional.

Finalmente, se puede indicar que, a pesar de haber muchos trabajos publicados donde se estudian los nanocompuestos formados por nanotubos de carbono, usando como matriz una poliamida o una mezcla de poliamidas con otro termoplástico [172, 173, 178, 193, 195, 198]; las investigaciones sobre compuestos conductores donde la matriz es una mezcla de poliamidas son realmente escasos, aún a día de hoy [199, 200]. Si las publicaciones sobre este tipo de compuestos son escasas, más aún lo son los estudios de las propiedades eléctricas, reológicas y morfológicas de mezclas miscibles o inmiscibles de poliamidas con nanotubos de carbono, que además incluyan el estudio de la formación de redes segregadas conductoras como estrategia para mejorar las propiedades eléctricas del material compuesto.

Todo esto prueba la relevancia y novedad de los objetivos propuestos, y finalmente desarrollados en el trabajo de tesis que, a continuación, se describe en esta memoria.

1.5.3 Estructura de la memoria de la tesis

A continuación, se expone un resumen de los contenidos que aparecen en cada capítulo de esta memoria.

Capítulo 1: Introducción. Está dedicado a una revisión profunda del estado del conocimiento acerca de los compuestos poliméricos conductores y sus aplicaciones. Además, se describen los objetivos de la tesis y la estructura de la memoria.

Capítulo 2: En este capítulo se describe el estudio de la influencia del contenido de nanotubos de carbono, ratio entre poliamida 6 / poliamida 66 y tipo de predispersión utilizada, en las propiedades piezoeléctricas de los nanocompuestos obtenidos.

Capítulo 3: Analiza el estado de dispersión de los nanotubos de carbono en función del ratio entre poliamida 6 / poliamida 66 y el tipo de predispersión utilizada; y como estas variables influyen en las propiedades eléctricas y reológicas de los compuestos conductores obtenidos.

Capítulo 4: En esta sección se estudia la formación de redes conductoras segregadas, con nanotubos de carbono, usando como matriz una mezcla inmiscible de poliamida 6 y poliamida 12. Finalmente, se determina el contenido umbral de percolación eléctrica y reológica.

Capítulo 5: En este capítulo se evalúa la influencia de la formación de una red conductora segregada con nanotubos de

carbono, en el estado cristalino y en la absorción de agua, de una mezcla inmiscible de poliamida 6 y poliamida 12.

Capítulo 6: La última parte de la memoria está dedicada al estudio de la conductividad térmica de compuestos poliméricos conductores, formados con nanotubos de carbono y una mezcla inmiscible de poliamida 6 y poliamida 12.

1.6. Referencias

1. Tuttle ME, Structural Analysis of Polymeric Composite Material,CRCPress (2004)

2. Plastic Additives Handbook, Carl Hanser Verlag. Munich (2001)

3. Hashim A. Advances in Nanocomposite Technology, InTech (2011)

4. Gay D, Hoa SV, Tsai SW. Composite Materials Design and Applications, CRCPress, 2003

5. Ajayan PM, Schadler LS, Braun PV. Nanocomposite science and technology. Weinheim: Wiley-VCh, p. 77-80 (2003)

6. Mallick PK. Fiber-reinforced composites: materials, manufacturing, and design. New York: Marcel Dekker Inc., 584 (1993)

7. Kotlensky WV. Chemistry & Physics of Carbon, 9: 173 (1973)

8. GuptaR.K.,E.Kennel,K.J.Kim, Polymer Nanocomposites Handbook,CRCPress (2010)

9. Öchsner A, Shokuhfar A, New Frontiers of Nanoparticles and Nanocomposite Materials, Novel Principles and Techniques,Springer (2013)

10. Kanatzidis M. Chemical & Engineering News, 36: 54 (1990)

11. González A., A. Romo, Memoria 2005, Ediciones de la Universidad Nacional Autónoma de México (2006)

12. Das P, Schipmann S, Malho JM, Zhu B, Klemradt U, Walther A. ACS Applied Materials and Interfaces, 5: 3738 (2013)

13. Podsiadlo P, Tang Z, Shim BS, Kotov NA. Nano Letters, 7: 1224 (2007)

14. Sun X, Sun H, Li H, Peng H. Advanced Materials, 25: 5153 (2013)

15. Shi Z, Chen X, Wang X, Zhang T, Jin J. Advanced Functional Materials, 21: 4358 (2011)

16. Shim BS, Zhu J, Jan E, Critchley K, Ho S, Podsiadlo P, Sun K, Kotov NA. ACS Nano Letters, 3: 1711 (2009)

17. Jalili R, Aboutalebi SH, Esrafilzadeh D, Konstantinov K, Moulton SE, Razal JM, Wallace GG. ACS Nano, 7: 3981 (2013)

18. Gunawidjaja R, Jiang C, Peleshanko S, Ornatska M, Singamaneni S, Tsukruk VV. Advanced Functional Materials, 16: 2024 (2006)

19. Kharlampieva E, Kozlovskaya V, Gunawidjaja R, Shevchenko VV, Vaia R, Naik RR, Kaplan DL, Tsukruk VV. Advances Functional Materials, 20: 840 (2010)

20. Markutsya S, Jiang C, Pikus Y, Tsukruk VV. Advanced Functional Materials, 15: 771 (2005)

21. Luzinov I, Minko S, Tsukruk VV. Soft Matter, 4: 714 (2008)

22. Kharlampieva E, Zimnitsky D, Gupta MK, Bergman KN, Kaplan DL, Naik RR, Tsukruk VV. Chemistry of Materials, 21: 2696 (2009)

23. Hussain I, Brust M, Papworth AJ, Cooper AI. Langmuir, 19: 4831 (2003)

24. Hou Y, Cheng Y, Hobson T, Liu J. Nano Letters, 10: 2727 (2010)

25. Beek WJE, Wienk MM, Janssen RAJ. Advanced Materials, 16: 1009 (2004)

26. Kabra D, Song MH, Wenger B, Friend RH, Snaith HJ. Advanced Materials, 20: 3447 (2008)

27. Shamir D, Siegmann A, Narkis M. Journal of Applied Polymer Science, 115: 1922 (2010)

28. Hu K, Chung DDL. Carbon, 49: 1075 (2011)

29. Friddle RW, LeMieux MC, Cicero G, Artyukhin AB, Tsukruk VV, Grossman JC, Galli G, Noy A. Nature Nanotechnology, 2: 692 (2007)

30. Jay Amarasekera. Reinforced plastics, 38 (2005)

31. Pardo SG, Arboleda L, Ares A, García X, Dopico S, Abad MJ. Polymer Composites, 34: 1938 (2013)

32. Grady BP. Carbon nanotube-polymer composites: manufacture, properties, and applications. Hoboken: John Wiley & Sons Inc., 368 (2011)

33. Koning C, Grossiord N, Hermant MC. Polymer carbon nanotube composites: the polymer latex concept. Singapore: Pan Stanford, 256 (2012)

34. Coleman JN, Khan U, Blau WJ, Gun'ko YK. Carbon, 44:1624 (2006)

35. Bauhofer W, Kovacs JZ. Composites Science and Technology, 69 (10): 1486 (2009)

36. Pandey G, Thostenson ET. Polymer Review, 52: 355 (2012)

37. Britnell L, Ribeiro RM, Eckmann A, Jalil R, Belle BD, Mishchenko A, Kim YJ, Gorbachhev RV, Georgiou T, Morozov SV, Grigorenko AN, Geim AK, Casiraghi C, Castro Meto AH, Novoselov KS. Science, 340: 1311 (2013)

38. El-Kady MF, Kaner RB. Nature Communications, 4 (1475): 1 (2013)

39. Kim J, Hong S.M, Kwak S, Seo Y. Physical Chemistry Chemical Physics, 11: 10851 (2009)

40. Tetsuka H, Asahi R, Nagoya A, Okamoto K, Tajima I, Ohta R, Okamoto A. Advanced Materials, 24: 5333 (2012)

41. Hu K, Gupta MK, Kulkarni DD, Tsukruk VV. Advanced Materials, 25:

2301 (2013)

42. Mannoor MS, Tao H, Clayton JD, Sengupta A, Kaplan DL, Naik RR, Verma N, Omenetto FG, McAlpine MC. Nature Communications, 3: 763 (2012)

43. Guo W, Cheng C, Wu Y, Jiang Y, Gao J, Li D, Jiang L. Advanced Materials 25: 6064 (2013)

44. Shahil KMF, Balandin AA. Solid State Communications, 152: 1331 (2012)

45. Ijima, S. Nature, 354: 56 (1991)

46. Saifuddin N, Raziah AZ, Junizah AR. Journal of Chemistry, 1 (2013)

47. Balasubramanian K, Burghard M. Small, 1 (2): 180 (2005)

48. Kumar M, Ando Y. Journal of Nanoscience and Nanotechnology, 10: 3739 (2010)

49. Harris PJF. Carbon Nanotubes and Related Structures, Cambridge University Press (2003)

50. Radushkevich LV, Lukyanovich VM. Soviet Journal of Physical Chemistry, 26: 88 (1952)

51. Davis WR, Slawson RJ, Rigby GR. Nature, 171: 756 (1953)

52. Oberlin A, Endo M, Koyana T. Journal of Crystal Growth, 32: 335 (1976)

53. Hamada N, Sawada S, Oshiyama A. Physical Review Letters, 68: 1579 (1992)

54. Abrahamson J, Wiles PG, Rhodes B. Carbon, 37: 1873 (1999)

55. Saifuddin N, Raziah AZ, Junizah AR. Journal of Chemistry, 1 (2013)

56. O'Connell, Carbon Nanotubes Properties and Applications, Taylor & Francis Group (2006)

57. Bethune DS, Kiang CH, de Vries MS, Gorman G, Savoy R, Vazquez J, Beyers R. Nature 363: 605 (1993)

58. Prasek J, Drbohlavova J, Chomoucka J, Hubalek J, Jasek O, Adamc V, Kizek R. Journal of Materials Chemistry, 21: 15872 (2011)

59. Terrones M. Annual reviews of materials research, 33: 419 (2003)

60. Popov VN. Materials Science and Engineering, 43: 61-102 (2004)

61. Li FK, Zhu W, Zhang X, Zhao CT, Xu M. Journal of Applied Polymer Science, 71: 1063 (1999)

62. Calvert P. Nature, 399 (6733): 210 (1999)

63. Peng-Cheng M, Naveed A.S, Gad M, Jang-Kyo K. Composites: Part A, 41:1345 (2010)

64. Alig I, Pötschke P, Lellinger D, Skipa T, Pegel S, Kasaliwal G.R., Villmow T. Polymer, 53: 4 (2012)

65. Moniruzzaman M, Winey KI. Macromolecules, 39: 5194 (2006)

66. Grossiord N, Loos J, Regev O, Koning CE. Chemistry of Materials, 18: 1089 (2006)

67. Du JH, Bai J, Cheng HM. Express Polymer Letters,1: 253 (2007)

68. Hua D, Lin L, Mizhi J, Shuangmei Z, Mingbo Y, Qiang F. Progresss in Polymer Science, 39: 627 (2014)

69. Sahoo NG, Rana S, Cho JW, Li L, Chan SH. Progress in Polymer Science, 35: 837 (2010)

70. Spitalsky Z, Tasis D, Papagelis K, Galiotis C. Progress in Polymer Science, 35: 357 (2010)

71. Kosmidou TV, Vatalis AS, Delides CG, Logakis E, Pissis P, Papanicolaou GC. Express Polymer Letters, 2: 364 (2008)

72. Ma PC, Liu MY, Zhang H, Wang SQ, Wang R, Wang K, Wong YK, Tang BZ, Hong SH, Paik KW, Kim JK. ACS Applied Materials and Interfaces, 1: 1090 (2009)

73. El Sawi I, Olivier PA, Demont P, Bougherara H. Composites Science and Technology, 73: 19 (2012)

74. Combessis A, Bayon L, Flandin L. Applied Physic Letters, 102 (011907): 1 (2013)

75. Sengupta R, Bhattacharya M, Bandyopadhyay S, Bhowmick AK. Progress in Polymer Science, 36: 638 (2011)

76. Ahir SV, Huang YYM, Terentjev EM. Polymer, 49: 3841 (2008)

77. Kuilla T, Bhadra S, Yao D, Kim NH, Bose S, Lee JH. Progress in Polymer Science, 35: 1350 (2010)

78. Al-Saleh MH, Sundararaj U. Carbon, 47: 2 (2009)

79. Huang YY, Ahir SV, Terentjev EM. Physical Review B, 73: 125422 (2006)

80. Villmow T, Kretzschmar B, Pötschke P. Composites Science and Technology, 70: 2045 (2010)

81. Gaurav K., Pegel S, Göldel A, Pötschke P, Heinrich G. Polymer 51: 2708 (2010)

82. Krause B, Pötschke P, Häußler L. Composites Science and Technology, 69:1505 (2009)

83. Deng H, Zhang R, Bilotti E, Loos J, Peijs T. Journal of Applied Polymer Science, 113: 742 (2009)

84. Deng H, Bilotti E, Zhang R, Peijs T. Journal of Applied Polymer

Science, 118: 30 (2010)

85. Pan YZ, Li L, Chan S, Zhao JH. Composites Part A, 41: 419 (2010)

86. Gorrasi G, Bredeau S, Di Candia C, Patimo G, De Pasquale S, Dubois P., Macromolecular Materials and Engineering, 120: 2663 (2011)

87. Khare RA, Bhattacharyya AR, Kulkarni AR. Journal of Applied Polymer Science: 120: 2663 (2011)

88. Ezat GS, Kelly AL, Mitchell SC, Youseffi M, Coates PD. Polymer Composites, 33: 1376 (2012)

89. Cheng HKF, Pan Y, Sahoo NG, Chong K, Li L, Chann SH, Zhao JH. Journal of Applied Polymer Science, 124: 1127 (2012)

90. Brigandi Paul J, Cogen JM, Pearson RA. Polymer Engineering and Science 54: 1 (2014)

91. Pötschke P, Bhattacharyya AR, Janke A, Pegel S, Leonhardt A, Taschner C. Fullerenes Nanotubes and Carbon Nanostructures, 13: 211 (2005)

92. Micusik M, Omastová M, Krupa I, Prokes J, Pissis P, Logakis E. Journal of Apllied Polymer Science, 113 (4): 2536 (2009)

93. Timmaraju MV, Gnanamoorthy R, Kannan K. Composites Part B: Engineering, 42: 466 (2011)

94. Timmaraju MV, Gnanamoorthy R, Kannan K. Materials Science and Engineering, A, 528: 2960 (2011)

95. Brown AS. Mechanical Engineering, 132(3): 36 (2010)

96. Brian P. Grady, Carbon nanotube-polymer composites: Manufacture, properties and applications, Wiley (2011)

97. Zhang W, Dehghani-Sanij AA, Blackburn RS. Journal of Materials Science, 42: 3408 (2007)

98. Li L, LiC, Ni C, Rong L, Hsiao B. Polymer, 48: 3452 (2007)

99. Sham ML, Li J, Ma PC, Kim JK. Journal of Composite Materials, 43: 1537 (2009)

100. Sumfleth J, Buschhorn ST, Schulte K. Journal of Materials Science, 46: 659 (2011)

101. Cardoso P, Silva J, Silva MC, van Hattum FWJ, Lanceros-Méndez S. Journal of Polymer Science Part B: Polymer Physics, 5: 1253 (2012)

102. Weber M, Kamal MR. Polymer Composites, 18:711 (1997)

103. Bangarusampath DS, Ruckdaschel H, Altstadt V, Sandler JKW, Garray D, Shaffer MSP. Polymer 50: 5803 (2009)

104. Lee JI, Yang SB, Jung HT. Macromolecules 42: 8328 (2009)

105. Hu GJ, Zhao CG, Zhang SM, Yang MS, Wang ZG. Polymer, 47: 480

(2006)

106. Chatterjee T, Yurekli K, Hadjiev VG, Krishnamoorti R. Advanced Functional Materials, 15: 1832 (2005)

107. Penu C, Hu G-H, Fernández A, Marchal P, Choplin L. Polymer Engineering and science, 52: 2173 (2012)

108. Lin B, Sundaraj U, Pötschke P. Macromolecular Materials and Engineering, 291: 227 (2006)

109. Pötschke P, Abdel-Goad M, Alig I, Dudkin S, Lellinger D. Polymer, 45: 8863 (2004)

110. Abbasi S, Carreau PJ, Derdorui A, Moan M. Rheolgica Acta, 48: 943 (2009)

111. Villmow T, Pötschke P, Pegel S, Häussler L, Kretzschmar B. Polymer, 49(16): 3500 (2008)

112. Kasaliwal G, Göldel A, Pötschke P. Journal of Applied Polymer Science, 112(6): 3494 (2009)

113. Balberg I, Anderson CH, Alexander S, Wagner N.Physical Review B, 30(7): 3933 (1984)

114. Pötschke P, Dudkin SM, Alig I. Polymer, 44: 5023 (2003)

115. Kasaliwal GR, Pegel S, Göldel A, Pötschke P, Heinrich G. Polymer, 51: 2708 (2010)

116. Kashiwagi T, Fagan J, Douglas J, Yamamoto K, Heckert A, Leigh S, Obrzut J, Du F, Lingibson S, Mu M, Winey KI, Haggenmueller R. Polymer, 48: 4855 (2007)

117. Bryning MB, Islam MF, Kikkawa JM, Yodh AG. Advanced Materials, 17: 1186-(2005)

118. Martin CA, Sandler JKW, Shaffer MSP, Schwarz MK, Bauhofer W, Schulte K, Windle AH. Composites Science and Technology, 64: 2309 (2004)

119. Pegel S, Pötschke P, Villmow T, Stoyan D, Heinrich G. Polymer, 50: 2123 (2009)

120. Deng H. Progress in Polymer Science, 39: 627 (2014)

121. Cardoso P, Silva J, Paleo AJ, van Hattum FWJ, Simoes R, Lanceros-Méndez S. Physica Status Solidi A, 207: 407 (2010)

122. Cardoso P, Silva J, Klosterman D, Covas J, van Hattum F, Simoes R, Lanceros-Méndez S. Nanoscale Research Letters, 6 (370): 1 (2011)

123. Aguilar JO, Bautista-Quijano JR, Avilés F. Express Polymer Letters, 4: 292 (2010)

124. Jeon K, Lumata L, Tokumoto T, Steven E, Brooks J, Alamo R. Polymer, 48: 4751 (2007)

125. Haggenmueller R, Guthy C, Lukes JR, Fischer JE, Winey KI. Macromolecules 40: 2417 (2007)

126. Alig I, Lellinger D, Dudkin SM, Pötschke P. Polymer, 48: 1020 (2007)

127. Kasaliwal GR, Göldel A, Pötschke P, Heinrich G. Polymer, 52(4): 1027 (2011)

128. Kasaliwal GR, Villmow T, Pegel S, Pötschke P, Influence of material and processing parameters on carbon nanotube dispersion in polymer melts. In: McNally T, Pötschke P, editors. Polymer-carbon nanotube composites: preparation, properties and applications. Woodhead Publishing Limited; p.92-132 (2011)

129. Pegel S, Pötschke P, Petzold G, Alig I, Dudkin SM, Lellinger D. Polymer, 49(4): 974 (2008)

130. Ha H, Kim SC, Ha K, Macromolecular Research,1 8(5): 512 (2010)

131. Zejler R, Handge UA, Dijkstra DJ, Meyer H, Altstädt V. Polymer, 52(2): 430 (2011)

132. Socher R, Krause B, Müller MT, Boldt R, Pötschke P. Polymer 53: 495 (2012)

133. Chen Hongyu, Valeriy V.Ginzburg, Jian Yang, Yunfeng Yang, Wei Liu, Yan Huang, Libo Du, Bin Chen, Thermal conductivity of polymer-based composites: Fundamentals and applications, Progress in Polymer Science 59: 41-85 (2016)

134. Han ZD, Fina A. Progress in Polymer Science, 36: 914 (2011)

135. J. H. Seol, A. L. Moore, I. Jo, L. Shi, “Thermal Conductivity Measurement of Graphene Exfoliated on Silicon Dioxide,” Journal of Heat Transfer, 133, 022403 (2011)

136. Huang XY, Jiang PK, Tanaka T. IEEE Electrical Insulation Magazine, 27: 8 (2011)

137. Tu H, Ye L. Polymer for Advanced Technologies, 20: 21 (2009)

138. Liu Z, Guo Q, Shi J, Zhai G, Liu L. Carbon, 46: 414 (2008)

139. Veca ML, Meziani MJ, Wang W, Wang X, LuF, Zhang P, Lin Y, Fee R, Connell JW, Sun Y. Advanced Materials, 21: 2088 (2009)

140. Tibbetts GG, Lake ML, Strong KL, Rice BP. Composites and Science Technology, 67: 1709 (2007)

141. Cheng Y, ting J, Ultra high thermal conductivity polymer composites, Carbon 2002; 40: 359-62

142. Wolff S, Wang MJ, Carbon black reinforcement of elastomers, In: Donnet JB, Bansal R.C, Wang M.J, editors, Carbon black science and technology, 2nd edition, New York: Marcel Dekker; 289-355 (1993)

143. Abdel-Aal N, El-Tantawy F, Al-Hajry A, Bououdina M. Polymer

Composites, 29: 511 (2008)

144. Fischer JF, Carbon nanotubes: structure and properties, In: Gogotsi Y, editor, Carbon nanomaterials, New York; Taylor and Francis Group; 51-8 (2006)

145. Zhang WB, Xu XF, Yang JH, Huang T, Zhang N, Wang Y, Zhou ZW. Composites Science and Technology, 106: 1 (2015)

146. Shen Z, Bateman S, Wu DY, McMahon P, Dell'Olio M, Gotama J. Composites Science and Technology, 69: 239 (2009)

147. Li C.C, Lu C.L, Lin Y.T, Wei B.Y, Hsu W.K. Physical Chemistry Chemical Physics, 11 (2009)

148. Biercuk MJ, Llaguno MC, Radosavljevic M, Hyun JK, Johnson AT, Fischer JE. Applied Physics Letters, 80: 2767 (2002)

149. Assael MJ, Antoniadis KD, Metaxa IN. Journal of Chemical and Engineering Data, 54: 2365 (2009)

150. Evseeva LE, Tanaeva SA. Mechanics of Composite Materials, 44: 87 (2008)

151. Pizza A, Metz R, Hassanzadeh M, Bantignies JL. The International Journal of Life Cycle Assessment, 19: 1226 (2014)

152. King JA, Barton RL, Hauser RA, Keith JM. Polymer Composites, 29: 421 (2008)

153. Ghose S, Working DC, Connel JW, Smith JG, Watson KA, Delozier DM, Sun YP, Lin Y. High Performance Polymers, 18: 961 (2006)

154. Yoo Y, Lee HL, Ha SM, Jeon BK, Won JC, Lee SG. Polymer International, 63: 151 (2014)

155. Zhang SA, Ke YC, Cao XY, Ma YM, Wang FS. Journal of Applied Polymer Science, 124: 4874 (2012)

156. Kusunose T, Yagi T, Firoz SH, Sekino T. Journal of Materials Chemistry A, 1: 1440 (2013)

157. Datsyuk V, Trotsenko S, Reich S. Carbon, 52: 605 (2013)

158. Kaul PB, Bifano MFp, Prakash V. Journal of Composite Materials, 47: 77 (2013)

159. Agarwal S, Khan MMK, Gupta RK. Polymer Engineering and Science, 48: 2472 (2008)

160. Wu HJ, Sun XW, Zhang W, Zhang XX, Lu CH. Composites A, 55: 27 (2013)

161. Zhou SX, Zhu Y, Du HD, Li BH, Kang FY. New Carbon Materials, 27: 241 (2012)

162. Yan HY, Tang YX, Long W, Li YF. Journal of Materials Science, 49: 5256 (2014)

163. Cai D, Song M. Carbon, 46: 2107 (2008)

164. Shenogin S, Xue L, Ozisik R, Keblinski P, Cahill DG. Journal of Applied Physics, 95: 8136 (2004)

165. Huxtabke ST, Cahill DG, Shenogin S,Xue L, Ozisik R, Barone P, Ursey M, Strano MS, Siddons G, Shim M, Keblinski P. Nature Materials, 2: 731 (2003)

166. Endo M, Hayashi T, Kim YA. Pure and Applied Chemistry, 78: 1703 (2006)

167. Paredes JI, Burghard M. Langmuir, 20: 5149 (2004)

168. Ke G, Guan WC, Tang CY, Hu Z, Guan WJ, Zeng DL, Deng F. Chinese Chemical Letters, 18: 361 (2007)

169. Göldel A, Kasaliwal G, Pötschke P. Macromolecular Rapid Communications, 30: 423 (2008)

170. Feng J, Chan CM, Li JX. Polymer Engineering and Science, 43: 1058 (2003)

171. Taguet A, Cassagnau P, López Cuesta JM. Progress in Polymer Science, 39: 1526 (2014)

172. Zhang L, Wan C, Zhang Y. Polymer Engineering and Science, 49: 1909 (2009)

173. Zhang L, Wan C, Zhang Y. Composites Science and Technology, 69: 2212 (2009)

174. Göldel A, Marmur A, Kasaliwal GR, Pötschke P, Heinrich G. Macromolecules, 44: 6094 (2011)

175. Göldel A, Kasaliwal GR, Pötschke P, Heinrich G. Polymer, 53: 411 (2012)

176. Abbasi MA, Azizeh J, Hossein N, Amir F, Volker A. Journal of Polymer Science, Part B: Polymer Physics, 53: 368 (2015)

177. Gültner M, Göldel A, Pötschke P. Composites Science and Technology, 72(1): 41 (2011)

178. Nayak GC, Sahoo S, Rajasekar R, Das CK. Composites Part A: Applied Science and Manufacturing, 43(8): 1242 (2012)

179. Dashan M, Kejun L, Hainan D, Jie Z. Polymers for advanced technologies, 25: 364 (2014)

180. Pang H, Chen C, Bao Y, Chen J, Ji X, Lei J, Li ZM. Materials Letters, 79: 96 (2012)

181. Al-Saleh MH, Sundararaj U. Composites A, 39: 284 (2008)

182. Huan P, Ling X, Ding-Xiang Y, Zhong-Ming L. Progress in Polymer Science, 39: 1908 (2014)

183. Du JH, Zhao L, Zeng Y, Zhang LL, Liu PF, Liu C. Carbon, 49: 1094 (2011)

184. Al-Saleh MH, Jawad SA, Ghanem HME. High Performance Polymers, 26: 205 (2014)

185. Wang BJ, LiHY, Li HZ, Chen P, Wang ZB, Gu Q. Composites Science and Technology, 89: 180 (2013)

186. Gupta S, Ou RQ, Gerhardt RA. Journal of Electronic Materials, 35: 224 (2006

187. Jurewicz I, King AAK, Worajittiphon P, Asanithi P, Brunner EW, Sear RP, Hosea TJC, Keddie JL, Dalton AB. Macromolular Rapid Communications, 31: 609 (2010)

188. Grossiod N, Wouters M, Miltner HE, Lu K, Loos J, Van Mele B, Koning CE Isotactic polypropylene/carbon nanotube composites prepared by latex technology: electrical conductivity study. European Polymer Journal 46 (9) 1833-1843 (2010)

189. Kyrylyuk AV, Hermant MC, Schilling T, Klumperman B, Koning CE, Shoot P. National Nannotechnology, 6: 364 (2011)

190. Chen J, Shi YY, Yang JH, Zhang N, Huang T, Chen C, Wang Y, Zhou ZW. Journal of Materials Chemistry, 22: 22398 (2012)

1891. Dai K, Xu XB, Li ZM. Polymer, 48: 849 (2007)

192. Zhang YC, Dai K, Tang JH, Ji X, Li ZM. Materials Letters, 64: 1430 (2010)

193. Baudouin AC, Devaux J, Bailly C. Polymer, 51: 1341 (2010)

194. Gubbels F, Jérome R, Teyssié P, Vanlathem E, Deltour R, Calderone A, Parenté V, Brédas JL, Selective localization of carbon black in inmiscible polymer blends: a useful tool to design electrical conductive composites, Macromolecules 1994; 27: 1972-4

195. Zonder L, Ophir A, Kenig S, McCarthy S. Polymer, 52: 5085 (2011)

196. Lu C, Hu XN, He YX, Huang XH, Liu Jc, Zhang YQ. Polymer Bulletin, 68: 2071- (2012)

197. Tan YQ, Fang LJ, Xiao JL, Song YH, Zheng Q. Polymer Chemistry, 4: 2939 (2013)

198. Lim SJ, Jong GL, Soo HH, Woo NKi. Macromolecular Research, 22(6): 632 (2014)

199. Besco S, Lorenzetti A, Roso M, Modesti M. Polymers for Advanced Technologies, 22: 1518 (2011)

200. Tomova D, Kressler J, Radusch HJ. Polymer, 41(21): 7773 (2000)

Página intencionadamente en blanco

Capítulo 2

Piezoresistive response of carbon nanotubes-polyamides composites processed by extrusion

Página intencionadamente en blanco

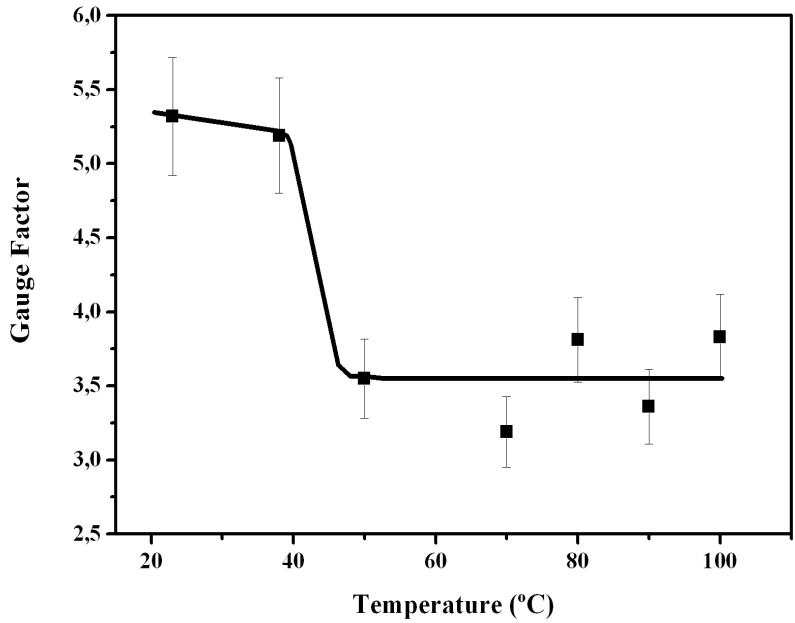

Estudio de la piezoresistividad de nanocompuestos CNT/poliamidas en función de la cantidad de CNT, del ratio poliamida 66 (PA66)/poliamida 6 (PA6) y de la masterbatch utilizada para incorporar los CNT en los nanocompuestos.

Este capítulo está basado en la siguiente publicación:

L. Arboleda, A. Ares, M.J. Abad, A. Ferreira, P. Costa, S. Lanceros-Méndez, Piezoresistive response of carbon nanotubes-polyamides composites processed by extrusion, Journal of Polymer Research, 20, p. 326-337 (2013)

Página intencionadamente en blanco

2.1. Introduction

Most polymers are known for their excellent insulating properties. Nevertheless, increasing number of applications demand from these materials dissipative or conductive characteristics. In this way, intrinsic conductive polymers and conductive composites based on conductive fillers such as carbon nanotubes (CNTs) and polymer matrices have been developed as functional components in the manufacture of sensors, microelectrodes, electromagnetic shielding, electroconductive rubbers and electrostatically paintable materials, among others [1].

Enhanced conductivity in polymers can be thus achieved either using inherently conductive polymers or adding electrical conductive fillers to the polymer matrix. Polyaniline, polypyrrole or polythiophene are, among others, inherently conductive polymers due to their conjugated π-electron system [2]. With these materials, transparent electrical conductive polymer films have been achieved, which are widely used, for example, in organic solar cells [3]. The main drawbacks of these materials are their high prices, the difficulties in melt compounding due to nonmeltability combined with thermal degradation, and their poor long-term stability.

In a second approach, electrical conductive fillers are incorporated in the polymer matrix. Above certain filler content, the electrical percolation threshold is achieved at which the conductive filler particles form electrical pathways through the polymer matrix. As conductive fillers, metal powders and carbon based additives are quite commonly used in industry [4].

Within this family, carbon nanotubes (CNTs) are known to produce composites with superior electrical and mechanical properties when compared to other carbon allotropes such as carbon black (CB) or carbon nanofibers (CNF) [5]. Strong increases in electrical conductivity and mechanical properties can be obtained in polymer nanocomposites with CNT concentrations below 5 wt.% [6-8].

Electrical, thermal and mechanical properties of the composites are affected both by the characteristics of the CNT and also by the processing technique used to prepare the polymer composite [9]. Effective use of the full potential of nanotubes to enhance the electrical conductivity of polymer composites depends primarily on the ability to disperse the nanotubes in the polymer matrix. Due to intermolecular van der Waals interactions and entanglement

between the nanotubes, destruction of primary agglomerates is not easily obtained [10].

Several methods have been used to solve this problem and, for example, in situ-polymerization is a method to generate composites with well-dispersed nanotubes [11-12].

However, this and similar approaches are not industrial-scale technically feasible solutions. Instead, if the composites are prepared using the melt mixing method, the results obtained can be easily scale up to an industrial level. In that case, the number and size of primary agglomerates can be minimized by appropriate application of shear during melt mixing [13-15]. Thus, it has been proven for many systems such as polycarbonate (PC) filled with multiwalled carbon nanotubes (MWCNT) that the processing by extrusion or injection moulding [16-17], as well as the post mixing processing (e.g., sample manufacture) [18-19] strongly influences the final properties of the composite, since the processing parameters influence the characteristics of the CNT network.

Usually, low electrical resistivity values of the composite are related to a more perfect conductive filler network formation related to an appropriate dispersion of CNTs or CNT clusters into the polymer matrix. A complete characterization of this network is quite difficult. Large aggregates resulting from non-dispersed primary agglomerates formed during inappropriate mixing can be observed by optical light microscopy (LM) [20] or scanning electron microscopy (SEM) [21]. Nevertheless, to properly examine CNT dispersion at the submicron scale and polymer-CNT interface, transmission electron microscopy (TEM) is commonly necessary, despite the drawbacks of not allowing a complete visualization of the complex three-dimensional structure of the individual nanotubes or their aggregates [10] by showing just a quite small section of the composite.

In recent years, CNT/polymer composites are gaining attention for smart materials applications [22-24] and in particular for the development for piezoresistive sensors for structural health monitoring systems [22,23,25], among others [26]. Several matrix such as thermoplastic poly(vinylidene fluoride) [27] and polymethylmethacrylate (PMMA) [24], thermoplastic elastomers such as silicone rubber or tri-block copolymer styrene-butadiene-styrene (SBS) [28,26] and epoxy resins [21], composites with CNT or carbon nanofibers have been prepared using laboratory methods and piezoresistive properties have been obtained that indicate the suitability of the materials for strain and pressure

sensor applications. The gauge factor of these composite samples strongly depend of matrix, carbon nanofiller type and content [26, 23] reaching values up to 1.4 to 15.3 [1] for thermoplastics, 0.6 to 2.2 for epoxy resins [29] and 1 to 6 for some elastomers [1].

Polyamides (PA) are semi-crystalline polymers particularly interesting as composite matrices due to their versatility and ease of processing [30]. Polyamides are tough and have excellent sliding and wear characteristics**.** Properties vary from the hard and tough PA 66 to the soft and flexible PA 12. Depending on the type, polyamides absorb different amounts of moisture, which also affect the mechanical characteristics and electrical response [31-32].

The influence of MWCNT addition in PA6 or PA66 properties has been addressed. One part of these studies has been focused on relationships among the processing parameters used to prepare the nanocomposites (rotation speed, time and mixing temperature) and electrical properties and crystallisation behaviour of the polymer composites [30] in order to obtain lowest electrical volume resistivity. A high mixing temperature, a low rotation speed, and a high mixing time were found to be the best conditions. Moreover, MWCNTs can modify the crystallization temperature of the polyamide matrix and, consequently, its crystalline degree [33-34]. The effect of different reactive couplings or modifiers on electrical, rheological and morphological behavior of polyamide/CNT composites has been also reported [35-36].

Despite the wide bibliography with respect of carbon nanotubes-polyamides composites both in PA66 and PA6, the study of blends with different ratios of these polyamides and different CNT content has been scarcely explored, despite the potential advantages in tailoring materials properties for specific applications taken into account the different materials characteristics.

Further, for upscaling processes and industrial applications it is important where and how the nanofiller is incorporated [35]. In the case of a polymer blend the fillers can be incorporated in either of the constituent masterbatches.

Therefore, this work reports on the dispersion level, thermal behaviour, electrical conductivity and electromechanical performance of polyamides/multi-wall carbon nanotubes (PA66/PA6/MWCNT) composites processed by extrusion. Different PA66/PA6 ratios are investigated as well as different CNT contents incorporated from PA66 or PA6 masterbatches, respectively.

This work is relevant as it demonstrates the feasibility of the polymer composites for the development of piezoresistive sensors that can be processed with standard up-scalable polymer processing techniques.

2.2. Experimental

2.2.1 Materials

The polymers used in this work were polyamide PA66 (PA66 Dinalon of Repol) and PA6 (Zytel of DuPont) with a density of 1.13 g/cm^3 and 1.14 g/cm^3 and a melt flow rate of 68 and 95 g/10 min (290 ºC, 2.16 kg), respectively. A masterbatch of 15 wt.% MWCNT dispersed in PA66 and another one of 15 wt.% MWCNT dispersed in PA6 were supplied by Nanocyl, Sambrevile, Belgium, in pellets form. The polyamides used in masterbatchs are similar to the polyamides added in the extruder blends. The CNTs are characterized according to the supplier by an average diameter of 9.5 nm, an average length of 1.5 μm, a carbon purity of 90% and a surface area of 250-300 m^2/g.

2.2.2 Preparation of composites

Previous to the blending, the masterbatches and the two polyamides were dried in an oven at 110 ºC for 6 h. To prepare the different formulations, the corresponding masterbatch was diluted with different contents of PA66 and PA6 to reach the desired ratio between the polyamides and the different MWCNT contents. Then, composites with different contents of MWCNTs and different ratios of polyamides were prepared using a co-rotating twin-screw extruder (Brabender DSE 20) operating at 20 rpm, with a barrel temperature of 255-270 ºC and a die temperature of 260 ºC. All the components (virgin polyamides and masterbatch) were premixed by tumbling and fed simultaneously into the extruder. The obtained pellets were compression moulded into 2 mm plaques at 285 ºC applying a pressure of 40 bar for 10 min. Finally, the plaques were cooled down by circulating water within the press plates under a pressure of 25 bar for 5 min.

Table 1 shows the composite formulations and the MWCNT content with respect to the overall polyamide content.

PA66/PA6/CNT	PA66 (wt.%)	PA6 (wt.%)	CNT (wt.%)
50/50 (MB)/1	49.50	49.50	1
50/50 (MB)/3	48.50	48.50	3
50/50 (MB)/5	47.50	47.50	5
50/50 (MB)/7.5	46.25	46.25	7.5
75 (MB)/25/3	72.75	24.25	3
25 (MB)/75/3	24,25	72.75	3
75/25 (MB)/3	72.75	24.25	3
25/75 (MB)/3	24.25	72.75	3

Table 1 Prepared composites of PA66/PA6 with different contents of CNT, in weight. MB indicates the matrix from which the nanotubes were dispersed in each sample

2.2.3 Morphological analysis by Scanning Electron Microscopy

The composite morphology was analysed by scanning electron microscopy (SEM). For SEM analysis, some specimens were cryo-fractured in liquid nitrogen and the fracture surfaces examined using a JEOL JSM-6400 scanning electron microscope (SEM) at an accelerating voltage of 20 kV. The samples were previously sputter-coated with a thin layer of gold.

2.2.4 Thermal analysis

Thermal measurements were carried out with a differential scanning calorimeter (DSC-7, Perkin-Elmer) under nitrogen atmosphere. The samples (6-10 mg) were heated from 10 ºC to 280 °C at a heating rate of 10 °C.min^{-1}.

Heating-cooling-heating cycles were performed for the different samples. The first heating scan was used to determine the melting temperature (T_m) and the heat of melting (ΔH_m). To allow comparison between samples with different MWCNT contents, the melting enthalpies (ΔH_m) were normalized to the polyamide fraction, further, a deconvolution procedure was applied to the melting thermograms to better understand the effects of nanotubes on the crystalline phase of each polyamide type. The degree of crystallinity (X_c) was calculated with equation 1:

$$X_c = \Delta H_m * 100 / \Delta H_0 * \omega_p \quad (1)$$

where ΔH_m is the melting enthalpy of sample, ω_p, weigh fraction of the corresponding polyamide, assuming ΔH_0=230 J/g for 100% crystalline PA6 [37] and ΔH_0=190 J/g for 100% crystalline PA66 [38].

2.2.5 Electrical conductivity measurement

Direct current (DC) electrical surface resistance measurements at room temperature were performed in rectangular samples with the dimensions 70 mm x 10 mm x 2 mm with a 4 prove method with a Keithley 487 picoammeter/voltage source. Previously, two parallel rectangular gold electrodes of 6 mm x 1 mm were deposited by magnetron sputtering. Copper wires were attached to the electrodes with silver paste to ensure good electrical contact. The surface resistivity ρ_s (Ω/sq) was calculated from:

$$\rho_S = \frac{R l_e}{d_e} \quad (2)$$

where R is the surface resistance in Ω, l_e is the electrode length and d_e is the distance between electrodes.

2.2.6 Electro-mechanical characterization

The sensitivity of a piezoresistive sensor can be quantified through the gauge factor (GF), which is defined as the relative change in electrical resistance due to an applied mechanical deformation:

$$GF = \frac{dR/R}{dl/l} \quad (3)$$

where *R* is the electrical resistance of the material without deformation and *dR* is the resistance change caused by the change *dl* in length *(l)* [39]. In the surface sensing mode, the GF can be written as:

$$GF = \frac{dR/R}{\varepsilon_l} = \frac{d\rho/\rho}{\varepsilon_l} + 1 + \nu \quad (4)$$

where $dl/l = \varepsilon_l$ and ν is the Poisson modulus of the material. Equation (3) shows that two effects contribute to the gauge factor:

an intrinsic piezoresistive effect $\left(\left(d\rho/\rho\right)/\varepsilon_l\right)$ and a geometric effect $\left(1+\nu\right)$ [39].

Electro-mechanical experiments were performed under 4-point-bending mechanical solicitation (Figure 1) using a universal mechanical tests Shimadzu-AG-IS while simultaneously recording the electrical resistance variation of the samples with a Agilent 34401A multimeter. The electromechanical measures of samples were calculated using Eq. (2).

The strain, calculated from the theory of pure bending of a plate to a cylindrical surface, valid between the inner loading points (Figure 1), is given by [40]:

$$\varepsilon = \frac{3dz}{5a^2} \qquad (5)$$

Four loading and unloading cycles were performed for each sample at different z-displacements between 0.3 to 1 mm, deformation speeds between 1 to 50 mm/min and temperatures from 25 to 100 ºC. The GF value was calculated for each cycle, from the z-displacement and the electrical resistance curves, by linear regression. Finally, the average value of the GF was calculated for each sample. The calculated value of the GF for the up or down mechanical cycles was the same, unless specifically specified.

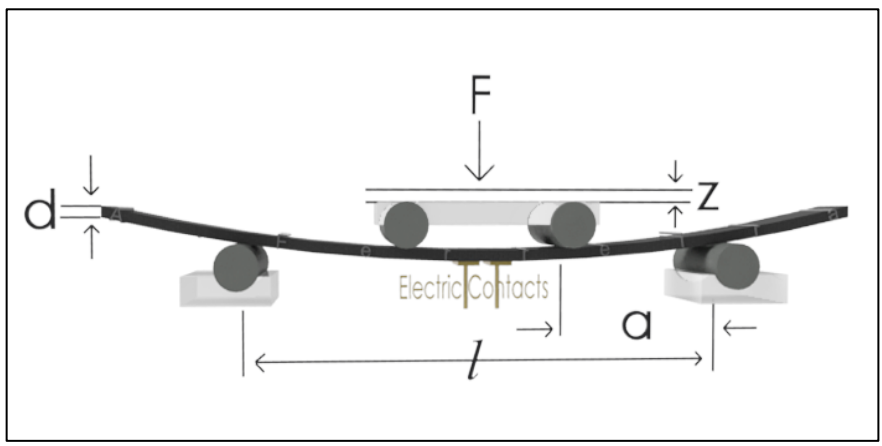

Figure 1 Schematic representation of the 4-point bending tests: *z* is the vertical displacement of the piston, *d* is the thickness of the sample, *a* is the distance between the first and the second bending points (15 mm) and *l* the distance between the lower supports (45 mm)

2.3 Results and Discussion

In the following, the main results are presented and discussed in terms of the influence of masterbatch type, filler content and polyamide ratio on the microscopic characteristics, thermal behavior and electrical and electromechanical response of the samples.

2.3.1 Morphological characteristics

Figure 2 shows the SEM images of composites with two different masterbatches (PA6 and PA66), different polyamide ratio but with the same concentration of filler (3 wt.% CNT). A similar dispersion level of carbon nanotubes is obtained for all composite samples. In this way, for 50/50 (MB) and different filler contents (1% to 7.5%), Figure 2a, b and c show that the carbon nanotubes are disperse homogeneously. In a similar way, for PA66 masterbatch and different PA66/PA6 ratios and 3% filler content, figures, 2e and 2f do not show agglomerates and the nanotubes are well distributed in the composite samples.

Differences are nevertheless obtained when comparing composites with different PA66/PA6 ratios with 3 wt.% CNT, a better dispersion of fillers being reached with higher content of PA66 and using PA6 masterbatch (75/25(MB)/3) (Figure 2d). This fact is attributed to the higher melting viscosity of PA66 when compared to PA6, as it has been proven that the most effective dispersion and distribution of primary MWCNT agglomerates was obtained when using high viscosity matrices albeit this could also result in increased nanotube shortening as compared to the use of lower viscosity matrices [10]. In the present case, the pre-dispersion of MWCNT in a low viscosity matrix as PA6, avoids this drawback, as the applied shear strength is reduced during the melt mixing.

The opposite behaviour is observed in the 25(MB)/75/3 composite (Figure 2e). In this case, the nanotubes mixed from a PA66 masterbatch during extrusion are more difficultly dispersed in the polymer matrix. The higher content of PA6, with a lower melt viscosity, is not able to generate shear enough to disperse uniformly the nanotubes during the extrusion.

Comparing 2b and 2d SEM images the only and exclusively influence of PA66 content could be analysed since the masterbatch type and CNT amount is the same in the two composites. In this

case, a better dispersion in the sample with a higher content of PA66 was obtained. On the other hand, if composites with the same ratio of polyamides (75/25) and the same CNT amount, such as 2d and 2f images, are compared, the influence of masterbatch could be analysed and the better dispersion has been got when MWCNT are initially pre-dispersed in the low viscosity matrix.

a) 50/50 (MB)/1

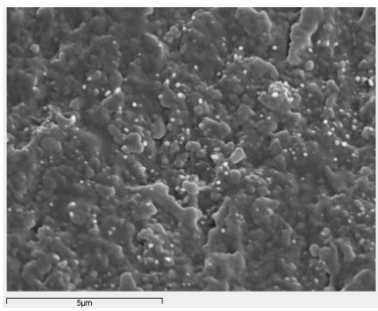

d) 75/25 (MB)/3

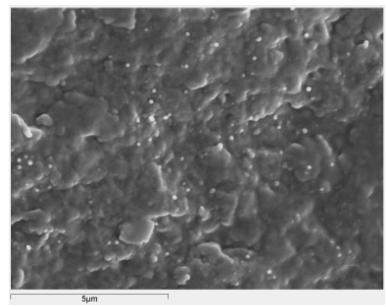

b) 50/50 (MB)/3

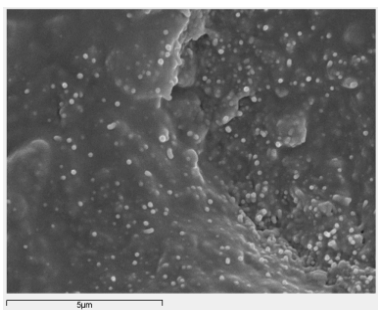

e) 25 (MB)/75/3

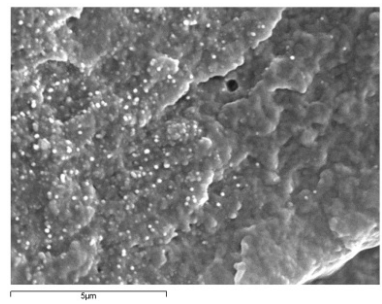

c) 50/50 (MB)/7.5

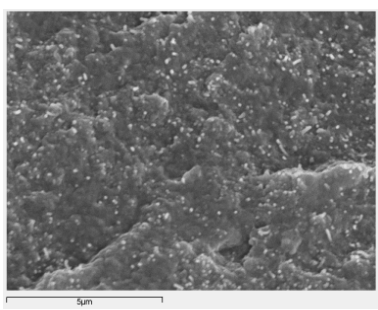

f) 75 (MB)/25/3

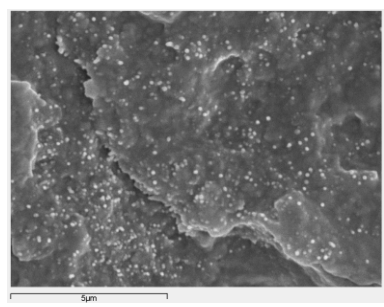

Figure 2 SEM images for several PA66/PA6 (25/75, 50/50 and 75/25) blends and CNT content (1, 3 and 7.5%)

The micrographs 2b and 2f show an intermediate behaviour. It is thus concluded that a higher content of PA66 improves the CNT dispersion, but if nanotubes are pre dispersed in a masterbatch of low viscosity, the effect can be further improved.

In conclusion, two important factors with a clear influence on observed CNT dispersion and distribution have appeared: on one side the content of PA66, the matrix with higher viscosity in the composites and on the other hand, the nanotubes must be included originally in a lower viscosity matrix. Keeping in mind the obtained electrical results detailed in section 3.3, we could suspect which one between these two aspects is more important for achieve the best conductivity values.

2.3.2 Thermal Properties

Both polyamides are miscible in the amorphous state within the range of processing temperatures [41]. However, during cooling, polyamides are able to form different crystalline structures, which could be modified by the presence of CNT [33]. In order to evaluate these aspects and their influence in the electrical and electromechanical behavior of the composites, the DSC analysis was limited to the first heating scan on samples processed in similar conditions as the ones to be used for the different characterization tests and thus with the same thermal history.

As observed in the DSC thermograms (Figure 3) and the corresponding data of Table 2 the crystallization of both polyamides depends on their ratio in the composite. Whereas for 50/50 and 25/75 ratios both polyamides form two separated melting peaks during sample cooling, for the 75/25 ratio the PA6 crystallization is inhibited by the larger proportion of PA66. A single melting peak, corresponding to the PA66 melt is shown in this sample. On the other hand, the degree of crystallization of both polyamides decreases when they are blended, the drop being more important in PA6. This fact can be attributed to the low viscosity of this polyamide, together with the miscibility with PA66 that, for certain relative concentrations of the polymers, encourages the diffusion of PA6 molecules within the PA66 matrix in the amorphous state, inhibiting the crystal formation [43].

For composites with equal quantity of the two polymers, the melting temperatures of both polyamides and the degree of crystallinity, Xc, of PA66 decreases as a function of CNT content. The drop is more significant at low loadings. Although, it has been

reported the nucleating effect of CNTs in polyamide matrices which can lead to an increase of the degree of crystallinity, in the present case this does not happen. With the combination of two polyamides with CNTs, the polymers are less able to diffuse in order to form crystalline structures. The decrease in the melting temperatures and crystalline degree with filler addition suggests that the crystallization of both polyamides is heterogeneous and the crystals formed are thinner [44].

For composites with 75/25 and 25/75 ratios, the crystallization of the polyamide in lower proportion is inhibited by the presence of the fillers. The melting thermograms show thus a single peak corresponding to the polyamide in the larger quantity (Figure 3). This behaviour seems to be related to the crystallization kinetic [44]. The low nanotube content (3 wt.%) encourages the crystals growth in the dominant polyamide. On the other hand, the crystallization of the other polyamide would be more difficult since it is diluted on the whole material as a secondary phase.

When the polyamide ratio is 50/50, the growth of crystals of both polyamides is affected by the presence of crystals of the other one. The growth of one limiting the growth of the other one. Because of this, the degree of crystallinity and the melting temperatures are lower than when one or the other polyamide is dominant in the composite. This effect is more important for PA6 as it crystallizes at lower temperatures, when PA66 is already crystallized.

Finally, the observed behaviour appears to be independent of the masterbatch used to disperse the nanotubes. The only difference was observed in the 25/75(MB)/3 sample, which displays a double peak when the CNTs are mixed from a PA6 masterbatch with respect to its twin sample (25(MB)/75/3), using a PA66 masterbatch. Again, differences in viscosity of the matrices and sample morphology (as discussed earlier) are at the origin of the different species of crystals formed in this sample.

For pure polyamides and all composites, the melting properties are summarized in Table 2.

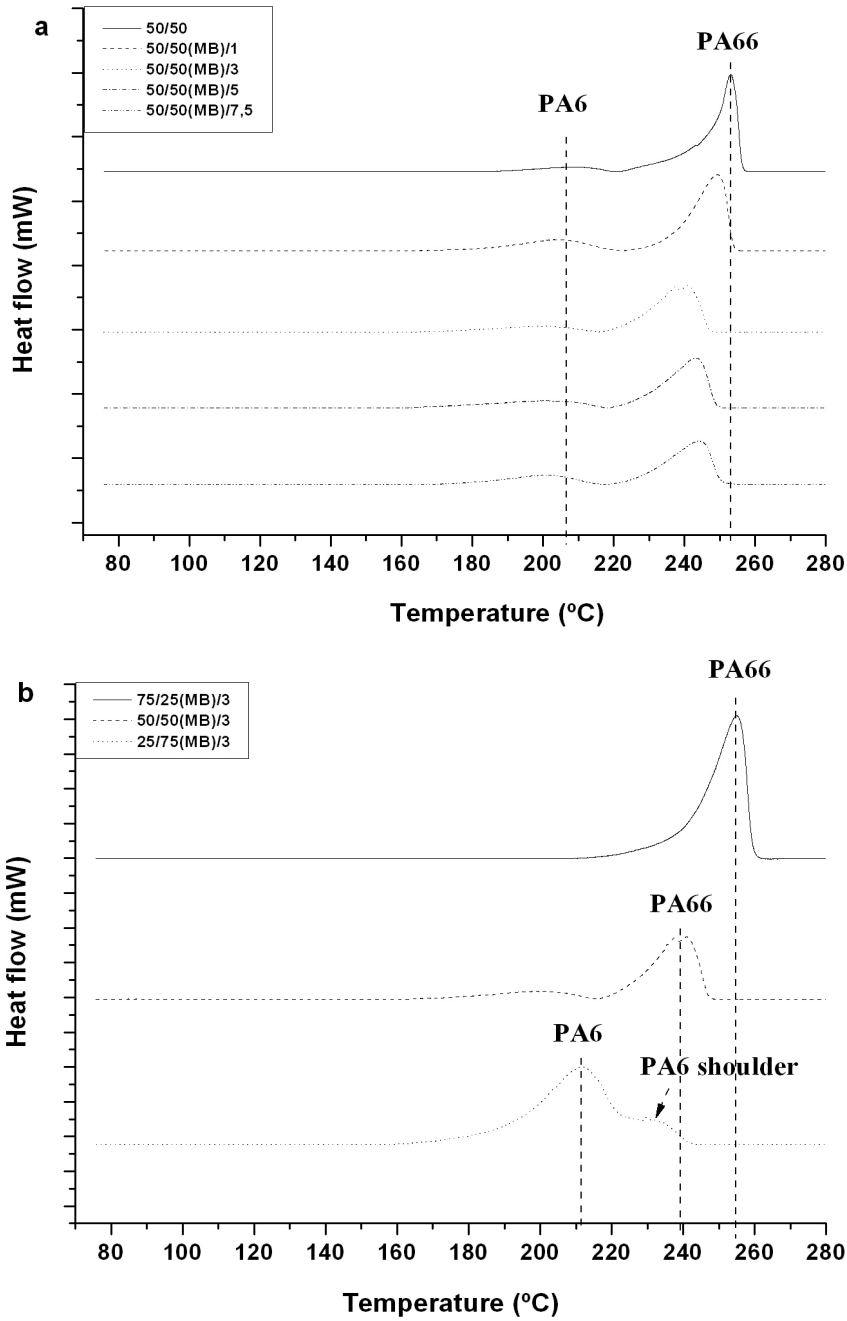

Figure 3 DSC scans of composites samples for a) PA66/PA6 (50/50) for CNT content up to 7.5%, and b) PA66/6 for 25/75, 50/50 and 75/25 ratios with 3% CNT

PA66/PA6/CNT	Tm_{PA6} (ºC)	ΔH_{mPA6} (J/g $_{PA6}$)	Xc_{PA6} (%)	Tm_{PA66} (ºC)	ΔH_{mPA66} (J/g $_{PA66}$)	Xc_{PA66} (%)	R^2
PA6	217.6	75.9	33.0	-	-	-	-
PA66	-	-	-	258.9	91.5	48.2	-
50/50	206.8	14.6	6.3	252.0	101.2	53.3	0.961
50/50(MB)/1	202.0	25.4	11.0	247.5	87.7	46.2	0.930
50/50(MB)/3	195.3	15.5	6.7	237.9 (240.9)	68.4	36.0	0.932
50/50(MB)/5	196.2	27.4	11.9	240.6	66.3	34.9	0.982
50/50(MB)/7.5	198.5	21.8	9.5	241.9	65.5	34.5	0.931
75/25	207.1	80.8	35.1	253.8	77.2	40.6	0.898
75(MB)/25/3	-	-	-	248.6	82.1	43.2	0.908
75/25(MB)/3	-	-	-	252.7	84.5	44.5	0.912
25/75	218.2	33.5	14.6	247.9	83.2	43.8	0.938
25(MB)/75/3	214.1	75.5	32.8	-	-	-	0.957
25/75(MB)/3	210.5(*229.7)	105.2	45.7	-	-	-	0.983

* **PA6 shoulder**

Table 2 Melting properties of PA6 and Pa66 for the different composites samples. R^2 is the regression coefficient obtained for the fitting

2.3.3 Electrical Properties

The composites with masterbatch PA6 with different PA66/PA6 ratios and CNT contents are shown in figure 4a. The electrical conductivity increases with CNT content for the three PA ratios, 75/25, 50/50 and 25/75 and the conductivity values also increase with increasing PA66 content in the composites. The presence of PA66 also decreases percolation threshold in the composites

samples from 3 wt.% CNT for the 25/75 ratio composites to 2% CNT in the composites with 75/25 ratio.

Figure 4b shows the electrical behaviour for the CNT composites obtained from PA66 masterbatch. The trend in conductivity with different PA66/PA6 ratios is similar to the one obtained for the PA6 masterbatch, but comparing the same CNT quantities; the values of the electrical conductivity are lower.

The explanation for this behavior is related with the differences in CNT dispersion observed (Figure 2). As previously stated, the nanocomposite with 75/25 polyamide ratio using PA6 masterbatch, results in the best dispersion of CNT in the polyamide matrix, due to the combination of higher quantity of PA66 (with high melt viscosity) and CNT pre-dispersed in PA6 masterbatch (with lower melt viscosity), and this better dispersion of the CNT improves the electrical conductivity.

As previously mentioned, there are two factors which have a clear influence on nanotube dispersion and distribution: on one side the content of PA66, the matrix with higher viscosity, in the composites and, on the other hand, the fact of the nanotubes are originally included in a lower viscosity matrix. In view of the result obtained, in this case, the fact of MWCNT are predispersed in a matrix with lower viscosity is more decisive for achieve the best conductivity values.

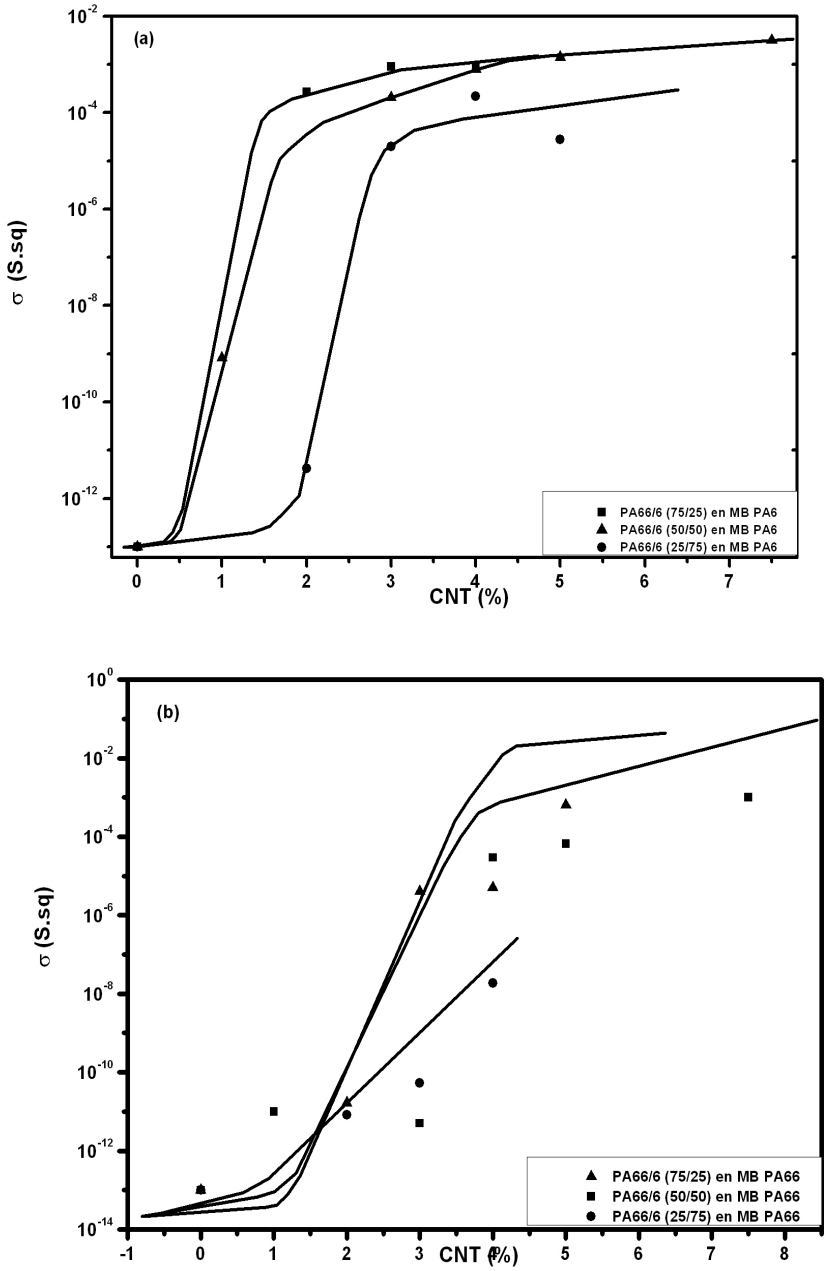

Figure 4 Electrical conductivity for composite samples with CNT up to 7.5% and polyamide ratios 75/25, 50/50 and 25/75 in masterbatch PA6 (a) and PA66 (b). The lines are for guiding the eyes

2.3.4 Piezoresistive Properties

The piezoresistive properties of the composites are measured in 4-point bending tests, studying the influence of the different masterbatch, polyamide ratio, and filler content.

Typical experiments with 4 loading-unloading mechanical cycles with simultaneous measurements of the electrical resistance variation are shown in Figure 5a. For each loading and unloading electromechanical tests a linear fit was performed for obtaining the value of the GF, as shown in figure 5b. As observed in Figure 5, proper linearity between mechanical strains and electrical resistance variation is obtained, indicating the suitability of the materials for sensor applications.

The behavior of the GF for the different composites samples is presented in figure 6.

For the composites prepared from the PA66 masterbatch the GF is higher for 75(MB)/25 samples, with a maximum value of GF~ 6, for 3% and 5% CNT (Figure 6a). For equal amounts of polyamides (50/50) (figure 6a) the GF is less than 2 for low CNT contents and increase to a maximum of ~ 3 with higher CNT loading. For the samples prepared from the PA6 masterbatch (Figure 6b), the GF is in general lower and less dependent both on the relative polyamide and filler contents than in the case of the PA66 masterbatch. It is thus concluded that the preparation of the composites from the PA66 masterbatch and the increase of PA66 content in these samples improves the electromechanical response of the composites. This fact is in contrast to the fact that the best values of the electrical conductivity are obtained for the PA6 masterbatch with large PA66 content. The explanation for this behavior is again related to the differences in CNT dispersion (Figure 2). Samples prepared from the PA6 masterbatch, show best dispersion of CNT in the polyamide matrix, which lead to better values of the conductivity but less variation of the conductive paths when the material is under mechanical deformation, the latter being at the basis of the electromechanical response and being the reason why the larger GF are typically obtained close to the percolation threshold [20, 27].

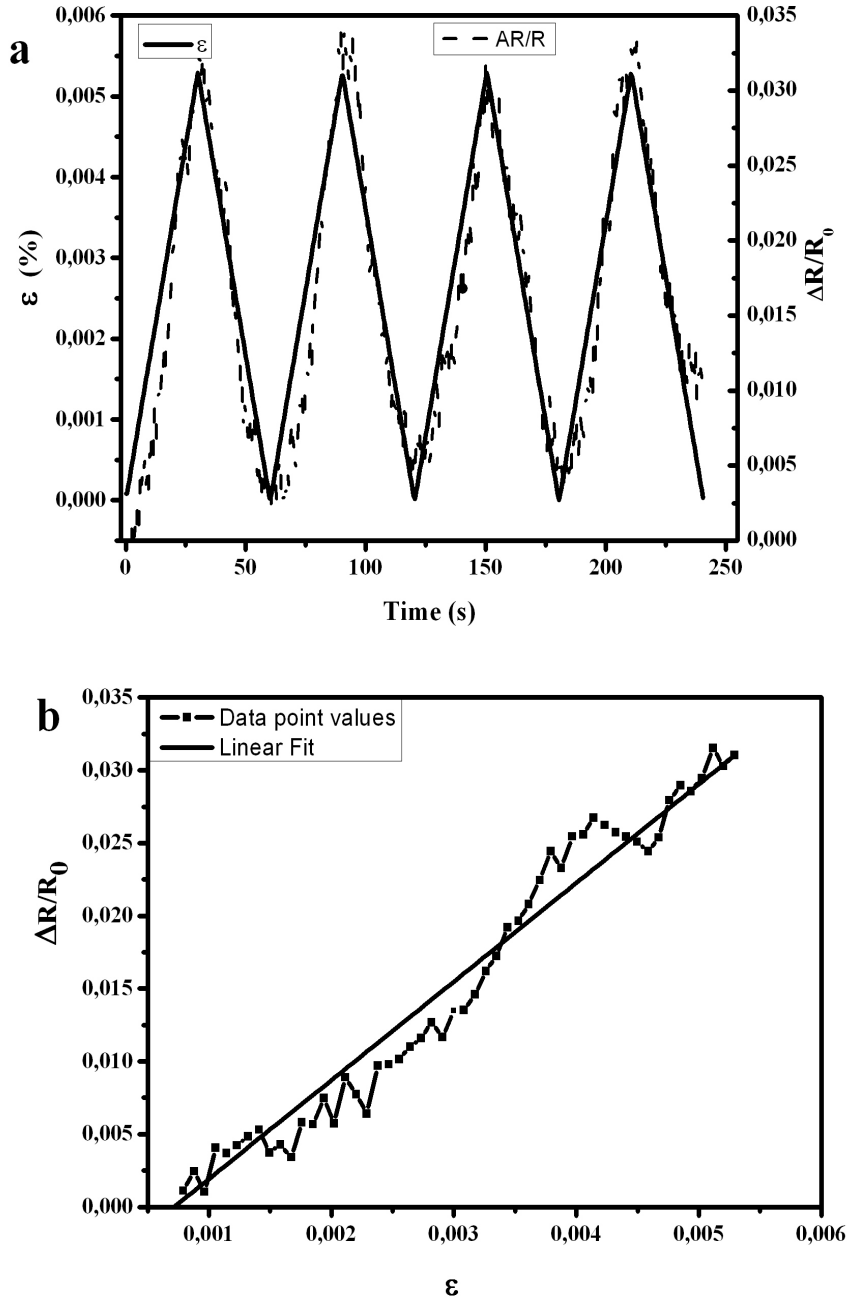

Figure 5 a) Variation of relative electrical resistance and mechanical strain over time for 75(MB)/25/3 composites during 4 loading and unloading cycles. b) Linear fit of relative electrical resistance and strain in the 75(MB)/25/3 composite

In the present case, due to the complex topology of the polymer microstructure, related to the different masterbatches and the different polymer characteristics (e.g. mechanical and crystalline characteristics of each phase within the blend), no specific trend is obtained (Figure 6). In any case, two important conclusions are drawn: first, the presence of PA66 improves the electromechanical response leading to large GF compatible with the upscale production of piezoresistive sensors, as the observed GF are among the largest obtained in the literature for thermoplastic composites due to a larger contribution of intrinsic piezoresistive response [45-48]; second, that the GF is not as strongly dependent on CNT concentration as in similar thermoplastic composites [47] and that the larger values of the GF are not related to the percolation threshold, indicating a complex blend topology and therefore CNT network characteristics.

To assess the application potential of the composites, the 75(MB)/25/3 sample was analyzed by performing electromechanical tests as a function of temperature, from room temperature to 100 ºC, for deformation speeds up to until 50 mm/min and different maximum strains.

With respect to the temperature behavior (Figure 7) the GF strongly decreases from the room temperature value above 5 to ~3.5 at 40 ºC remaining this value stable until 100 ºC. The large GF values, in the temperature range from room temperature to 100 ºC, prove the suitability of the material for applications. The decrease of the GF around 40 ºC is not related to any temperature induced transition of the polymer and thus can only be attributed to an annealing effect leading the filler network to a most favourable energy configuration and therefore less sensitive to mechanical variations.

The influence of the mechanical deformation speed on the GF is shown in Figure 8. The GF is larger for low speeds (GF≈ 6), decreasing abruptly for deformations speeds above 5 mm/min. After these deformations the GF is practically independent of deformation speed up to deformations of 50 mm/min, the GF remaining in the rage $3.3 < GF < 4.7$. This behaviour is directly related to the time response of the semicrystalline polymer [27].

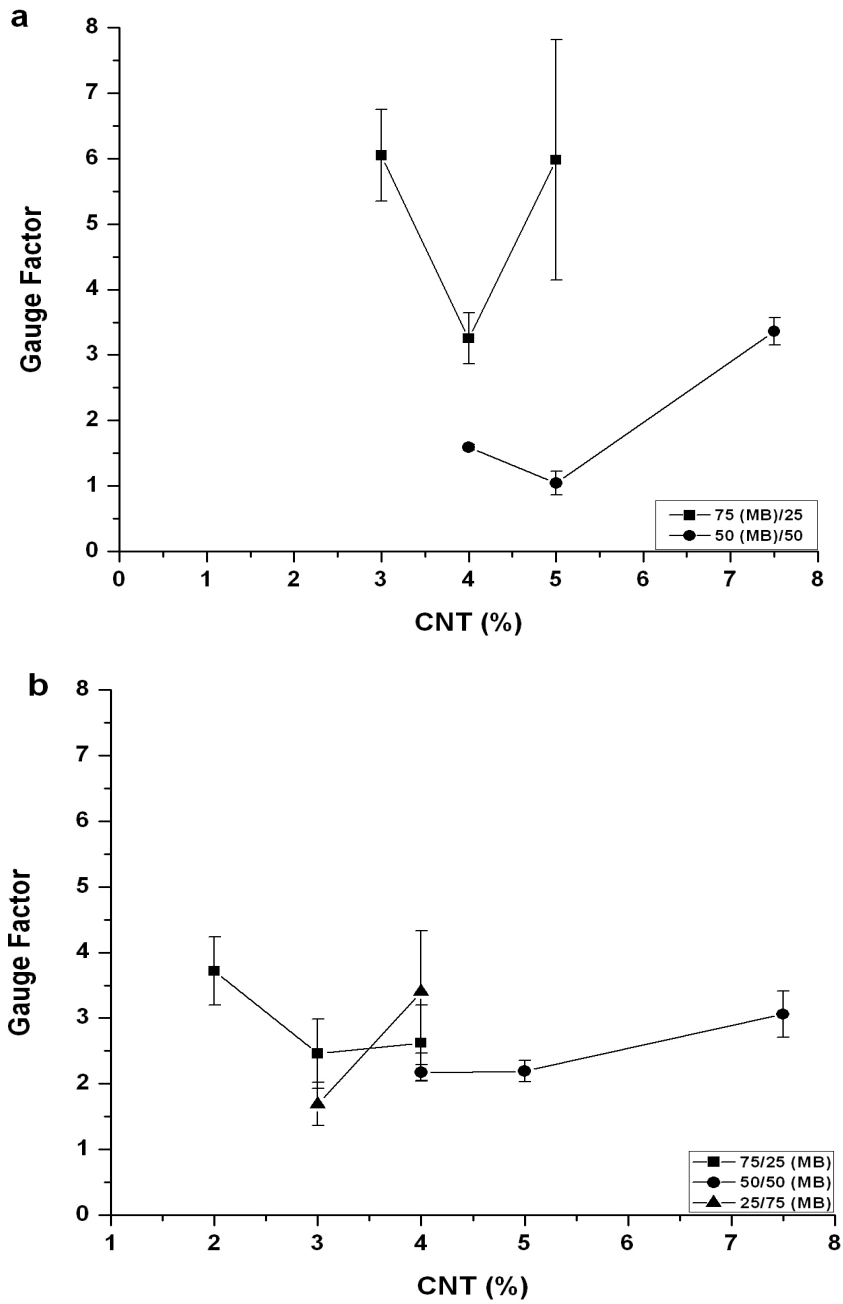

Figure 6 Gauge Factor values for composites samples: a) 50(MB)/50 and 75(MB)/25 and b) 25/75(MB), 50/50(MB) and 75/25(MB) for several CNT contents

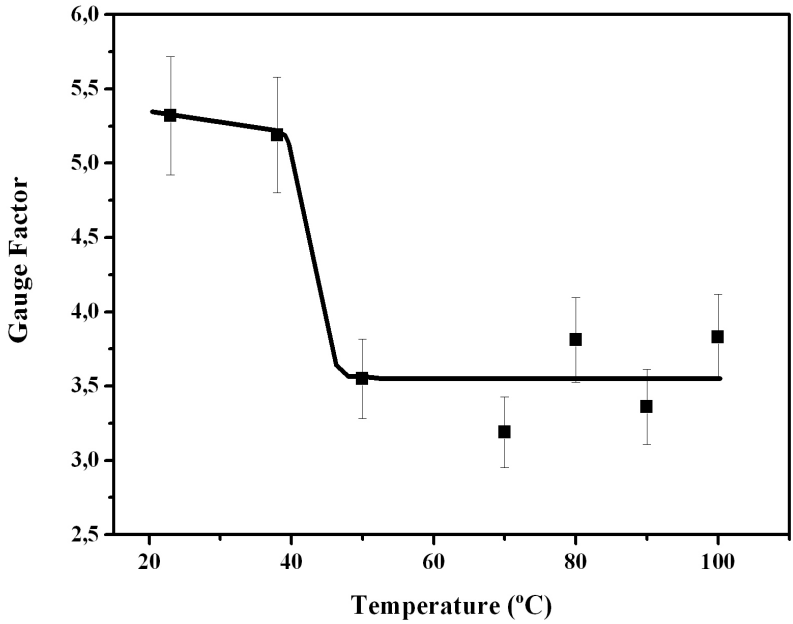

Figure 7 Temperature dependence of Gauge Factor for composite 75(MB)/25/3. The line is for guiding the eyes

The maximum deformation of the composite sample also influences the piezoresistive response, the value of the GF increasing with increasing strain. For low strains the GF value is around zero and reaches values up to 6 at 1 mm displacement, indicative of the larger variations of resistance and therefore of sensor sensitivity for increasing mechanical deformations [27,48].

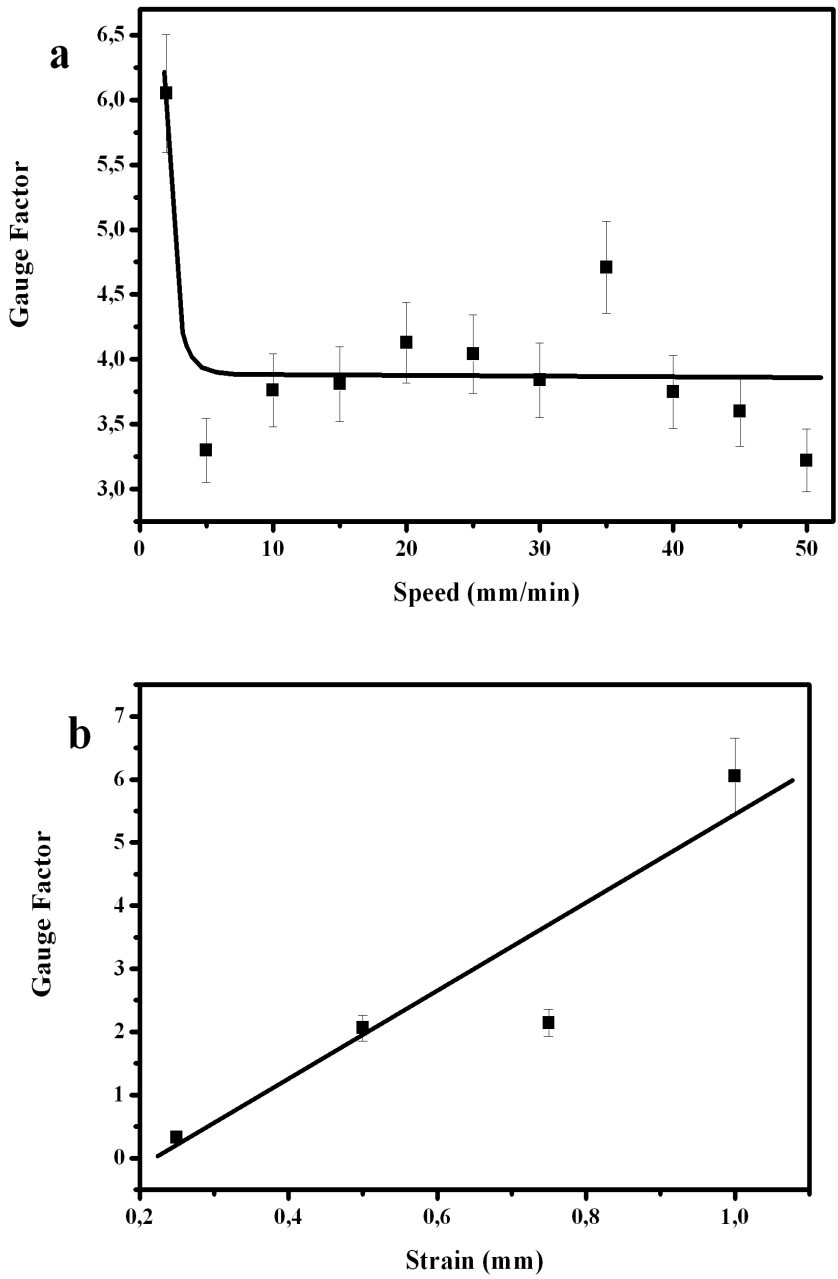

Figure 8 a) Mechanical deformation speed (fixed strain of 1 mm) and b) strain (fixed speed of 1 mm/min) dependence of Gauge Factor for the 75(MB)/25/3 composite. The lines are for guiding the eyes

2.4 Conclusions

In this work, the electrical, thermal and electromechanical behaviour of different CNT/polyamide composites were studied as function as their composition. The aim was to investigate the effect of matrix viscosity in the CNT dispersion and consequently, in the macroscopic properties of nanocomposites.

The data show that there are two factors, which clearly influence the nanotube dispersion into the polyamide matrix: the PA66/PA6 ratio and the fact of the CNTs were originally pre-dispersed in a PA66 masterbatch or in a PA6 masterbatch.

The morphologic study displays the best dispersion of MWCNTs was obtained when the polyamide ratio is rich in PA66 (the higher viscosity matrix) and the nanotubes are included from the lower viscosity masterbatch (PA6 MB). These nanocomposites also achieved the best conductivity values.

Respect to the thermal behaviour, the data show that the nanocomposites have a heterogeneous crystallization depending on the polyamide ratio and the CNT amount. General speaking, both polyamides (PA66 and PA6) can crystallize separately and can form different crystals. However, for composites with 75/25 and 25/75 polyamide ratios, the crystallization of the polyamide in lower proportion is inhibited by the presence of the fillers. When the polyamide ratio is 50/50, the crystallization of both polyamides is affected by the presence of the other one.

The piezoresistive response of CNTs/PA composites prepared with PA66 and PA6 masterbatchs has been evaluated. The GF depends on filler content and PA type concentration, being larger for composites with larger PA66 content. The GF reaches values above 6, which indicates a main contribution from intrinsic piezoresistive effect and demonstrates the suitability of the materials for sensor applications. From the processing point of view, it is concluded that the inclusion of the CNT in the PA6 masterbatch helps to improve dispersion leading to larger values of the electrical conductivity in the composites prepared with larger PA66 content. Gauge Factors, on the other hand, are better for the composites prepared from the PA66 masterbatch, the increase of PA66 content improving also the electromechanical response.

2.5. References

1. Luo S, Liu T. Carbon, 59: 315 (2013)

2. György I. Conductive polymers a new era in electrochemistry. Springer-Verlag: Berlin Heidelberg (2008)

3. Hoppe H, Sariciftci NS. Journal of Materials Research, 19 (7): 1924 (2004)

4. Zhang W, Dehghani-Sanij A, Blackburn RS. Journal of Materials Science, 42: 3408 (2007)

5. Lorenz H, Fritzsche J, Das A, Stöckelhuber KW, Jurk R, Heinrich G, Klüppel M. Composites Science and Technology, 69: 2135 (2009)

6. Du J-H. Express Polymer Letters, 1: 253 (2007)

7. Ma P-C, Siddiqui NA, Marom G, Kim J-K. Composites Part A: Applied Science and Manufacturing 41: 1345 (2010)

8. Sahoo NG, Rana S, Cho JW, Lin L, Chan SH. Progress in Polymer Science, 35: 837 (2010)

9. Castillo FY, Socher R, Krause B, Headrick R, Grady BP, Prada-Silvy R, Pötschke P. Polymer, 52: 3835 (2011)

10. Socher R, Krause B, Müller MT, Boldt R, Pötscke P. Polymer, 53: 495 (2012)

11. Kelar K, Jurkowski B. Journal of Applied Polymer Science, 104: 3010 (2007)

12. Saeed K, Park S. Journal of Applied Polymer Science, 106: 3729 (2007)

13. Andrews R, Jacques D, Minot M, Rantell T. Macromolecular Materials and Engineering, 287: 395 (2002)

14. Hagerstrom JR, Greene SL. Electrostatic dissipating composites containing Hyperion fibril nanotubes. Commercialization of nanostructured materials conference proceedings. Miami, Florida, USA, 6 (2000)

15. Ferguson DW, Bruant EWS, Fowler HC (1998). ESD thermoplastic product offers advantages for demanding electronic applications. ANTEC conference proceedings, Atlanta, Georgia, USA: Society of Plastics Engineers: 1219 (1998)

16. Pötschke P, Dudkin SM, Alig I. Polymer, 44: 5023 (2003)

17. Mack C, Sathyanarayana S, Weiss P, Mikonsaari I, Hübner C, Henning F, Elsner P. Materials Science and Engineering, 40: 1 (2012)

18. Pegel S, Pötschke P, Petzold G, Alig I, Dudkin SM, Lellinger D. Polymer, 49: 974 (2008)

19. Villmow T, Pegel S, Pötschke P, Wagenknecht U. Composites Science and Technology, 68: 777 (2008)

20. Paleo AJ, Sencadas V, van Hattum FWJ, Lanceros-Méndez S, Ares A. Polymer Engineering and Science, 54 (1): 117 (2014)

21. Cardoso P, Klosterman D, Covas J A, van Hattum FWJ, Lanceros-Méndez S. Polymer Testing, 31: 697 (2012)

22. Xiao H, Li H, Ou J (2010). Sensors & Actuators A: Physical, 160: 87 (2010)

23. Theodosiou TC, Saravanos DA. (2010). Composites Science and Technology, 70: 1312 (2010)

24. Oliva-Avilés AI, Avilés F, Sosa V. Carbon, 49: 2989 (2011)

25. Chiacchiarelli LM, Rallini M, Monti M, Puglia D, Kenny JM, Torre L. Composites Science and Technology, 80: 73 (2013)

26. Wang ZF, Wang P, Ye XY, Jiang B. Nanotechnology, 8: 756 (2009)

27. Ferreira A, Cardoso P, Klosterman D, Covas JA, van Hattum, FWJ, Vaz F, Lanceros-Mendez S. Smart Materials and Structures, 21 (7): 75008 (2012)

28. Costa P, Silva J, Sencadas V, Simoes R, Viana JC, Lanceros-Méndez. Journal of Materials Science, 48: 1172 (2012)

29. Slobodian P. Carbon, 50: 3446 (2012)

30. Krause B, Pötschke P, Häußler L. Composites Science and Technology, 69:1505 (2009)

31. Timmaraju MV, Gnanamoorthy R, Kannan K. Composites Part B: Engineering, 42: 466 (2011)

32. Timmaraju MV, Gnanamoorthy R, Kannan K. Materials Science and Engineering: A 528: 2960 (2011)

33. Phang IY, Ma J, Shen L, Tianxi L Zhang W-D. Polymer International, 55: 71 (2006)

34. Logakis E, Pandis C, Peoglos V, Pissis P, Stergiou C, Pionteck J, Pötschke P, Micusik M, Omastova M. Journal of Polymer Science Part B: Polymer Physics, 47: 764 (2009)

35. Bose S, Bhattacharyya AR, Kulkarni AR, Pötschke P. Composites Science and Technology, 69: 365 (2009)

36. Bhattacharyya AR, Pötschke P. Macromolecular Symposia, 233: 161 (2006)

37. Edith Turi A. Thermal characterization of polymeric materials. Polytechnic University Brooklyn, New York, Vol. 2 (1997)

38. Menczel JD, Jaffe M, Bessey WE. Thermal characterization of polymeric material. San Diego: Academic Press (1997)

39. Beeby S, Ensell G, Kraft M, White N. MEMS Mechanical Sensors, Artech House, Boston (2004)

40. Zhu S, Chung DDL. Carbon, 45:1606 (2007)

41. Tomova D, Kressler J, Radusch H. Polymer, 41 (21): 7773 (2000)

42. Li Y, Liu H, Zhang Y, Yang G. Journal of Applied Polymer Science, 98: 2172 (2005)

43. Caamaño C, Grady B, Resasco DE. Carbon, 50: 3694 (2012)

44. Hu N, Karube Y, Yan C, et al. Acta Materialia, 56: 2929 (2008)

45. Castillo-Castro T del, Castillo-Ortega MM, Herrera-Franco PJ. Composites Part A, 40: 1573 (2009)

46. Ferreira A., Rocha JG, Ansón-Casaos A, Martínez MT, Vaz F, Lanceros-Méndez S. Sensors and Actuators A: Physical, 178: 10 (2012)

48. Paleo AJ, van Hattum FWJ, Rocha JG, Lanceros-Méndez S. Microsystem Technologies, 18 (5): 591 (2012)

Página intencionadamente en blanco

Capítulo 3

Influence of polyamide ratio on the CNT dispersion in polyamide 66/6 blends by dilution of PA66 or PA6-MWCNT masterbatches

Página intencionadamente en blanco

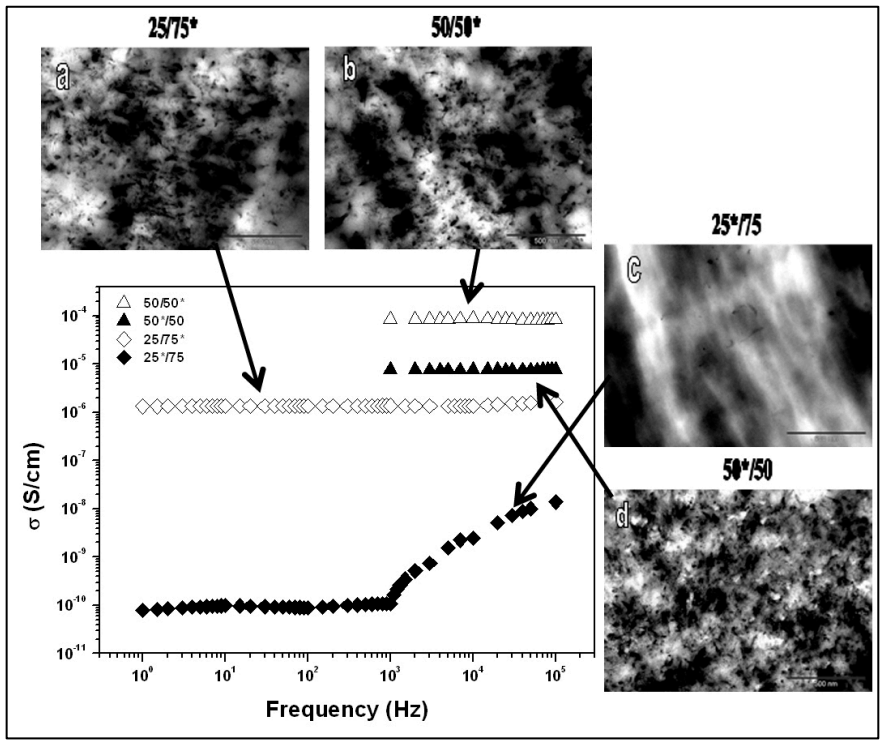

Estudio de la influencia de la masterbatch utilizada y el ratio entre la poliamida 66 y la poliamida 6 en la microestructura de nanocompuestos con un 3% en peso de CNT y las relaciones entre la microestructura y las propiedades físicas obtenidas (propiedades dieléctricas, cristalinidad y reología)

Este capítulo está basado en la siguiente publicación:

Laura Arboleda-Clemente, Ana Ares-Pernas, Xoán García, Sonia Dopico, María José Abad, Influence of polyamide ratio on the CNT dispersion in polyamide 66/6 blends by dilution of PA66 or PA6-MWCNT masterbatches, Synthetic Metals, 221, p. 134-141 (2016)

Página intencionadamente en blanco

3.1 Introduction

Dispersing conductive fillers, as carbon nanotubes (CNT), in a polymeric matrix is a relatively simple route to develop new electrically conductive polymer composites (CPCs). The targets to obtain are easy processing, low cost and obviously, tunable electrical properties. The final properties of CPCs depend on both material composition and morphology obtained. If the CPC matrix is a blend of two immiscible polymers, the material morphology is given by the polymer composition as well as the rheological properties of polymers and the processing variables [1].The addition of carbon nanotubes can also alter the morphology of immiscible blends. Recent researches [2] have proved that the nanoparticles addition can change the blend morphology in three important aspects: reduction of the domain size of the dispersed phase (compatibilizer effect), change sea-island into co-continuous morphology and phase inversion. These ones are related with changes in the viscosity ratios due to the selective distribution of nanoparticles in one polymer or another. All these variables directly affect the final properties of composites, specifically the electrical properties [3]. Since there are no general rules, which are able to predict the macroscopic behaviour, it is necessary a study of each conductive nanocomposite.

CNT dispersion in the polymer matrix seems to be a key factor to obtain the desirable final properties. This one influences greatly viscoelastic properties of CNT composites [4-6] and for this reason, nanofiller dispersion level can be evaluated from rheological studies [7-13]. To obtain high electrical conductivity, an initial dispersion of nanotubes in polymer matrix during mixing process is required. However, according to previous literature [14-16], reaggregation of well-dispersed nanotubes encourages their interconnectivity reducing the distance between the tubes to the tunnelling range and, as consequence, decreasing the filler amount required for electrical percolation. Both dispersion and re-aggregation of CNTs are controlled by diffusion mechanisms, which are related to attractive forces between polymer chains and nanotubes, as well as external forces applied during the melt-blending. Initially, the polymer chains infiltrate into the primary agglomerates, removing the CNT on their surface and reducing their size or dissolving them. This process depends on the melt viscosity of the polymer resin and the interfacial energy between CNTs and matrix. Then, the wetted CNTs are distributed within the

polymer matrix. The mixing parameters applied (shear strain and mixing time), establish the degree of nanofiller dispersion [17].

The study of CPCs obtained from CNTs and polyamide blends with different viscosities are particularly interesting and novel from both academic and industrial frameworks. The polyamides are widely used in important industrial sectors as in automotive, electronics and packaging; therefore, the success achieved could have a high socio-economic impact.

In this research, our attention is concentrated on the study of conductive polymer composites based on CNT dispersed in blends of polyamide 66 (PA66) and polyamide 6 (PA6), with different ratios. The masterbatch dilution technique was used to produce the CNT/PA66/PA6 composites by extrusion, from two masterbatchs, namely PA6/MWCNT and PA66/MWCNT. Previously, others researchers have probed that this technique is suitable to produce CNT nanocomposites with good electrical properties [18]. In contrast with other preparation methods, the nanocomposites obtained from CNT masterbatch dilution, could be produced industrially, expanding the range of potential applications.

Notwithstanding many parameters can directly influence the electrical conductivity of PA66/PA6/MWCNT composites (filler content, state of dispersion and distribution, aspect ratio, matrix crystallinity, blend morphology, etc), this work is focused on the effect of polyamide ratio and the masterbatch used on the microstructure of CNT composites. Then, an effort has been made to draw the relations between the nanocomposites microstructure and their dielectric properties, crystallization behaviour and rheological performance.

3.2 Experimental

3.2.1 Materials

Two polyamides, PA66 (PA66 Dinalon supplied by Repol) and PA6 (Zytel supplied by DuPont) were used in this study. PA66 has a density of 1.13 $g.cm^{-3}$, a Melt Flow Rate of 68 g/10 min (290°C, 2.16 kg), a melting point of 259°C and a viscosity of 332 Pa.s (290°C, 0.1 $rad.s^{-1}$). PA6 has a density of 1.14 $g.cm^{-3}$, a Melt Flow Rate of 95 g/10 min (290°C, 2.16 kg), a melting point of 218°C and a viscosity of 181 Pa.s (290°C, 0.1 $rad.s^{-1}$). To prepare the nanocomposites, CNT were dispersed into the polyamide blend from two different masterbatches supplied by Nanocyl (Nanocyl S.A**,** Sambrevile, Belgium). Plasticyl PA1501contents 15 wt.% of MWCNT (NC7000, Nanocyl) pre-dispersed in PA66 (PA66 Dinalon,

Repol) and Plasticyl PA1503, 15 wt.% of MWCNT (NC7000, Nanocyl) pre-dispersed in PA6 (Zytel, DuPont).

MWCNTs, characterized according to the supplier, have an average diameter of 9.5 nm, a length of 1.5 μm, a carbon purity of 90% and a surface area of 250-300 $m^2.g^{-1}$.

3.2.2 Preparation of composites

PA66/PA6/CNT	PA66 (%.wt)	PA6 (%.wt)	CNT from PA66 masterbach (%.wt)	CNT from PA6 masterbach (%.wt)
0/100*	0	97	-	3
100*/0	97	0	3	-
25/75	25	75	-	-
50/50	50	50	-	-
25/75*	24.25	72.75	-	3
50/50*	48.50	48.50	-	3
25*/75	24.25	72.75	3	-
50*/50	48.50	48.50	3	-

Table 1 Binary blends, binary composites and ternary composites of PA66/PA6/MWCNT

Table 1 shows the composite formulations with different PA66/PA6 ratios and a fixed content of 3 wt.% MWCNT respect the overall polyamide amount. In a previous study, it was demonstrated that electrical threshold is lower than this CNT amount and for this reason, the conductive network should be formed in all nanocomposites [19]. Before extrusion, masterbatches and pristine polyamides were dried in an oven at 110°C for 6 h. Then, the different composites were extruded using a co-rotating twin-screw extruder (Brabender DSE 20) operating at 20 rpm, with a temperature profile between 255-270°C. All the components were premixed by tumbling and then, fed simultaneously into the extruder. For dielectrical measurements the obtained pellets were compression moulded into square plaques with an area of 25 mm x 25 mm and thickness around 0.5 mm at 285°C applying a pressure of 40 bar for 5 min. Finally, the plaques were rapidly cooled down by circulating water under a pressure of 25 bar for 1 min. For a better understanding of the relationships between electrical

behaviour and composite morphology, the samples used in morphological study were moulded in the same conditions.

For rheological tests, the samples were shaped into discs by compression moulding at 285°C applying a pressure of 40 bar for 5 min.

3.2.3 Characterization

The state of CNT macrodispersion in the composites was studied and quantified using a light transmission microscopy (Leica DM2500 microscope combined with a DFC295 camera). Thin sections of 5 μm thickness of each sample were cut from compression moulded samples with a microtome (Microm HM 355, Thermo Fisher Scientific) at room temperature.

The agglomerate area ratio A/A_0 was determined from the micrographs by calculating the ratio of the area *A* of remaining agglomerates to the total area of the micrograph A_0 (~ 4.2x10^6 μm^2) using the software Image J Version 1.49K (General Public License). Agglomerates larger than 50 μm^2 were taken into account for this calculation. For the quantification of the mean values and their standard deviations at least five cuts for each sample were analysed. The mean size of the agglomerates ($\bar{A}$) in each sample was also calculated using the same software.

An analytical TEM (JEOL JEM 1010) was used to investigate the CNT network formation in the different composites at nanoscale. Ultra-thin sections with a thickness of 70 nm were cut, at room temperature, from compression moulded samples.

The rheological measurements were performed using a controlled strain rheometer (ARES, TA Instruments) with parallel-plate geometry (25 mm diameter, 1 mm gap) at 290°C. The complex viscosity (η^*), storage modulus (G'), and loss modulus (G'') were measured as a function of frequency (ω). The rheological tests were performed in the linear viscoelastic region (LVE). This linear viscoelastic region was determined previously from a strain sweep test. The frequency sweep measurements were set up in the frequency range 1x10^{-1} to 10^2 rad.s^{-1}.

The dielectric measurements were performed on the compression moulded samples at room temperature in the frequency range between 1 to 10^5 Hz with an applied signal of 1V using a dielectric analyzer DEA 2970 (TA Instruments) (This model works in a range from 0.003 Hz to 100 kHz). Sensor parallel plate mode has been used. The ac conductivity was calculated by the software of the equipment with these dielectric measurements.

Thermal measurements were carried out with a differential scanning calorimeter (DSC-7, Perkin-Elmer) under nitrogen atmosphere. The samples (6-10 mg) were heated from 10°C to 280°C at a rate of 10°C.min^{-1} and mantained 5 min. at 280°C to erase their thermal history. Finally, they were cooled to 10 °C at a rate of 10 °C.min^{-1}.

3.3 Results and discussion

3.3.1 Morphology characterization

The objective of this section is to describe and quantify the dispersion of individual nanotubes together with the distribution of their agglomerates or clusters into the polymeric matrices. These outcomes strongly influence the final filler network and therefore, the electrical properties of nanocomposites. With this general purpose, two microscopy techniques were used: Light Microscopy (LM) and Transmission Electronic Microscopy (TEM).

3.3.1.1 Light microscopy

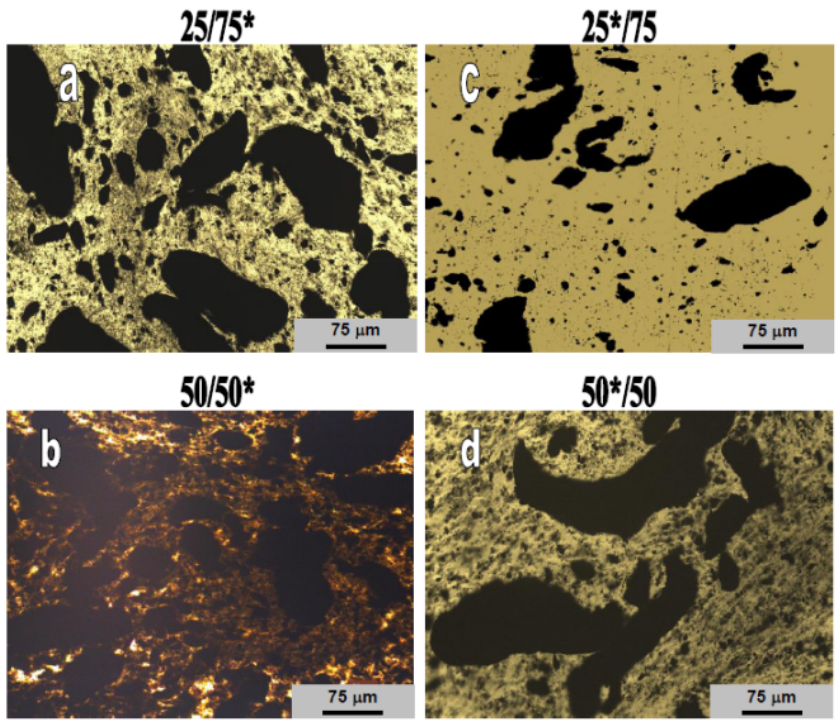

Figure 1 Ligth microscopy images of composites based on different polyamide ratio and masterbach containing 3 wt.% MWCNT

Figure 1 shows the micrographs of different nanocomposites after compression moulding obtained by light microscopy. A large amount of self-organized MWCNT agglomerates was observed in all samples.

To quantify the dispersion of nanotubes, the agglomerate area ratio A/A_0 and the mean size of the agglomerates ($\bar{A}$) were estimated (Table 2). In view of the data, it seems that the composites show an incomplete CNT dispersion, leading to high agglomerate area ratios.

PA66/PA6	$A/A_0(\%)$	$\bar{A}$**(μm²)**	σ***(S.cm^{-1})**	**ω_c; G_c**
25/75	-	**-**	**-**	G'' > G'
50/50	-	**-**	**-**	G'' > G'
25/75*	14.9 ± 2.0	1593 ± 595	1.6 x 10^{-6}	8 ; 5612
50/50*	38.5 ± 3.2	2117 ± 690	8.3 x 10^{-5}	11 ; 4872
25*/75	2.5 ± 0.9	438 ± 158	1.4 x 10^{-8}	14 ;7340
50*/50	34.4 ± 0.9	2488 ± 869	7.7 x 10^{-6}	17 ; 5834

Table 2 Agglomerate area ratio A/A_0, agglomerate $\bar{A}$, conductivity (*at 100000 Hz) and G'/G'' crossover points in composites.

The 50/50 PA66/PA6 nanocomposites have the highest A/A_0 ratios together with the greatest sizes of agglomerates, showing that these composites present the worst state of nanotubes dispersion. This fact is independent of the type of masterbatch used. The micrographs of these nanocomposites (Figure 1b and 1d) display many and big agglomerates although apparently well distributed within the polymer matrix.

For the other two nanocomposites (25/75 PA66/PA6), A/A_0 ratios are lower and smaller agglomerates are present. The composite prepared from PA66 masterbatch presents lowest A/A_0 ratio and $\bar{A}$ ($A/A_0 \approx 2.5\%$ and $\bar{A} \approx 400\mu m^2$). Spacing small agglomerates and large areas without nanotubes are mainly present and therefore distances between nanotubes are higher. This morphology is the logical outcome of the increased rupture of larger agglomerates as a result of that the CNTs are included in PA66, a more viscous matrix.

3.3.1.2 Transmission electron microscopy (TEM)

In order to get more information about the microstructures of MWCNT composites, the dispersion and distribution of nanotubes, transmission electron microscopy was used in this study. Figure 2 shows the most representative TEM images, although the following discussion is based also on a variety of micrographs taken from the samples. All nanocomposites show isolated nanotubes and CNT bundles.

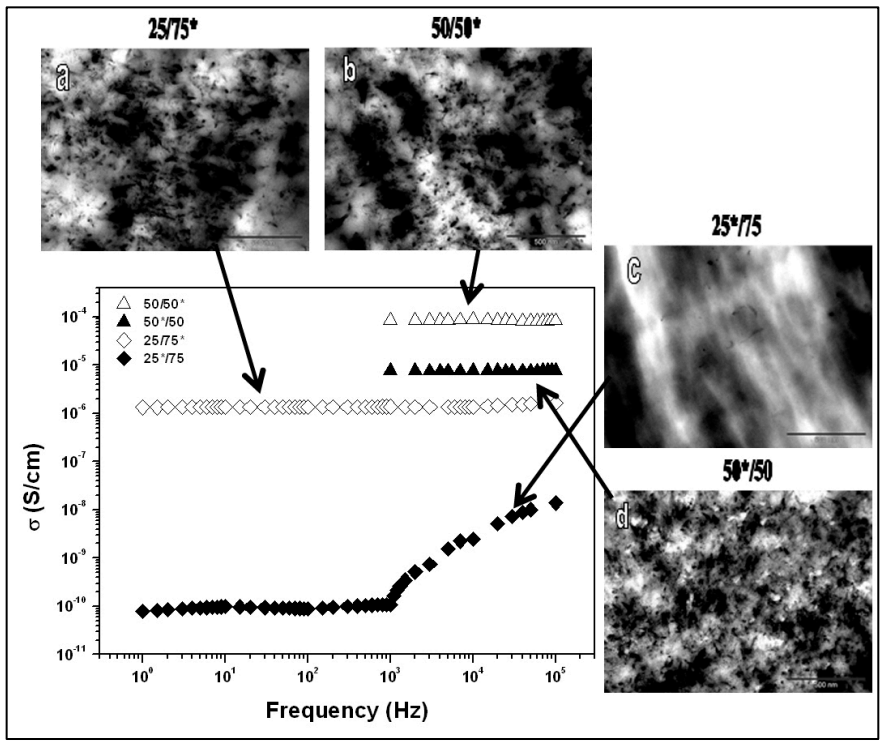

Figure 2 Electrical conductivity and morphological characterization by TEM of PA66/PA6/MWCNT composites (scale bar 500 nm)

The distribution of, MWCNT clusters and isolated nanotubes at the nanoscale is homogeneous and quite similar in 50/50 PA66/PA6 composites, but show clear differences with respect to the others samples. In Figure 2b and 2d, small nanotubes bundles are finely distributed in the matrix and partially connected, which eventually forms a dense 3D interconnected network of nanoparticles. This network can facilitate electrons flow and significantly boost the electrical conductivity, as other authors also

pointed out [20-21]. As it previously observed (in LM characterization), the morphology at nanoscale is independent of the masterbatch used.

Contrary to the observed in the above ratio, the 25/75 PA66/PA6 composites present differences in the distribution and size of CNT clusters depending of the masterbatch used. This effect is more obvious in Figure 2c (nanocomposite prepared from PA66 masterbatch), where very small clusters and single isolated nanotubes were observed but many areas without MWCNT are mainly present.

In conclusion, the better CNT distribution has been got in CNT composites with a PA66/PA6 ratio of 50/50. In 25*/75 composite (CNT predispersed in PA66), the CNT agglomerates are smaller and not uniformly distributed where even, at the nanoscale, nanotubes free areas are observed.

3.3.2 Rheological characterization

The morphological behaviour of nanocomposites could be related to the differences in their rheological properties. Viscosity values of different nanocomposites and polyamide blends are plotted in Figure 3a. Binary blends show a Newtonian behaviour. As expected, PA6 has a minor viscosity than PA 66 so that, the viscosity of 50/50 PA66/PA6 is higher than those of 25/75 blend. Binary blends display minor viscosity than matrices; this is a clear indicative of the immiscibility between them.

Besides, all composites show shear-thinning behaviour as previously observed in other filled melts [22-27]. When a 3% of nanotubes are included, viscosity increases with respect to PA66/PA6 blends. Anyway, the differences in viscosity among nanocomposites are not significant.

Regarding storage modulus behaviour of composites (Figure 3b), it increases with CNT amount and trends to be frequency-independent. This particular response with CNT addition is associated with the transition from liquid-like to solid-like viscoelastic behaviour (rheological percolation effect) indicating the formation of interconnected structures. This effect is more pronounced in G' than in G'' (not showed here). At low frequencies range, G' is slightly greater in 25*/75 composite. This behaviour could be related to a better dispersion of nanotubes in polyamide blend than in the other ones. This, previously reported by other authors [28], is also consistent with the fact that CNT agglomerates

are smaller in 25*/75 composite, as was proved from morphologic data.

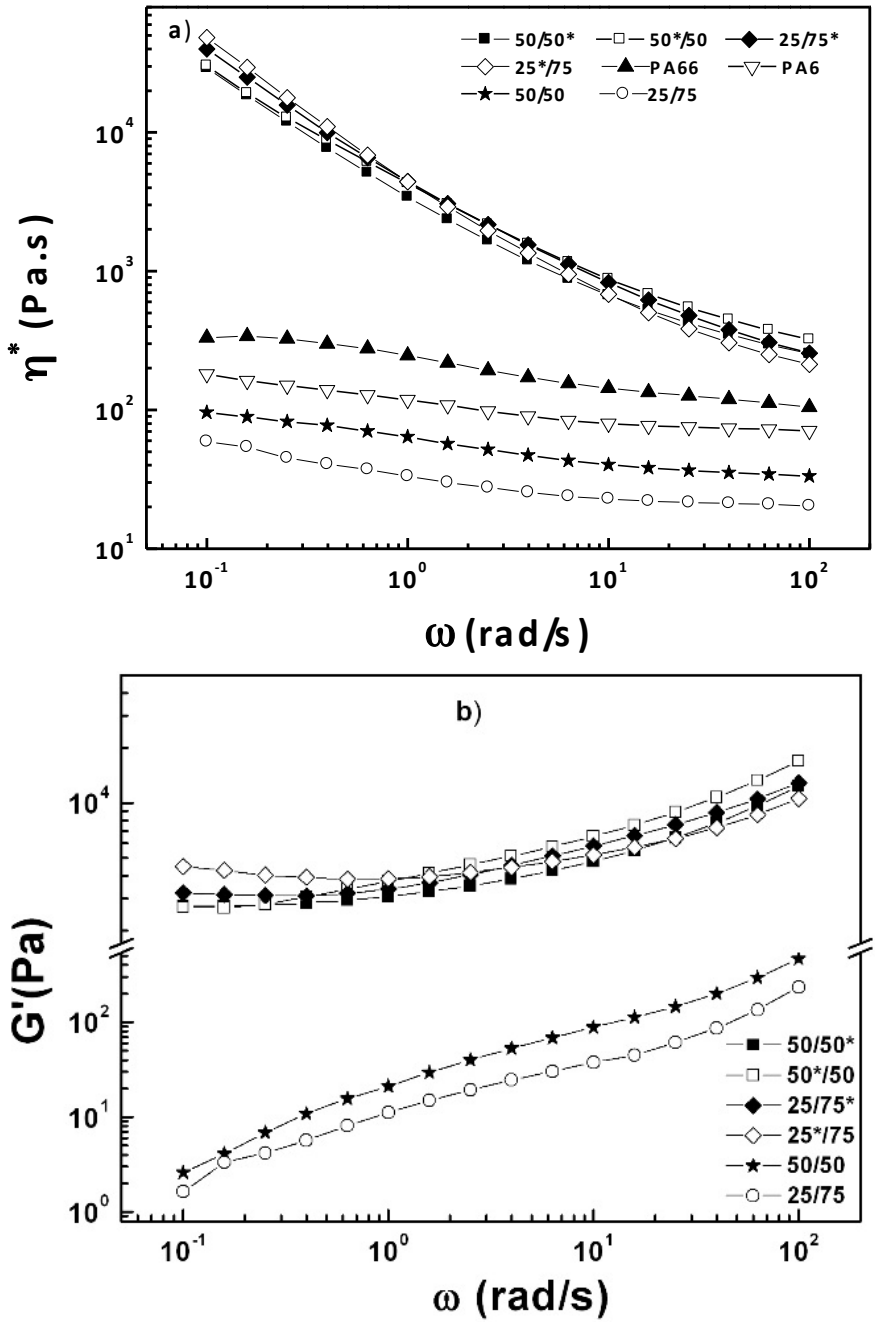

Figure 3 a) Complex viscosity (η*) for polyamides, binary blends, and composites; b) Storage modulus (G') for binary blends and composites

Figure 4a presents the storage modulus of PA66/PA6/MWCNT composites relative to the storage modulus of their corresponding binary blends. Adding CNTs, the storage modulus in both polyamide ratios, enhanced respect to the pristine blends, but the increase is higher in the 25/75 PA66/PA6 composites. This behaviour could indicate a higher degree of CNT dispersion in these composites, according to it previously observed in the morphology section.

To study the changes in viscoelastic parameters, the storage modulus G' and loss modulus G'' were plotted simultaneously for nanocomposites in Figure 4b. In this plot, analogous to Cole-Cole plots used in dielectric spectroscopy [29,30], composites that appears in the left of dot line (G'>G'') are totally percolated whereas composites that appears in the right zone (G''>G') not formed interconnected structure [31]. All our nanocomposites appear in the left side indicating an interconnected structure. Only binary blends appear in the right side.

Moreover, differences in stiffness are appreciated in composites and to evaluate them, the crossover point (ω_c, G_c), the point at which curves of G' and G'' against frequency intersect are also recorded in Table 2. This point is characteristic of the transition from viscous to elastic behaviour [31-36]. For binary blends, G'' is higher than G' in all frequency range, indicating a liquid-like behaviour. For nanocomposites, a crossover point is observed in all cases. The little differences appreciated in this parameter can be related to morphology of samples. CNT composites obtained from PA66 masterbatch, present higher elastic modulus than the others and their crossover points also appear at higher frequencies, due to the fact that some CNTs remain in PA66 phase (more viscous and with a higher melting point). The crossover points shift to the lower-left side in composites processed from PA6 masterbatch (more fluid and with a lower melting point) indicating that these composites begin to elastic-like behaviour at lower frequencies [32-36]. The left-shift of crossover point is related with the formation of percolation network that occurs earlier in these composites and lead to higher polymer relaxation times.

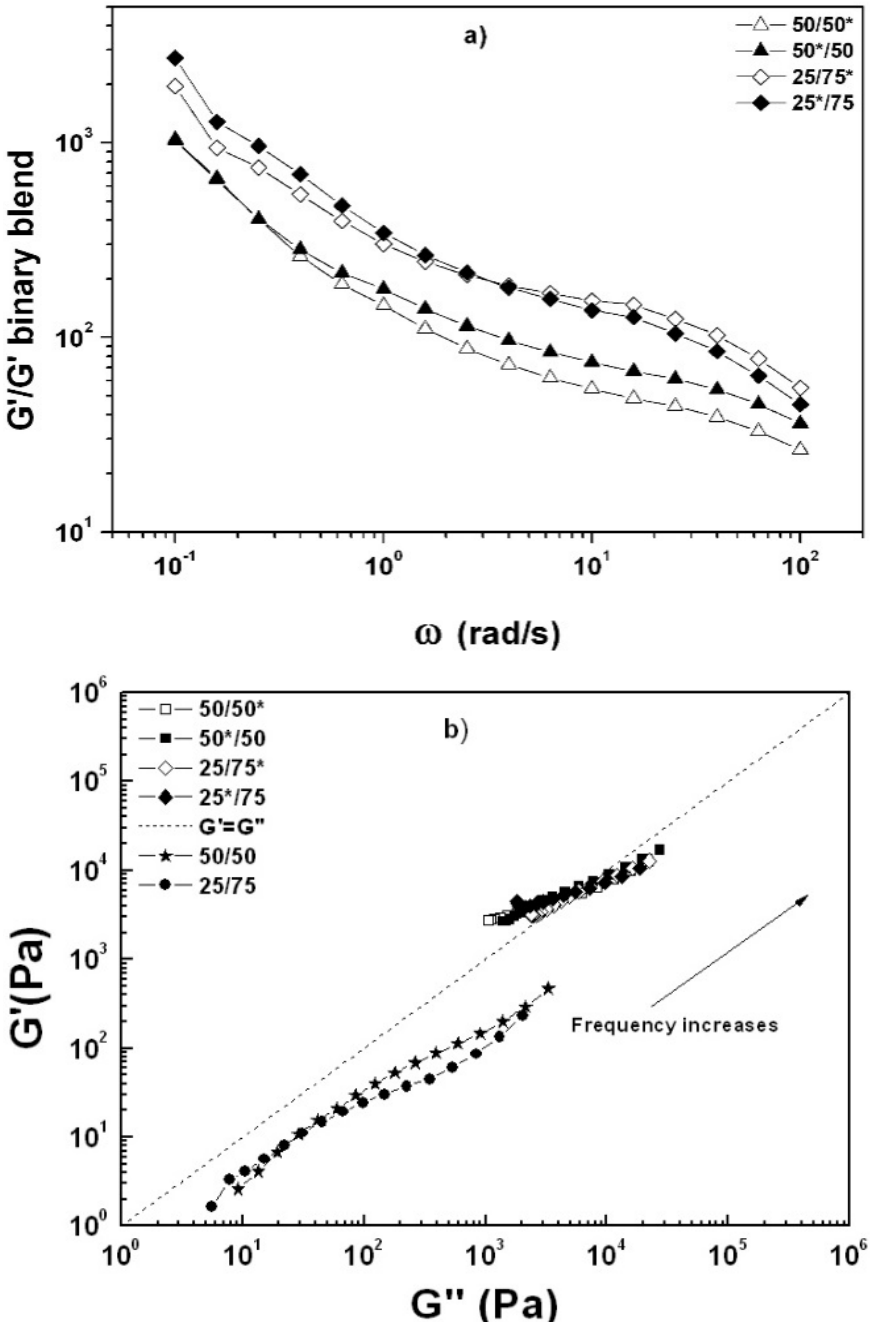

Figure 4a) Variation of relative storage modulus of PA66/PA6/MWCNT composites; b) Storage modulus (G') as function of loss modulus (G'') for binary blends and composites

3.3.3 Dielectric analysis

Dielectric properties of MWCNT composites and pristine PA66/PA6 blends were carried out in order to evaluate the frequency dependent electrical conductivity.

The conductivity data for the different nanocomposites are shown in Figure 2.

According to this picture, if nanocomposites with the same PA66/PA6 ratio are compared, ac conductivity is always greater in those which are prepared from PA6 masterbatch (open symbols). The greatest difference can be seen in the 25/75 pair where the 25/75* sample shows an increase of two orders of magnitude (at 10^5 Hz) with respect to the composite with the same ratio but prepared from the PA66 masterbatch (25*/75). It is important to point out that between these two samples take place the highest differences in the A/A_0 ratios and average sizes ($\bar{A}$) and this fact can be decisive to understand their electrical behaviour.

It is clear that in the two 50/50 PA66/PA6 composites and 25/75*, the dc plateau spreads to the whole frequency range indicating that the percolating “network-like structure” of MWCNT is already formed.

However, in the case of the 25*/75 composite, a different electrical behaviour was observed. A dc plateau, where conductivity is independent of frequency, appears below a critical frequency f_c (≈ 10^3 Hz), and above this point σ increases following a power law. This power law is characteristic for transport in disordered systems and is also well present in the frequency response of the conductivity in PA/CNT nanocomposites. At the crossover region a hump in the conductivity is observed due to space charge polarization. This type of conduction can be attributed to the formation of physical paths in the bulk formed by the nanotubes [37].

3.3.4 Conductivity, rheology and morphology relationships

The differences in conductivity of the nanocomposites, with the same MWCNT content, can be explained when rheology and morphology results are matched. Looking at data of Table 2, we can conclude that the conductivity of the samples seems to be more related to the agglomerate distribution than the CNT dispersion within the matrix considering that the highest conductivity values correspond to nanocomposites with high ratio

A/A_0 and big agglomerates (the worst state of dispersion). The differences are directly related to the morphology obtained during the extrusion and latterly, the compression moulding.

Unfortunately, the morphology of PA66/PA6 blends could not be detected in the morphologic tests, since there is not any selective solvent which removes one phase without damaging the other one.

As has been proved by Lee and col [1], the morphology of immiscible blends is formed during the extrusion process and differs depending on processing conditions. In the beginning, the polymer with a lower melting temperature (in our case PA6) melts while the particles of the other polymer (PA66) form a suspension in the PA6 continuous phase. As the suspension moves along the extrusion, the mixture temperature rises and the PA66 starts to melt. The liquid mixture forms a dispersed morphology where the droplets of PA66 are dispersed in the continuous phase (PA6). In this moment, there are two options: either this morphology allows along the extrusion or a phase inversion may take place, where the PA66 forms the continuous phase and the PA6, the dispersed phase. One or other option depends on the blend composition, viscosity ratio and extrusion parameters.

In this work, two PA66/PA6 ratios were studied, 25/75 and 50/50 PA66/PA6. In 25/75 PA66/PA6 blend where a polyamide is majority, typical sea-island morphology is expected, where continuous phase is formed by the PA6 and the dispersed phase, by the other. Due to the viscosity ratio is greater than 1 (η_{PA66}/η_{PA6} = 1.48, measured at 290°C and 100 rad.s^{-1}), PA66 trends to display a gross dispersion. For the 50/50 PA66/PA6 blend, a co-continuous morphology is expected. The external shear stress induces the deformation of the dispersed particles and promotes the formation of co-continuous morphology. We are going to start from these assumptions in the following discussion.

As it is known, CNT can modify the morphology of polyamide blends, related with an increase in viscosity of the preferential polymer. According to the Young's equation, the localization of the nanofiller in an equilibrium state can be estimated [38], based on the fact that the system tries to reach a minimum interfacial energy state. In our case, the thermodynamically more favorable phase is PA6 ($\sigma_{PA6/CNT}<\sigma_{PA66/CNT}$) [39]. The CNT will trend to remain in PA6 matrix or to move towards it, during the extrusion. For this reason, the viscosity of PA6 phase increases during the blending changing the viscosity ratio. Besides, the viscosity ratio also depends on the

masterbatch used to introduce the CNT in the composites. Using PA6 masterbatch, most CNTs remain in PA6 phase, increasing its melt viscosity.

In the worst case (if the CNT migration to PA6 is complete), the viscosity of this phase could increase up to reach the viscosity of PA6 with 6 wt.% CNT (see supplementary material). Comparing with the pristinePA6, it is clear that there is an increase in viscosity of several orders of magnitude (especially at low frequencies). In theory, this fact could induce a phase inversion. In practice, it is so difficult because of two reasons: the viscosity differences at shear rate of extrusion process are much lower due to that the typical pseudoplastic behavior of PA6 with 6 wt.% CNT and the difference in melting temperatures between PA66 and PA6 (about 40 °C), which causes that two polyamide are simultaneity melted very short time into extruder.

In 25/75* composite (Figure 5a), the infiltration of PA6 molecules into the CNT clusters reduces their break strength. This one promotes a better dispersion of bundles and individual CNTs and to improve the distribution of remained clusters during the extrusion process. Then, in the compression moulding, the lower melting temperature of PA6 improves the CNTs mobility and promotes the CNT re-agglomeration in new clusters or the growth of existing ones (increasing A/A_0 and $\bar{A}$). The rheological data show that the conductive network is formed earlier and this improved network produces a higher conductivity.

Using PA66 masterbatch (25*/75 composite), a part of CNTs remained in PA66 phase and other part could migrate to PA6 phase (Figure 5b). The complete migration is difficult due to the higher melting temperature of PA66 which reduces the CNT mobility during the extrusion process. The nanoparticles mainly affect to the PA66 viscosity which increases. But the viscosity ratio η_{PA66}/η_{PA6} remains greater than 1, and so, no morphology changes are expected. During the extrusion, the greater shear strength supported due to the higher viscosity of PA66 phase could cause the clusters break or at least, their size reduction. Latterly, during the compression moulding, the re-agglomeration is hindered by the higher melting temperature and melt viscosity of PA66, which reduce the CNT mobility(morphologic data show lower $A/A_0$and $\bar{A}$ values). It leads to the presence of single isolated nanotubes and many areas without MWCNT as was observed in their LM micrographs.

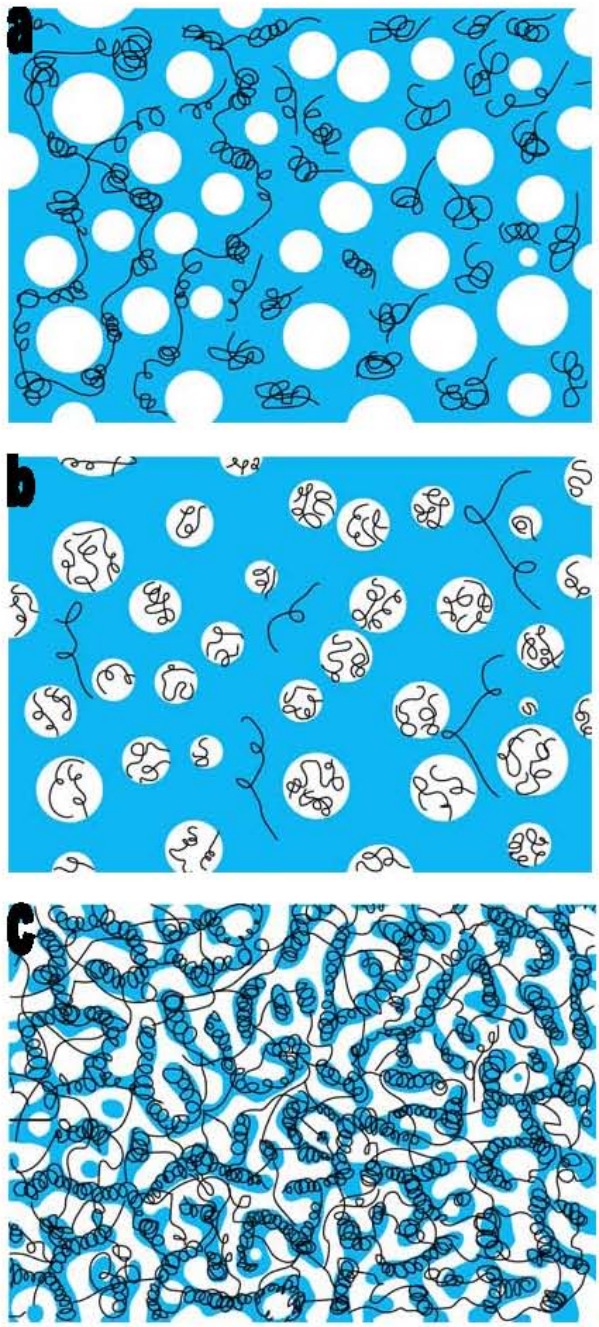

Figure 5 Schematic representations of the composites morphology: a) 25/75*; b) 25*/75 and c) 50*/50 and 50/50*. The blue part represents PA6 phase, the white part represents PA66 phase and the black lines represent MWCNTs

Direct connections and contacts between the nanotubes are less numerous and the polymer matrix could wrap the nanofiller with an insulating layer which reduces the electrical conductivity [40]. As a result, the conductive network is poorer in comparison with composites obtained from PA6 masterbatch (in rheological tests, crossover point appears at higher frequencies), and although the system is percolated (as rheological data show), the electrical conductivity is lower.

The nanocomposites with a 50/50 PA66/PA6 blend are worth special mention. The likely co-continuous morphology reached during the extrusion process, is remained when the CNT are added, regardless the masterbatch used (Figure 5c). The co-continuous morphology can encourage the formation of the conductive network, because of the higher degree of continuity reached in the matrix. But the truth is that, due to this morphology, the polyamides ratio and a higher miscibility degree [41], there are more interfacial surface between polyamides in 50/50 PA66/PA6 composites, helping to the CNT migration to PA6 during extrusion, when PA66 masterbatch is used.

For the same reasons, the re-agglomeration of CNT (during the compression moulding) produces more and bigger agglomerates than 25/75 composites. However, there are not significant differences in morphology between 50*/50 and 50/50* which can explain the conductivity differences. More information is necessary to explain the conductivity values.

3.3.5 Crystallization behavior

CNT ability as nucleating agent on polymers is well known. So, the selective localization of nanotubes in PA66 or PA6 can be proved studying the crystallization behaviour of nanocomposites. Figure 6 shows the DSC thermograms of PA66/PA6/CNT nanocomposites, obtained during the cooling scan. The curves of PA blends (without CNT) show that the PA6 crystallization is reduced according as the PA66 content increases. Taking into account that the crystallization temperature (T_c) of PA66 is higher than the other polyamide, when PA6 molecules began to crystallize the crystals of PA66 are already formed and can hindered the formation or growth of PA6 crystals. As contrary, it does not happen.

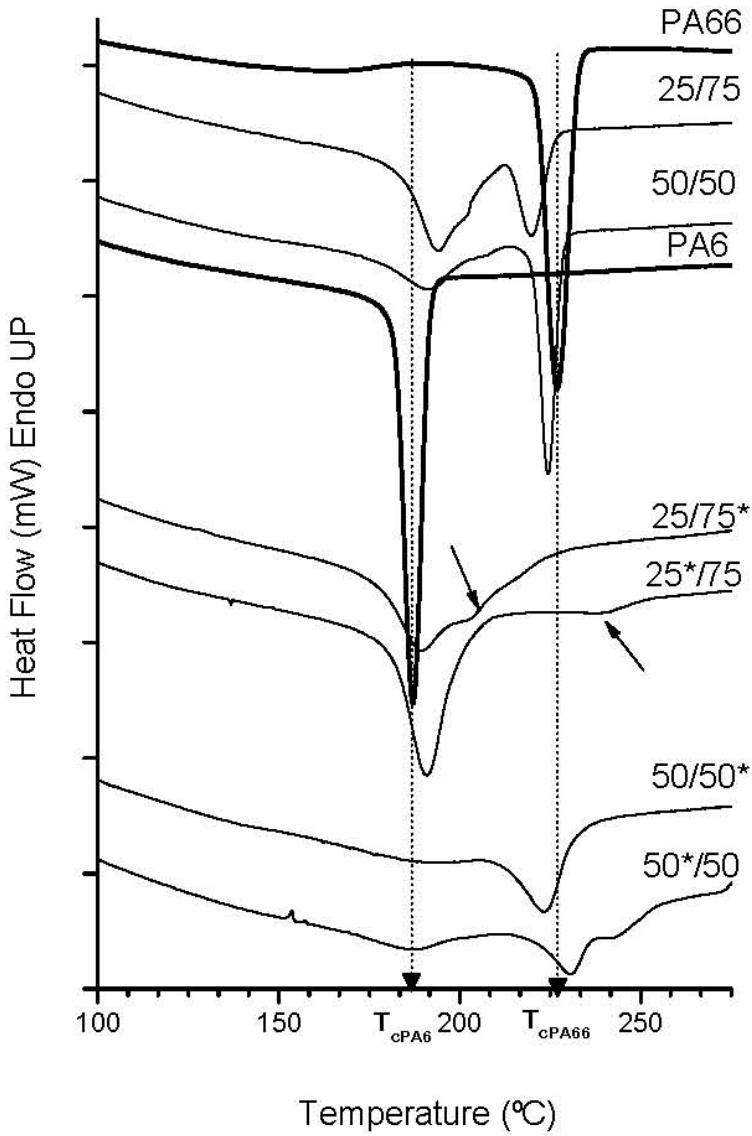

Figure 6 DSC cooling scans of PA66/PA6/CNT for polyamides, binary blends and nanocomposites (endo up)

In 25/75 PA66/PA6 blend, T_c of both polyamides are slightly closer, pointing a heterogeneous nucleation effect (mainly in PA6) due to the presence of other polymer. For 50/50 blend, crystallization temperatures of both polyamides remained constant respect the neat polyamides

When CNT are added to polyamides blends the crystallization behaviour changes. In 25*/75 and 25/75* nanocomposites, CNT produces a nucleating effect in PA6 phase, greater when PA6 masterbatch is used. In this latter case, the shoulder at higher temperature displays a heterogeneous nucleation of PA6, due to the CNT network formed. For the other masterbatch (25*/75 composite), the nucleation effect in PA6 is minor, besides a slight shift of T_{cPA66} at higher temperatures can be observed.

For 50*/50 nanocomposite, (using PA66 masterbatch), the T_c of PA66 clearly increases (nucleating effect of CNT). Both facts prove that CNT migration towards the PA6 phase is not complete, and there are nanotubes which remained in PA66 matrix when the masterbatch PA66 is used. Besides, the cooling thermogram of 50*/50 nanocomposite shows a shoulder at higher temperature than $T_{cPA66.}$ Its origin can be the heterogeneous nucleation of PA66 induced for the CNT network and CNT clusters. Other authors pointed at a partial introduction of CNT network in the no preferential phase (in our case PA66), as cause of this heterogeneous nucleation [2].

Finally, the crystallization behaviour of 50/50* nanocomposite is different. The both polyamides crystallize in wider peaks (PA6 peak in greater proportion) and trend to crystallize in the same temperature range. It is possible that CNTs act, in this case, as compatibilizer, improving the polyamides miscibility and reducing the crystallinity of both polyamides [17]. These facts could explain the higher conductivity of this sample respect to 50*/50 nanocomposite with similar morphology.

3.4 Conclusions

The electrical properties of PA66/PA6/MWCNT composites depend on the polyamide ratio, masterbatch used and the crystalline state. The results obtained allow drawing the following conclusions:

All nanocomposites are rheologically percolated, with little differences appreciated in their crossover point (ω_c, G_c), that can be related to the CNT localization in one or another polyamide.

In the case of 25/75 PA66/PA6 composites, a high degree of filler dispersion together with a low conductivity were obtained. Using PA6 masterbatch (25/75*nanocomposite), conductivity was a little higher, due to the majority localization of CNT in PA6 phase.

This fact encourages the CNT re-agglomeration during the compression moulding.

The highest conductivity values correspond to 50/50 PA66/PA6 nanocomposites. These ones present high ratio A/A_0 and big agglomerates, so electrical conductivity seems to be more directly related to agglomerate distribution than the CNT dispersion within the matrix during extrusion and latterly, their re-agglomeration. It can be explained only if they present a co-continuous morphology which allows an increase in CNT-CNT junctions through the well-distributed agglomerates.

The nanocomposites with 50/50 PA66/PA6 ratio display similar morphology, so the higher conductivity measured in 50/50* PA66/PA6 composite could be due to compatibilizing effect of nanotubes observed in DSC scans, which increases the polyamides miscibility and reduces their crystallization.

3.5 References

1. Lee JK, Han CD. Polymer, 41: 1799 (2000)
2. Xiang F, Shi Y, Li X, Huang T, Chen C, Peng Y, Wanga Y. European Polymer Journal, 48: 350 (2012)
3. Pang H, Xu L, Yan DX, Li ZM. Progress in Polymer Science, 39: 1908 (2014)
4. Knauert ST, Douglas JF, Starr FW. Journal of Polymer Science Part B: Polymer Physics, 45*:* 1882 (2007)
5. Starr FW, Schroder TB, Glotzer SC. Macromolecules, 35: 4481 (2002)
6. Song YS, Youn JR. Korea-Australia Rheology Journal, 16: 201 (2004)
7. Wu D, Wu L, Zhang M, Zhao Y. Polymer Degradation and Stability, 93: 1577 (2008)
8. Y.S. Song. Polymer Engineering and Science, 46: 1350 (2006)
9. Abdalla M, Dean D, Robinson P, Nyairo E. Polymer, 49: 3310 (2008)
10. Seyhan AT, Gojny FH, Tanoglu M, Schulte K. European Polymer Journal, 43: 2836 (2007)
11. Pötschke P, Brüning H, Janke A, Fisher D, Jehnichen D. Polymer 46: 10355 (2005)
12. McNally T, Pötschke P, Halley PJ, Murphy M, Martin D, Bell S, Brennan GP, Bien DCS, Lemoine P, Quinn JP. Polymer, 46: 8222 (2005)
13. Du F, Scogna RC, Zhou W, Brand S, Fisher JE, Winey KI. Macromolecules, 37: 9048 (2004)
14. Alig I, Skipa T, Lellinger D, Pötschke P. Polymer, 49: 3524 (2008)
15. Skipa T, Lellinger D, Böhm W, Saphiannikova M, Alig I. Polymer, 51: 201 (2010)
16. Pegel S, Pötschke P, Petzold G, Alig I, Dudkin SM, Lellinger D. Polymer, 49: 974 (2008)
17. Krause B, Pötschke P, Häubler L. Composites Science and Technology, 69: 1505 (2009)
18. Micusik M, Omastova M, Krupa I, Prokes J, Pissis P, Logakis E, Pandis C, Pötschke P, Pionteck J. Journal of Applied Polymer Science, 113: 2536 (2009)
19. Arboleda L, Ares A, Abad MJ, Ferreira A, Costa P, Lanceros- Méndez S. Journal of Polymer Research, 20: 326 (2013)
20. Aguilar JO, Bautista-Quijano JR, Avilés F. Express Polymer Letters, 4: 292 (2010)

21. Cardoso P, Silva J, Klosterman D, Covas JA, van Hattum FWJ, Simoes R, Lanceros-Mendez S. Nanoscale Research Letters, 6: 370 (2011)

22. Pötschke P, Fornes TD, Paul DR. Polymer, 43: 3247 (2002)

23. Ares A, Pardo SG, Abad MJ, Cano J, Barral L. Rheologica Acta, 49: 607 (2010)

24. Hashmi SAR, Sharma P, Chand N. Journal of Applied Polymer Science, 107: 2196 (2007)

25. Bera O, Trunec M. Plastic Rubber and Composites, 41: 384 (2012)

26. Paleo AJ, Sencadas V, van Hattum FWJ. Polymer Engineering and Science, 54: 117 (2014)

27. Ares A, Lasagabaster A, Abad MJ, Noguerol R, Cerecedo C, Valcárcel V, Caamaño JM, Guitián F. Journal of Composite Materials, 48: 3141 (2014)

28. Vural S, Dikovics KB, Kalyon DM, Soft Matter, 6: 3870 (2010)

29. Cole KS, Cole RH. Journal of Chemical Physics, 9: 341 (1941)

30. Havriliak JS, Havriliak SJ. Dielectric and Mechanical Relaxation in Materials: Analysis, Interpretation and Application to Polymers; Hanser Gardner Publications: Munich (1997)

31. Chin SJ, Vempati S, Dawson P, Knite M, Linarts S, Ozols K, McNally T. Polymer, 58: 209 (2015)

32. Lozano K, Yang S, Zeng Q. Journal of Applied Polymer Science, 93:155 (2004)

33. Tang XG, Hou M, Zou J, Truss R, Zhu Z, Yang W. Journal of Macromolecular Science, Part B: Physics, 51: 1498 (2012)

34. Wanjale SD, Jog JP. Journal of Macromolecular Science, Part B: Physics, 45: 1053 (2006) 1053

35. Banerjee S, Joshi M, Ghosh AK. Journal of Applied Polymer Science, 130: 4464 (2013)

36. Lim ST, Lee CH, Choi HJ, Jhon MS. Journal of Polymer Science Part. B.: Polymer Physics, 41: 2052 (2003)

37. Logakis E, Pandis C, Peoglos V, Pissis P, Piontek J, Pötschke P, Micusik M, Omastová M. Polymer, 50: 5103 (2009)

38. Sumita M, Sakata K, Asai S, Miyasaka K, Nakagawa H, Polymer Bulletin, 25: 265 (1991)

39. Taguet A, Cassagnau P, López-Cuesta JM. Progress in Polymer Science, 39: 1526 (2014)

40. Abbasi M, Javadi A, Nazockdast H, Fathi A, Altstaedt V. Journal of Polymer Science Part B: Polymer Physics, 53:368 (2015)

41. D. Tomova, J. Kressler, H. Radush. Polymer, 41:7773 (2000)

Capítulo 4

Segregated conductive network of MWCNT in PA12/PA6 composites: electrical and rheological behavior

Página intencionadamente en blanco

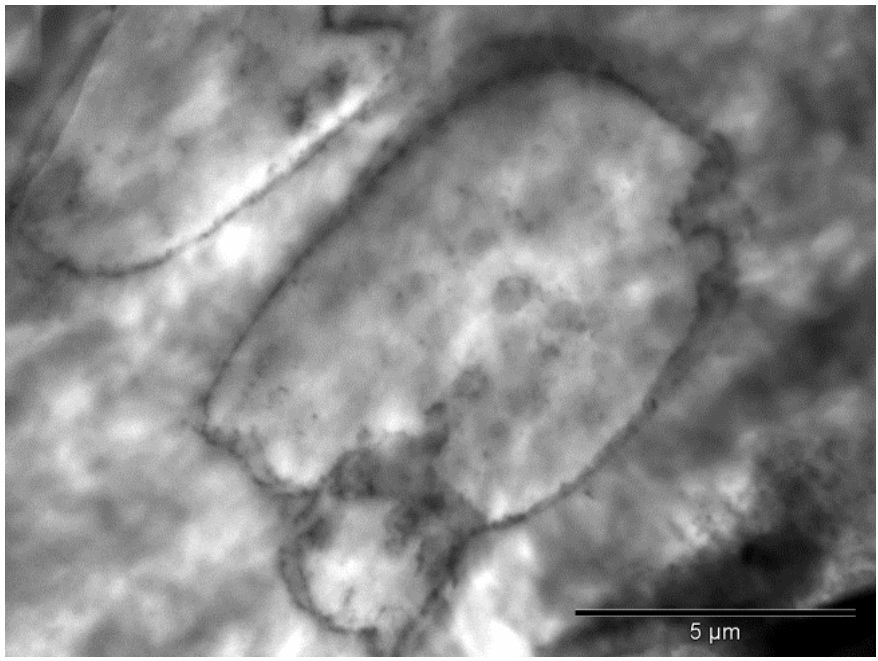

Obtención de nanocompuestos poliméricos conductores con un bajo umbral de percolación utilizando nanotubos de carbono multipared (MWCNTs) y una mezcla inmiscible de poliamida 12/poliamida 6 (PA12/PA6) debido a la formación de una red segregada conductora.

Este capítulo está basado en la siguiente publicación:

Laura Arboleda-Clemente, Ana Ares-Pernas, Xoán García, Sonia Dopico, María José Abad, Segregated Conductive Network of MWCNT in PA12/PA6 Composites, Polymer Composites, publicado online (2015), doi: 10.1002/pc.23865

Página intencionadamente en blanco

4.1. Introduction

The dispersion of conductive fillers (such as carbon nanotubes) (CNTs) in a polymer matrix or a polymer blend can result in electrically conductive polymer composites (CPCs) [1-5]. In CPC achievement, the use of melt mixing technologies (extrusion and injection molding) is a great advantage for industrial end-applications. Besides, the use of polyamide 12/polyamide 6 (PA12/PA6) blends, both commodity polymers in the industry, could be able to overcome some of PA 6 drawbacks such as high sensitivity to notch propagation under impact test in particular at sub-zero temperatures, high moisture sorption, and poor dimensional stability.

General speaking, the properties of CNT composites (such as electrical conductivity) are related with both material composition and morphology reached during their processing. In detail, electrical conductivity depends on the formation of a three dimensional conductive network into the insulating polymer above a critical filler concentration, called percolation threshold (p_C) [6, 7]. As conductive fillers, carbon nanotubes (CNT) have exceptional electrical properties and high aspect ratio (L/D≈1000) allowing to get typical p_C values in the range 1-3 wt.% [6]. Moreover, for immiscible polymer blends (such as polyamide 12/polyamide 6 blend in our case) the nanocomposite morphology is not only governed by thermodynamics and/or kinetic effects but also, by the viscosity ratio of polymers [8]. In theory, a morphology where CNTs migrate at the interfaces between the polymers (instead of randomly distributed in the immiscible polymer blend) would enable the formation of a segregated structure with a lower percolation threshold [9].

The percolation threshold of nanocomposites can be investigated by means of electrical conductivity measurements as well as by the evaluation of their rheological behavior. These techniques together provide insight into the nanoscale structure and organization of the MWCNTs in polymeric matrices [6, 7, 10].

Thus, the principal aim of this work is to design new CNT nanocomposites with electrical conductivity and a low percolation threshold, using an immiscible blend of polyamides as matrix. The percolation threshold p_c will be determined through rheological tests and alternating current (ac) measurements, to discuss in detail the frequency dependence of conductivity. Furthermore, light

microscopy (LM) and transmission electronic microscopy (TEM) were used to investigate the nanocomposites morphology and CNT localization in polymer matrix, finding out that this is a key aspect to explain the macroscopic properties of nanocomposites.

4.2. Experimental

4.2.1 Materials

A blend of Polyamide 12 (PA12 Grilamid supplied by EMS Grivory) and Polyamide 6 (PA6 Zytel supplied by DuPont) was used in this study. PA6 has a density of 1.14 $g.cm^{-3}$, a melting temperature of 220°C and a zero shear viscosity of 723.8 Pa.s measured at 235°C. On the other hand, PA12 has a density of 1.01 $g.cm^{-3}$, a melting temperature of 180°C and a zero shear viscosity 391.7 Pa.s measured at 235°C. To prepare CNT composites, a masterbatch of MWCNT (NC7000, Nanocyl S.A**,** Sambrevile, Belgium) pre-dispersed at 15 wt.% in PA12 was used. MWCNTs have an average diameter of 9.5 nm, a length of 1.5 μm, a carbon purity of 90% and a surface area of 250-300 $m^2.g^{-1}$, according to the supplier.

4.2.2 Methods

4.2.2.1 Extrusion

Composites with different MWCNT contents (between 0.15 and 5.05 %vol.) in 50 %vol./50 %vol. PA12/PA6 blend were prepared by extrusion using a co-rotating twin-screw extruder (Brabender DSE 20) operating at 30 rpm and a temperature profile between 220-235°C.

All the components were premixed by tumbling and then, fed simultaneously into the extruder. Previously, the masterbatch and the neat polyamides were dried in an oven at 110°C for 6 h.

4.2.2.2 Compression molding conditions

For dielectrical measurements, the obtained pellets were compression molded into square plaques with an area of 25 mm x 25 mm and thickness around 0.5 mm at 245°C applying a pressure of 30 bar for 5 min. For rheological tests, the samples were shaped into discs by compression molding at 245°C applying a pressure of 30 bar for 5 min.

4.2.2.3 Morphological analysis

The morphological analysis was carried out by light transmission microscopy (Leica DM2500 microscope combined with a DFC295 camera). Films of 50 ∓m thickness of each sample were prepared by compression molding at 245°C by applying 170 bars for 5 min and they were rapidly cooled down by circulating water. For transmission electron microscopy, an analytical TEM (JEOL JEM 1010) was used to investigate the CNT network formation in the different composites at nanoscale. Ultra-thin sections of 70 nm were cut, at room temperature, from compression molded samples.

4.2.2.4 Rheological measurements

The rheological measurements were performed using a controlled strain rheometer (ARES, TA Instruments) with parallel-plate geometry (25 mm diameter, 1 mm gap) at 235°C. The rheological tests were achieved in the linear viscoelastic region (LVE) previously determined from a strain sweep test. The frequency sweep measurements were set up in the frequency range $1x10^{-1}$ to 10^{2} rad.s^{-1}.

4.2.2.5 Dielectrical measurements

The dielectric measurements were carried out at room temperature in the frequency range between 1 to 10^{5} Hz with an applied signal of 1V using a dielectric analyzer DEA 2970 (TA Instruments). Sensor parallel plate mode has been used.

To obtain acceptable fittings, a total of 11 CNT compositions, in the mentioned range, were used in the threshold calculi. However, for the rheological and dielectrical analysis, only the most relevant CNT compositions (8 of them) were drawn to simplify the graphical representations.

4.3. Results and discussion

4.3.1 Characterization of nanocomposites

4.3.1.1 Rheological measurements

Rheological measurements have been carried out to characterize the percolation state of MWCNT and their dispersion in the polyamide blend. The frequency dependence of the complex viscosity η^*, is shown in log-log plots in Figure 1.

PA12/PA6 blend and composite with 0.15 %vol. MWCNT show a Newtonian behavior at low frequencies whereas the other nanocomposites exhibit a significant shear thinning behavior. Viscosity increases according to the growing amount of MWCNT. This effect is more pronounced at low frequencies, due to the shear-thinning effect, indicating that the relaxation of polymer chains in the nanocomposites is restrained by the presence of CNTs. As it can be seen in Figure 2a, a small amount of nanotubes improves G' modulus of the polyamide blend. Starting from 0.31 %vol. MWCNT, there is a plateau in G' at low frequencies corresponding with the pronounced shear thinning noticed in η^*.

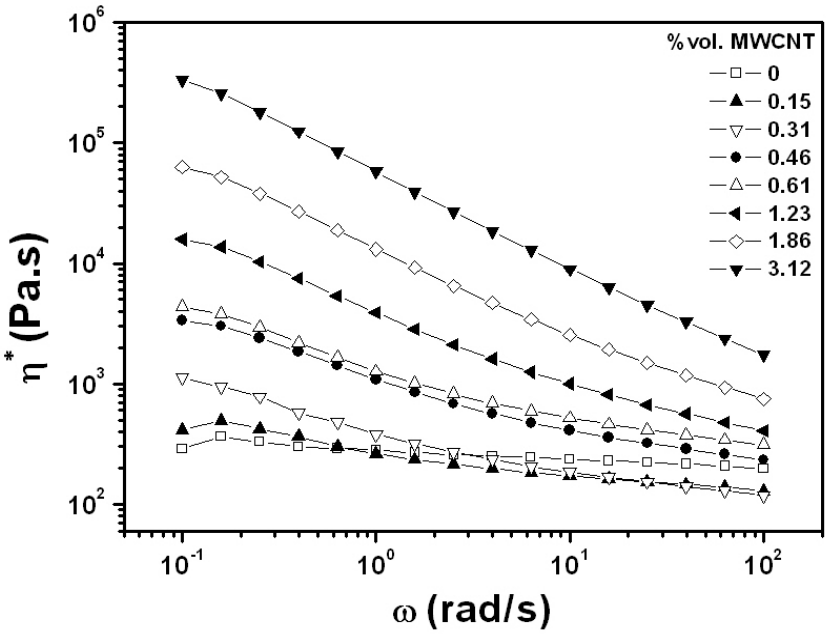

Figure 1 The effect of CNT content on the complex viscosity (η^*) for PA12/PA6 composites

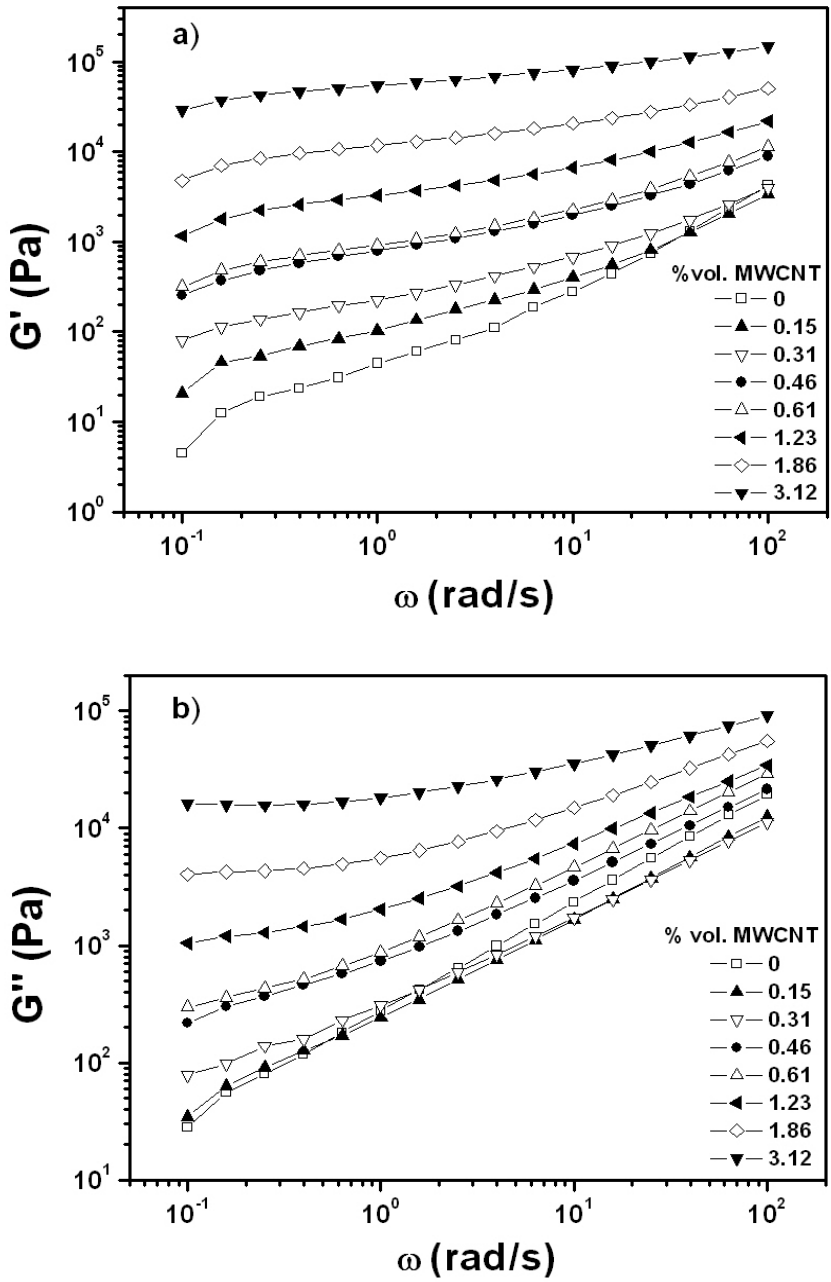

Figure 2 a) Storage modulus (G') and b) Loss modulus (G'') for PA12/PA6 composites

As it is well known, the rheological threshold can be identified in viscosity plots at low frequencies, monitoring the change from a Newtonian behavior to a frequency-dependent behavior and the plateau in the storage modulus [11]. So, the percolated network starts to form about 0.31 %vol.; with 0.15 %vol. CNT, the nanotubes are still quite dispersed in the matrix, providing a more viscous response (G''>G') (see Figure 2a and 2b). With 0.46 %vol., MWCNTs are already percolated into a network, and this makes that the material behaves more like a solid (G'>G''). The percolated network increases the amount of interfaces between MWCNTs, improving the elastic response (solid-like behavior) and increasing the dissipation energy component (G''). These facts could explain the moduli growth and the remarkable shift in the shape of the moduli and viscosity plots for nanocomposites with 0.15 %vol. and 0.31 %vol. CNT [12].

These graphical methods are frequently used to determine the rheological percolation threshold; however it depends very much on the number of experiments realized near the percolation threshold and the visual judgment of the analyst. For that reason, in this study, the power-law relation was also used to calculate the rheological percolation threshold as will be seen hereinafter.

4.3.1.2 Bulk ionic conductivity by dielectric analysis

Dielectric properties describe the ability that an electrical medium can be polarized by an applied electric field. In dielectric experiments, the measures of capacitance and conductance are used to calculate two variables which provide valuable information about molecular motion: permittivity (ε'), which is proportional to capacitance and measures the alignment of dipoles, and loss factor (ε''), which is proportional to conductance, and represents the energy required to align dipoles and move ions. With these parameters, DEA available software calculates bulk ionic conductivity (σ).

Figure 3 displays the conductivity data for PA12/PA6 blend and CNT/polyamide composites.

For the materials with 0 and 0.15%vol. MWCNT, ac conductivity increases approximately linearly with the frequency in a logarithmic scale, exhibiting typical capacitor behavior. From CNT amounts of 0.31 %vol, a dc plateau, where conductivity is independent of frequency, appears below the critical frequency f_c which enhances with nanofiller content. From 1.86 %vol. CNT, the dc plateau spreads to the whole frequency range. Thus, the dc conductivity

plateau is clearly achieved between 0.15 %vol. and 0.31 %vol., indicating that the percolation threshold (p_c), the transition from the insulating to the conducting phase, is located in the same range.

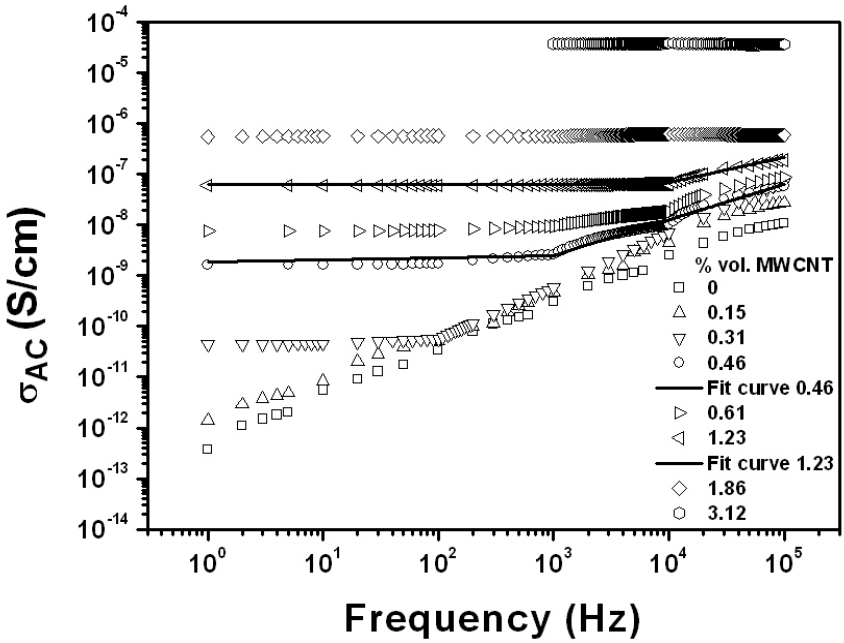

Figure 3 Frequency dependence of conductivity for PA12/PA6 composites with different MWCNT contents.

Above the critical frequency (f_c), σ increases following the power law characteristic for transport in disordered systems and it is also well present in the frequency response of the conductivity in PA/MWCNT nanocomposites. This conductivity change is due to space charge polarization attributed to accumulation and release of charge carriers at the interfaces between regions, with different permittivities and conductivities (Maxwell-Wagner-Sillars (MWS) relaxation), such as PAs and MWCNT. This type of conduction can be attributed to the formation of physical paths in the bulk formed by the nanotubes [10].

4.3.1.3 Composites Morphology and CNT localization

The micrographs obtained by light microscopy (LM) for composites with 0.31, 0.61, 1.86 and 3.12 %vol. MWCNT are showed in Figure 4.

In view of the obtained micrographs, it is seem there are two different behaviors: the nanocomposites with low content of nanotubes, such as 0.31 and 0.61 %vol. MWCNT, display spacing agglomerates with different sizes but most of them are small and apparently well distributed within the polymer matrix. This fact is an important aspect to consider given that can determine the final filler network and therefore, the electrical properties of composites.

On the other hand, nanocomposites with 1.86 and 3.12 %vol. MWCNT (Fig.4.c and Fig.4.d) show a greater number of CNT agglomerates with a very homogeneous distribution within the polymer matrix. This morphology could indicate that the interconnected network is already formed.

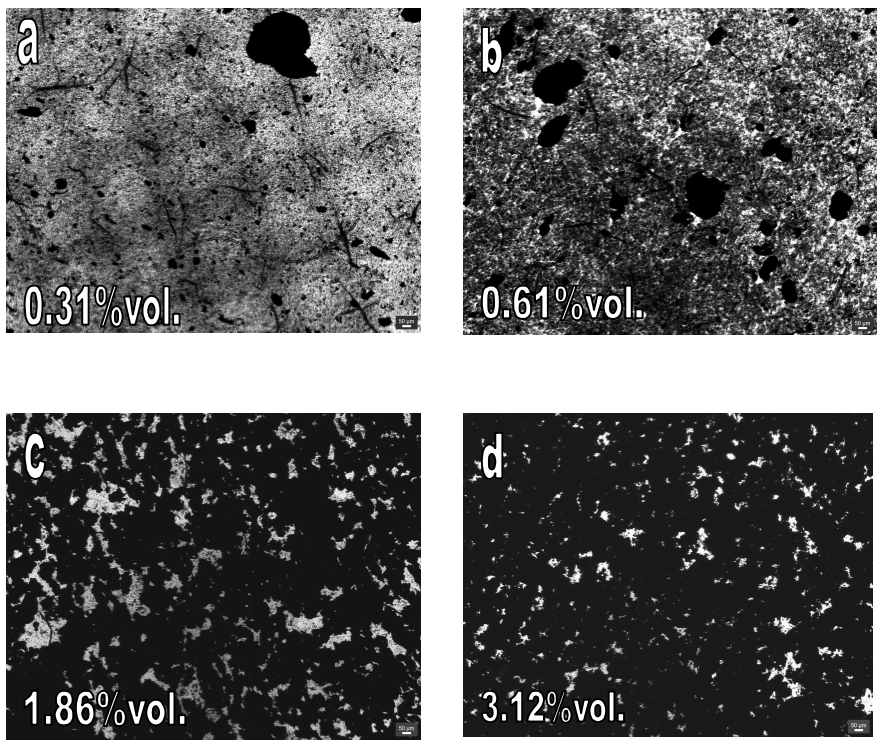

Figure 4 Light microscopy images of PA12/PA6/MWCNT composites. Legend inside; shows the respective nanotube contents

In order to localize the CNT into the polyamide blends, TEM micrographs were taken (Figure 5). The micrographs displays that the two polyamides are distributed in two different phases (island-

sea morphology) and CNTs are mainly found in the interphase between polyamides (see zoom).

As mentioned previously, this preferential localization is the desired morphology to form a segregated network and to obtain low percolation thresholds [9]. The achievement of this morphology depends on two key factors: viscosity ratio between the immiscible polymers and the interfacial energy of CNT/polymers. In this case, the viscosity ratio PA12/PA6 is 0.54 and CNT were pre-dispersed within the lower viscosity polyamide (PA12). This fact is advantageous to obtain a good dispersion of nanotubes/agglomerates in the polymer matrix during the mixing process and thus, to obtain the segregated network.

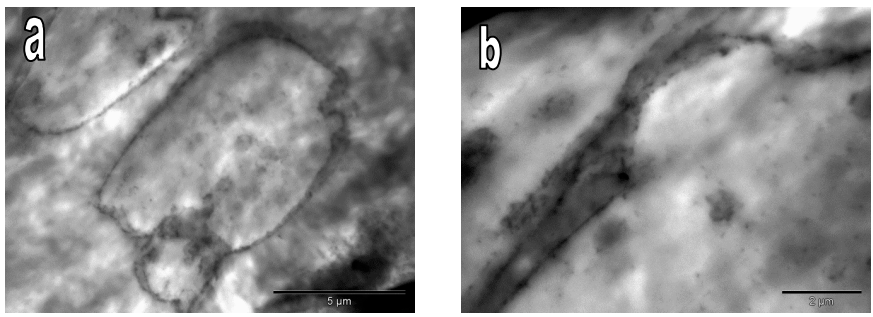

Figure 5 TEM micrographs of PA12/PA6/MWCNT composites with 0.46 %vol. CNT a); Zoom of interface between polyamides b)

Secondly, to support the TEM morphology, the CNT localization in the immiscible polyamide blend was estimated by mean of the wettability parameter. According to the Young's equation the localization of the filler in an equilibrium state can be estimated by calculation of the wetting coefficient ω_a (equation 1) [13], based on the fact that the system tries to reach a minimum interfacial energy state.

$$\omega_{AB} = \frac{\sigma_{CNT-B} - \sigma_{CNT-A}}{\sigma_{A-B}} \qquad (1)$$

where σ_{CNT-B} is the interfacial energy between CNT and polymer component B, $\sigma_{CNT-A}$is the interfacial energy between CNT and

polymer component A and the σ_{A-B} is the interfacial energy between polymer components A and B.

As described by Sumita et al. [13], and afterwards Fenouillot et al. [14], if $\omega_{AB} > 1$, the particles are present only in polymer A; if $\omega_{AB} < -1$, the particles are present only in polymer B and if $-1 < \omega_{AB} < 1$, the particles are situated at the interface between the two polymers.

The interfacial energies between CNT and polyamides in our nanocomposites were estimated using the harmonic-mean (equation 2) and geometric-mean equations (equation 3) [15], from the dispersion and polar components of surface energies reported in the literature [8].

$$\sigma_{12} = \sigma_1 + \sigma_2 - 4\left[\frac{\sigma_1^d \sigma_2^d}{\sigma_1^d + \sigma_2^d} + \frac{\sigma_1^p \sigma_2^p}{\sigma_1^p + \sigma_2^p}\right] \quad (2)$$

$$\sigma_{12} = \sigma_1 + \sigma_2 - 2\left(\sqrt{\sigma_1^d \sigma_2^d} + \sqrt{\sigma_1^p \sigma_2^p}\right) \quad (3)$$

where σ_1, σ_2 are surface energies of the components 1 and 2, σ_1^d, σ_2^d are disperse part of the surface energies of components 1 and 2, and σ_1^p, σ_2^p are polar part of the surface energies of components 1 and 2.

The Table 1 shows the calculated interfacial energies at 240°C and the wetting coefficient according to equation 1, estimated used the harmonic-mean and the geometric-mean equations (equations 2 and 3, respectively).

Regardless of the equation used, the findings show CNTs will tend to migrate at the interface between the two polyamides during the melt blending, as could be seen in TEM micrographs.

Interfacial energy (mJ/m^2)	**Harmonic mean equation**	**Geometric- mean equation**
$\sigma_{PA12/PA6}$	4.19	2.21
$\sigma_{PA12/CNT}$	4.43	2.36
$\sigma_{PA6/CNT}$	1.96	0.94
Wetting coefficient ($\omega_{PA12/PA6}$)	-0.59	-0.64

Table 1 Interfacial energies and wetting coefficient

4.3.2 Percolation threshold calculation

To assess if the preferential localization of CNT in the polyamides interphase observed in morphological analysis reduced the percolation threshold, it was calculated from the rheological and dielectric data.

4.3.2.1 Electrical threshold

In general, the frequency dependence of ac conductivity at constant temperature follows power law behavior and can be expressed by the following equation [16]:

$$\sigma'(\omega) = \sigma(0) + \sigma_{ac}(\omega) = \sigma_{dc} + A\omega^{s} \qquad (4)$$

where ω is the angular frequency, σ_{dc} is the dc conductivity (at $\omega \to 0$), A is a temperature-dependent constant and s is an exponent dependent on both frequency and temperature with $0 \leq s \leq 1$. This is a typical behavior for a wide variety of materials and is called by Jonscher 'universal dynamic response' (UDR) [16, 17]. The value of σ_{dc} can be estimated from the plateau values of conductivity. Also, for some compositions there is a critical frequency f_c beyond which a power law is followed [18, 19].

In order to obtain values of σ_{dc}, f_c and s, a non-linear curve fitting procedure was applied to the experimental curves of Figure 3. The following equation was used [18].

$$\sigma'(f) = \begin{cases} \sigma_{dc}, f < f_c \\ \sigma_{dc}\left(f / f_c\right)^{s}, f \geq f_c \end{cases} \qquad (5)$$

The fitting was done in Origin 8.0. All the parameters obtained are listed in Table 2. It is seen that σ_{dc} and f_c increase as the amount of CNT increases. Furthermore, the critical exponent s is unaffected by the amount of CNT and only a small divergence is reported for the sample with 0.31%vol. MWCNT. Such a value of s (~ 0.7) implies that the system is described by an equivalent 3D network of capacitors corresponding to the matrix region between the particles [19].

MWCNT (%vol.)	σ_{DC} (S/cm)	f_c (Hz)	s
0.31	5.0×10^{-11}	95	1.04
0.46	1.8×10^{-9}	647	0.70
0.61	$9.0 \times .10^{-9}$	2300	0.60
0.92	$3.0 \times .10^{-8}$	4500	0.60
1.23	6.3×10^{-8}	8400	0.50

Table 2 DC conductivity (σ_{dc}), crossover frequency (f_c) and exponent s for the samples indicated on the table

Figure 6 shows the extrapolated values of dc conductivity $\left(\sigma_{dc} = \sigma'(\omega \to 0)\right)$, obtained from the fitting procedure described above vs. CNT volume content (p) for the nanocomposites above p_c [20]. In order to get an estimate for p_c the well-known scaling law [21] (equation 6) was fitted to the experimental σ_{dc} data for $p > p_c$, where t is a critical exponent related with the dimensionality of the investigated system (see inset to Figure 6).

$$\sigma_{dc}(p) \propto (p - p_c)^t \qquad (6)$$

The best linear fit (R^2=0.99) was found for $p_c = 0.258 \pm 0.001$ %vol. and $t = 2.5 \pm 0.1$. This value of the critical exponent t is concordance with the previous reported values (between 0.7 and 3.1) for the CNT-filled nanocomposites in literature [22- 24].

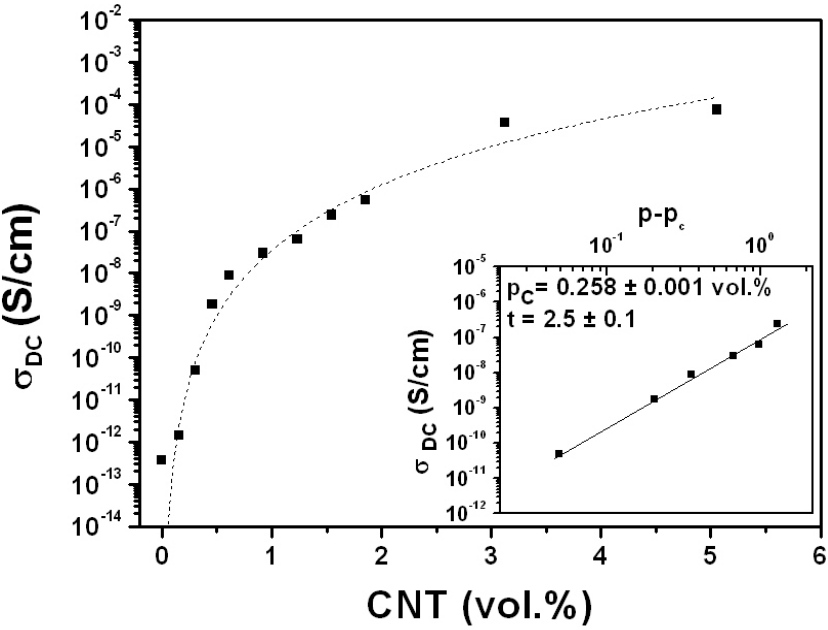

Figure 6 σ_{dc} vs. CNT vol.% concentration (p) for nanocomposites above pc. The inset shows a log–log plot of σ_{dc} vs. $\left(p - p_c\right)$

4.3.2.2 Rheological threshold

Similar to the electrical percolation threshold, the rheological percolation is correlated with the onset of a power-law dependence of rheological properties on the mass fraction [25]. According Kota and coworkers [26, 27], G' is one of the best rheological parameters to be used in order to estimate the onset of the rheological percolation threshold. This parameter has physical significance in terms of the flow and firmness of materials and must be evaluated at low frequencies, where the effect of incorporation of MWCNTs is more evident.

To determine the rheological threshold of PA12/PA6/MWCNT nanocomposites, a modified power law relation is drawn as following equation:

$$G'(p) \propto \left(p - p_{c,G'}\right)^{t_{c,G'}} \qquad (7)$$

where G' is storage modulus (at 0.1 rad.s^{-1}), $p_{c,G'}$ is the rheological percolation threshold and $t_{C,G'}$, the critical exponent analogous to

t in the electrical power law relation. The best fitting (R^2 = 0.94) is shown in Figure 7 with $p_{c,G'} = 0.09 \pm 0.01$ %vol. and $t_{C,G'} = 1.9 \pm 0.2$. From theory, a rheological percolation exponent of 2.1 ± 0.2 belong to percolating bonds, which resist stretching but are free to rotate [28]. The fitting realized from both electrical and rheological data exhibits that both they are sensitive to the interconnectivity of MWCNTs in the PA12/PA6 blend.

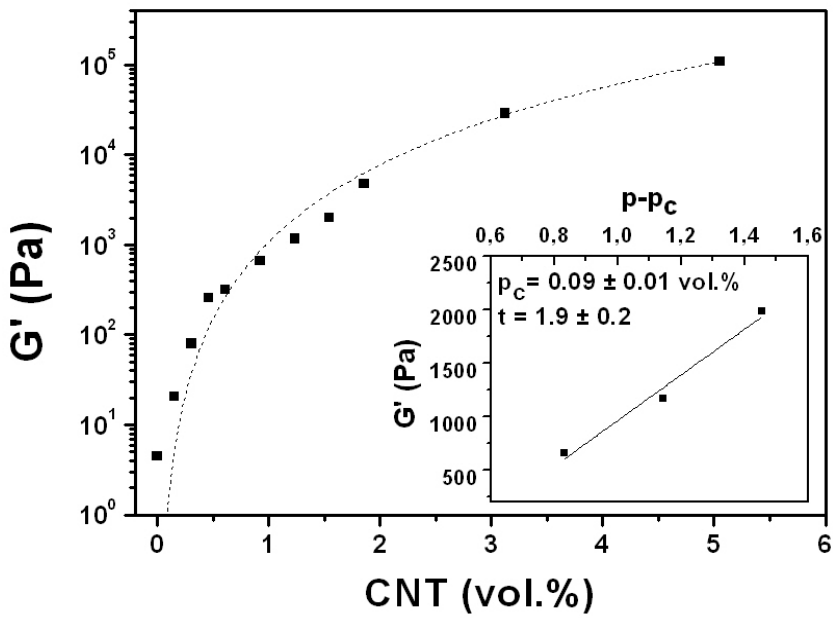

Figure 7 Storage modulus of PA12/PA6 composites as a function of MWCNT loading at a fixed frequency of 0.1 rad/s. Inset log–log plot of G' vs. $(p - p_c)$

4.3.3 CNT aspect ratio

The low values for percolation thresholds would be difficult to explain, if the high aspect ratio of the MWCNTs is not kept after melt mixing; in spite of high shear tends to break the CNT into shorter segments [29].

To corroborate this feature, the aspect ratio of CNT was calculated from the experimentally measured values of conductivity using a model proposed by Garboczi et al. [30]. This model is valid for prolate fibres with high aspect ratio and a difference in

conductivity between matrix and filler of many orders of magnitude. Intrinsic conductivity of conducting filler in an insulating matrix is defined as:

$$[\sigma] = \lim_{\phi \to 0} \sigma_{red} \tag{8}$$

where σ_{red} is the reduced conductivity given by

$$[\sigma_{red}] = \frac{\sigma_{eff} - \sigma_m}{\sigma_m \phi} \tag{9}$$

In the above equation, σ_{eff} is the conductivity of the composite, σ_m is the conductivity of the matrix (determined from dc measurements), and ϕ is the filler content. In Figure 8 the reduced conductivity of the nanocomposites, which are above the percolation threshold, is plotted vs. the volume fraction of CNT.

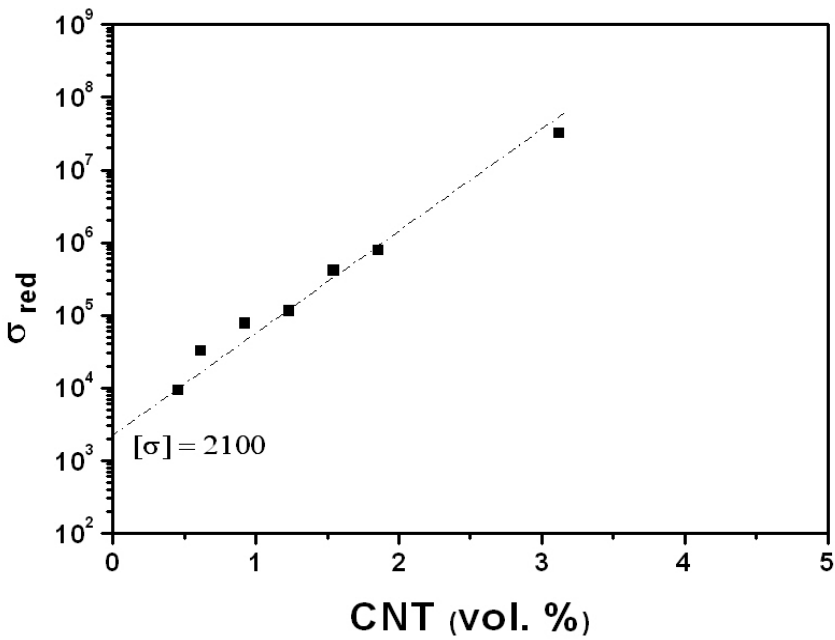

Figure 8 Reduced conductivity of PA12/PA6 composites plotted versus the volume content of the filler. The intrinsic conductivity is determined by the linear extrapolation to a volume content of 0 vol.%.

For the intrinsic conductivity $[\sigma]$, determined by a linear extrapolation of the reduced conductivity to $\phi_{CNT} = 0$, a value of $[\sigma] \approx 2100$ is obtained. The intrinsic conductivity is given as [29]:

$$\sigma = \frac{(L/d)^2}{\ln(L/d)} \qquad (10)$$

where L is the length of the prolate filler and d its diameter. In this work, the experimental value determined for the intrinsic conductivity ($[\sigma] \approx 2100$), corresponds to an aspect ratio $L/d \approx 98.1$. Keeping in mind that aspect ratio supplied by Nanocyl is L/d=158, the value obtained denotes a minimum decrease of CNT aspect ratio during the melt blending by extrusion and subsequent nanocomposite molding. Comparing with the literature data for similar systems, the diminution obtained in L/d is close or even lower than the reported values [31, 10].

4.4. Discussion

In the previous section a rheological percolation threshold smaller than the electrical one was obtained. This one implies that when the rheological percolation threshold is reached, the MWCNT are not in direct contact with each other yet or at least no “infinite” cluster is formed. According to some authors [24, 32], the rheological percolation is reached when the CNT-CNT average distance is between the polymer entanglement distance and twice the radius of gyration, namely, from 10 to 100 nm. However, the electrical percolation threshold is achieved when a conductive path is formed across the material from one end to the other. So, either conductive fillers are in direct contact with each other (direct conduction mechanism) or the tube-tube distance is less than 5 nm (electron hopping/ tunneling mechanism) [24, 33].

On the other part, both electrical threshold, $p_c = 0.258\%vol.$ or $p_c = 0.42\,wt.\%$, and rheological threshold, $p_{c,G'} = 0.09\%vol.$ or $p_{c,G'} = 0.15wt.\%$, obtained are lower than the published data in literature. Logakis et al [10], calculated an electrical threshold around 1.7 vol.% while Meincke et al [31], found that the rheological percolation threshold was around 2-4 wt.% and the electrical one around 3-7 wt.% in PA6/MWCNT nanocomposites.

On the other hand, Socher et al [34], calculated an electrical threshold around 0.7 %vol. for MWCNT in PA12. In the case of Bose et al [35], found that the rheological percolation threshold in MWCNT/PA6-ABS nanocomposites was around 1-2 wt.%, which was significantly lower than the corresponding electrical percolation of around 3-4 wt.%.

Our lower percolation thresholds are consistent with the fact that CNTs are preferentially located in the interface between the two polyamides and with the morphological results. This morphology could encourage the formation of a segregated conductive network into polymer matrix and theoretically, reduce the percolation threshold of conductive polymer nanocomposites [9]. Besides, the small reduction in L/d ratio of CNT after material processing, benefits the procurement of high conductivities with low CNT contents.

4.5. Conclusions

In this work, different MWCNT quantities (between 0.15 and 5.05 %vol.) were dispersed in an immiscible blend of 50/50 PA12/PA6. The rheological, electrical and morphological properties of nanocomposites were assessed and discussed as function of the nanofiller content. The main conclusions are summarized below:

Nanocomposites morphology showed that although CNTs reached different dispersion degree in the matrix as function of the filler content, their preferential localization is in the interface between the two polyamides. It proves that the mixing strategy used (CNT dispersion from a PA12 masterbatch) encouraged the formation of a segregated conductive network even with low CNT contents.

Respect to the rheological percolation threshold, graphically the transition from the liquid like to solid like behavior was observed between 0.15 %vol. and 0.31 %vol. MWCNT. Nevertheless, the estimated rheological percolation threshold, using the power-law relation, is 0.09 %vol. MWCNT.

The dielectrical measurements exhibited that the material transition from insulating to the conducting is located between 0.15 and 0.31 %vol. MWCNT. The electrical threshold calculus, using the power-law relation, obtained a p_c value of 0.26 %vol. MWCNT, confirming the previous statement.

Rheological percolation threshold is lower than the electrical one, suggesting that the rheological percolation is originated from a combined nanotubes-polymer network whereas the electrical percolation is mainly related to the network formed by the nanotubes alone.

The low percolation thresholds obtained for PA12/PA6/MWCNT composites can be explained by the preferential localization of CNT in the polyamides interface, just as by high aspect relation of nanotubes, kept after extrusion and subsequent nanocomposites molding.

4.6. References

1. Stankovich S, Dikin DA, Dommett GHB, Kohlhaas KM, Zimney EJ, Stach EA, Piner RD, Nguyem ST, Ruoff RS. Nature, 442: 282 (2006)

2. Deng H, Lin L, Ji MZ, Zhang SM, Yang MB, Fu Q. Progress in Polymer Science, 39: 627 (2014)

3. Al-Saleh MH, Sundararaj U. Carbon, 47: 2 (2009)

4. Tiusanen J, Vlasveld D, Vuorinen J. Composite Science and Technology, 72: 1741 (2012)

5. Mechrez G, Suckeveriene RY, Zelikman E, Rosen J, Ariel-Sternberg N, Cohen R, Narkis M, Segal E. ACS Macro Letters, 1: 848 (2012)

6. Luo S, Liu T. Carbon, 59: 315 (2013)

7. Pötschke P, Abdel-Goad M, Alig I, Dudkin S, Lellinger D. Polymer, 45: 8863 (2004)

8. Taguet A., Cassagnau P, Lopez-Cuesta J-M. Progress in Polymer Science, 39: 1526 (2014)

9. Pang H, Xu L, Yan D-X, Li Z-M. Progress in Polymer Science, 39: 1908 (2014)

10. Logakis E, Pandis C, Peoglos V, Pissis P, Pionteck J, Pötschk, Mikusik M, Omastova M. Polymer, 50: 5103 (2009)

11. Satapathy BK, Weidisch R, Pötschke P, Janke A. Composites Science and Technology, 67: 867 (2007)

12. Martins, J. N., Bassani, T. S., Barra, G. M. O., Oliveira, R. V. B. Polymer International, 60: 430 (2011)

13. Sumita M, Sakata K, Asai S, Miyasaka K, Nakagawa H. Polymer Bulletin, 25: 265 (1991)

14. Fenouillot F, Cassagnau P, Majesté JC. Polymer, 50: 1333 (2009)

15. Wu S, *Polymer interface and adhesion*, Marcel Dekker Inc, New York (1992)

16. Jonscher AK, *Nature*, **267**, 673 (1997)

17. Dyre JC, Schroder TB. Reviews of Modern Physics, 72: 873 (2000)

18. Allig I, Lellinger D, Dudkin SM, Pötschke P. Polymer, 48: 1020 (2007)

19. Ezquerra TA, Kulescza M, Santa Cruz C, Baltá Calleja FJ. *Advanced Mater*ials, 2: 597 (1990)

20. Peoglos V, Logakis E, Pandis Ch, Pissis P, Pionteck J, Pötschke P, Micusik M, Omastova M. Journal of Nanostructured Polymer Nanocomposites, 3: 116 (2007)

21. Stauffer D, Aharony A. Introduction to percolation, Taylor and Francis, London (1994)

22. Martin CA, Sandler JKW, Saffer MSP, Schwarz MK, Baunhofer W, Schulte K. Composites Science and Technology, 64: 2309 (2004)

23. Baunhofer W and Kovacs ZJ. Composites Science and Technology, 69: 1486 (2009)

24. Hu G, Zhao C, Zhang S, Yang M, Wang Z. Polymer*,* 47: 480 (2006)

25. McNally T, Pötschke P, Halley P, Murphy M, Martin D, Bell S, Gerad B, Bein D, Lemoine P, Quinn JP. Polymer*,* 46: 8222 (2005)

26. Kota AK, Cipriano BH, Duesterberg MK, Gershon AL, Powell D, Raghavan SR, Bruck HA. Macromolecules, 40: 7400 (2007)

27. Paleo AJ, Silva J, van Hattum FWJ, Lanceros-Méndez S, Ares AI. Journal of Polymer Science Part B: Polymer Physics, 51: 207 (2013)

28. Sahimi M, Arbabi S. Physical Review B, 47: 703 (1993)

29. Lin B, Sundararaj U, Pötschke P. Macromolecular Materials and Engineering, 291: 227 (2006)

30. Garboczi EJ, Snyder KA, Douglas JF. Physical Review E, 52: 819 (1995)

31. Meincke O, Kaempfer D, Weickmann H, Friedrich C, Vathauer M, Warth H. Polymer, 45: 739 (2004)

32. Mitchell CA, Bahr JL, Arepalli S, Tour JM, Krishnamoorti R. Macromolecules, 35: 8825 (2002)

33. Mitchell CA, Krishnamoorti R. Macromolecules*,* 40: 1538 (2007).

34. Socher R, Krause B, Boldt R, Hermasch S, Wursche R, Pötschke P. Composites Science and Technology*,* 71: 306 (2011)

35. Bose S, Bhattacharyya AR, Kulkarni AR, Pötschke P. Composites Science and Technology, 69: 365

Página intencionadamente en blanco

Capítulo 5

Water sorption of PA12/PA6/MWCNT composites with a segregated conductive network: structure-property relationships

Página intencionadamente en blanco

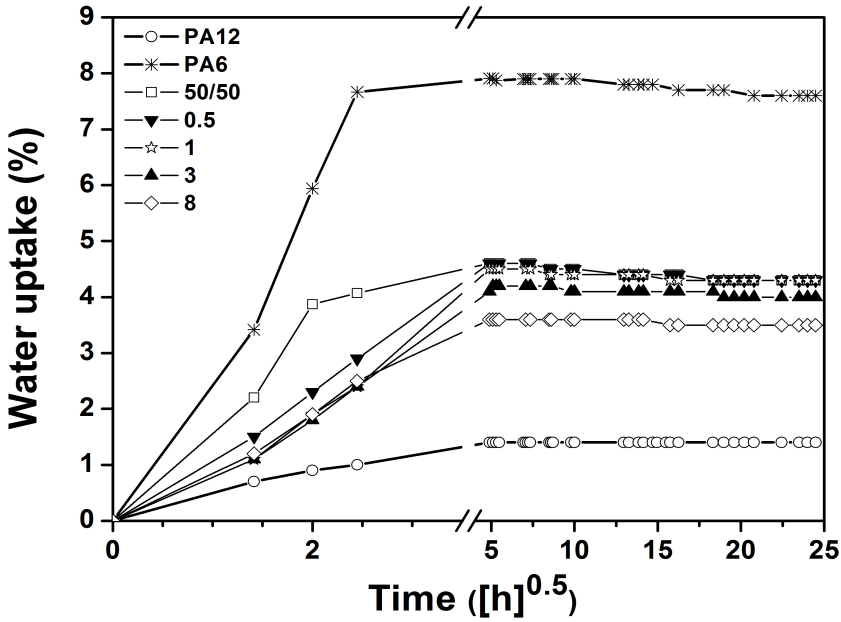

Estudio de la influencia del contenido de relleno en el comportamiento de difusión del agua en una mezcla inmiscible poliamida 12/poliamida 6.

Este capítulo está basado en la siguiente publicación:

Laura Arboleda-Clemente, Ana Ares-Pernas, Xoán-Xosé García-Fonte, María-José Abad, Water sorption of PA12/PA6/MWCNT composites with a segregated conductive network: structure-property relationships, Journal of Materials Science, 51 (17), p. 8674-8686 (2016)

Página intencionadamente en blanco

5.1. Introduction

In order to reduce CO_2 emission and fuel consumption, the automotive industry wishes to reduce the mass of vehicles. Polyamide composites reinforced with fillers, such as carbon nanotubes, are suitable substitutes of metals in automotive parts. They combine an affordable price and a reasonable stiffness due to the complex shapes allowed by the injection molding process. The blend of polyamides with other polymers has been extensively studied [1-3] but the scientific literature about blending of nylons themselves is still quite limited [4, 5]. The use of polyamide 12/polyamide 6 (PA12/PA6) blends, both commodity polymers in the industry, could be able to overcome some of PA6 drawbacks, such as high sensitivity to notch propagation under impact test in particular at subzero temperatures, high moisture sorption, and poor dimensional stability. These polyamides are nowadays increasingly used for structural applications such as engine mounts or clutch pedals which are submitted to complex cyclic movements. Furthermore, important variations of the temperature and relative humidity can be induced by the service conditions (under-bonnet temperature and climatic variations) [6]. Both temperature and relative humidity are known to have a strong impact on the mechanical properties of polyamides [7-10]. These reasons explain the number of studies about the water diffusion in polyamides. The great part of them is focused on establishing the diffusion mechanisms, considering the physical consequences of water sorption and evaluating the water diffusion rate [11-18].

Focusing on polyamides blends, Besco and collaborators studied the physical properties of PA66/PA12/clay nanocomposites, analyzing the influence of different PA66/PA12 ratios and an organically-modified layered silicate (OMLS) in the water uptake behavior of polymer blend [4]. Their data showed a possible compatibilizing effect of OMLS in the immiscible PA66/PA12 blends.

Regarding polyamide/carbon nanotube (CNT) nanocomposites, few studies analyze the influence of nanotubes amount in the water sorption of materials, such as Logakis et col [19]. In this paper, the researchers noticed a systematic enhancement of water uptake normalized to the amorphous fraction of polymer, with increasing CNT content. The authors concluded that the free volume increased in the nanocomposites due to loosened molecular packing of the polymer chains, in agreement with an observed decrease in Tg value. However, in another study, Sengupta [20]

observed that water absorption decreases remarkably with increasing nanotubes concentration in PA66/MWCNT films. Notwithstanding the research reported, water diffusion mechanisms are still controversial. The phenomenon has been linked to free volume [11, 12], to formation of hydrogen bonds between water and the polymer [13, 14] or to cluster formation [15-18]. To our knowledge, there is not any study about the water diffusivity in CNT nanocomposites using a blend of immiscible polyamides as matrix.

In a previous work, we had assessed the electrical properties of PA12/PA6/CNT nanocomposites, showing that the nanotubes form a segregated conductive structure into the polymer matrix and that they are preferable placed in the interface between polyamides. By extrusion, the CNTs previously included in PA12 matrix, were melt-mixed with PA6. The immiscible polyamides were selected with a viscosity ratio, PA12/PA6; lower than 1 to promote the CNT migration from PA12 to PA6. Following this mixing strategy, a suitable morphology was obtained and, as consequence, a low electrical threshold and a high electrical performance [5].

It is well-known, CNTs are able to change the crystalline state of polyamides and as a result, they could modify the water uptake of nanocomposites. Besides, CNT could affect to PA6 and PA12 in different way, due to the CNT migration and their selective localization in the polyamides interface. To further study this question in depth, it is necessary to examine the water uptake behavior of these PA12/PA6/CNT nanocomposites and related it with their morphology (CNTs form a segregated conductive structure into the polymer matrix) and their crystalline state. This aspect is a novelty and, to our knowledge, it has previously not been addressed.

The effect of carbon nanotubes on the crystal organization of polyamides has been widely studied by Differential Scanning Calorimetry (DSC) and X Ray Diffraction (XRD), both techniques are complementary. Phang [21] studied the crystalline structure of PA6/MWCNT composites and obtained that the presence of nanotubes enhanced the crystallization of PA6 by acting as a heterogeneous nucleation agent. Logakis [19] confirmed that CNT promote the formation of the $\mapsto$ form crystals, making it the dominant phase in the crystalline state of PA6. Concerning DSC, the quantitative analysis of polyamide crystallinity may be misinterpreted because of the placement of the baseline and the presence of moisture absorbed during sample preparation [22].

The analysis of wide-angle-X ray diffraction (WAXD) patterns of semicrystalline polymers offers information on several important structural parameters related to various levels of the organization of macromolecules, the determination of the size of the crystallites and crystallinity. Moreover, in the case of polymorphism, the weight fractions of individual crystalline phases can be estimated. The prerequisite for all procedures dedicated to determining structural data mentioned above by means of the WAXD technique is the possibility of resolving the patterns into crystalline and amorphous components, i.e, crystalline peaks and an amorphous halo.

In spite of the shortcomings of both techniques, they provide reliable results in polyamide samples with high crystallinity [22].

Therefore, the main target of this study is to assess the influence of the carbon nanotubes content in the water diffusion behavior of an immiscible blend of polyamides. Previously, the crystalline state of both polyamides (PA12 and PA6), evaluated by DSC and XRD, the nanocomposites morphology and their rheological properties were analyzed. This paper is focused in finding out the structure-properties relationships of such CNT composites.

5.2. Experimental

5.2.1 Materials

A blend of Polyamide 12 (PA12 Grilamid supplied by EMS Grivory) and Polyamide 6 (PA6 Zytel supplied by DuPont) was used in this study. PA6 has a density of 1.14 $g.cm^{-3}$, a melting temperature of 220 °C and a zero shear viscosity of 723.8 Pa.s measured at 235 °C. On the other hand, PA12 has a density of 1.01 $g.cm^{-3}$, a melting temperature of 180 °C and a zero shear viscosity 391.7 Pa.s measured at 235 °C. To prepare CNT composites, a masterbatch of MWCNT (NC7000, Nanocyl S.A, Sambrevile, Belgium) pre-dispersed at 15 wt.% in PA12 was used (Plasticyl PA1502, Nanocyl S.A, Sambrevile, Belgium). MWCNTs have an average diameter of 9.5 nm, a length of 1.5 ∓m, a carbon purity of 90% and a surface area of 250-300 $m^2.g^{-1}$, according to the supplier.

Sample	PA12 (wt.%)	PA6 (wt.%) (wt.%)	MWCNT (wt.%) (wt.%)	ω_c; G_c (rad/s) (Pa)
PA12	100	0	0	G'' > G'
PA6	0	100	0	G'' > G'
0	50	50	0	G'' > G'
0.5	49.75	49.75	0.5	0,2 ; 131
1	49.50	49.50	1	1,1 ; 950
3	48.50	48.50	3	47 ; 35880
8	46.00	46.00	8	G''< G'

Table 1 Formulations of PA12/PA6/MWCNT nanocomposites and G'/G'' crossover points.

5.2.2 Preparation of composites

Composites of a 50/50 PA12/PA6 blend and different MWCNT contents were prepared by diluting the masterbatch with the same PA12 as used in the masterbatch (Table 1). Before extrusion, masterbatch and pristine polyamides were dried in an oven at 110 °C for 6 h. Then, the different composites were extruded using a co-rotating twin-screw extruder (Brabender DSE 20) operating at 30 rpm, with a temperature profile between 220-235 °C. All the components were premixed by tumbling and then, fed simultaneously into the extruder.

For rheological tests, the samples were shaped into discs by compression molding at 245 °C applying a pressure of 30 bar for 5 min. For the rest of experiments, the samples were cut from square plaques molded by compression with an area of 25 mm x 25 mm and thickness around 0.5 mm at 245 °C applying a pressure of 30 bar for 5 min. In all cases, before the compression-molding of nanocomposites, the pellets were dried at an oven at 110 °C for 6 h.

5.2.3 Characterization

The composite morphology was analyzed by scanning electron microscopy (SEM). For SEM analysis, some specimens were cryo-fractured in liquid nitrogen and the fracture surfaces examined using a JEOL JSM-6400 scanning electron microscope (SEM) at

an accelerating voltage of 20 kV. The samples were previously sputter-coated with a thin layer of gold.

The rheological measurements were performed using a controlled strain rheometer (ARES, TA Instruments) with parallel-plate geometry (25 mm diameter, 1 mm gap) at 235°C. The storage modulus (G'), and loss modulus (G'') were measured as a function of frequency (ω). The rheological tests were performed in the linear viscoelastic region (LVE). This linear viscoelastic region was determined previously from a strain sweep test. The frequency sweep measurements were set up in the frequency range $1x10^{-1}$ to 10^2 rad.s^{-1}.

Thermal measurements were carried out with a differential scanning calorimeter (DSC 2910, TA) under nitrogen atmosphere. The samples (6-10 mg) were heated from 0 °C to 250 °C at a rate of 10 °C.min^{-1} and maintained 10 min at 250 °C to erase their thermal history, then they were cooled to 0 °C at a rate of 10 °C.min^{-1} and finally, heated to 250 °C (second heating) at a rate of 10 °C.min^{-1}.

A deconvolution procedure using the Origin 8.5 software was applied to the thermograms to obtain the thermal data. The crystallinity degree (Xc) was calculated following equation 1, where ΔH_m^* is the melting enthalpy normalized to the polyamide fraction.

$$X_C^{DSC}(\%) = \frac{\Delta H_m^*}{\Delta H_0} \times 100 \qquad (1)$$

The cold crystallization enthalpy normalized to the polyamide fraction (ΔH_c^*) was considered for the calculus of the crystallinity degree, in the thermograms where it could be measured (equation 2).

$$X_C^{DSC}(\%) = \frac{\Delta H_m^* - \Delta H_c^*}{\Delta H_0} \times 100 \qquad (2)$$

The heat of fusion of 100% crystalline polyamide is taken as ΔH_0 = 230 J/g for PA6 [23] and ΔH_0 = 209 J/g for PA12 [24].

The X-ray diffraction patterns were recorded using a Bruker D5000 diffractometer using Cu $K_{\mapsto}$ radiation ($\lambda = 0.154 nm$) with Bragg-Brentano geometry with a radius of 250 mm. The assay range is from 1.15 to 40 degrees and steps of 0.005 degrees at room temperature.

Water-absorption experiments were realized from square-shaped samples with an area of 25 mm □ 25 mm and thickness around 0.5 mm obtained by compression molding. In a first step, all samples were dried in an oven at 105°C for a period of 48 hours and then, weighted at room temperature to obtain the dry weights. Afterward, the specimens were placed in deionised water at 50 °C, using a temperature bath. Periodically, the samples were removed and dried with filter paper. Then, after reaching to room temperature in a desiccator, they were weighed and finally returned to the water bath. The procedure was repeated until the samples reached the saturation level.

5.3. Results and discussion

Before the kinetic analysis of solvent sorption experiments as function of composition, this section studies the morphology, rheological behavior and crystalline state of different CNT composites. The final propose is to find the relationships between the sample microstructure and the water uptake behaviour.

5.3.1 Morphology

Figure 1 shows the SEM micrographs of PA12/PA6 nanocomposites with different CNT contents. The micrographs show an acceptable dispersion level of nanotubes in polyamide matrix, as CNT content increases.

Besides, as was proven in a previous work [5] from TEM micrographs, the two polyamides are distributed in two different phases (island-sea morphology) and CNTs are mainly found in the interphase between polyamides. The achievement of this morphology depends on two key factors: viscosity ratio between the immiscible polymers and the interfacial energy of CNT/polymer. In this case, the viscosity ratio PA12/PA6 is 0.54 and CNT were pre-dispersed within the lower viscosity polyamide (PA12). This fact is advantageous to obtain a good dispersion of nanotubes in the polymer matrix during the mixing process, as shown in this case in the SEM micrographs.

This preferential localization of carbon nanotubes (in the polyamides interphase) is the desired morphology to form a segregated network and to obtain low percolation thresholds [25]. The effect of this morphology will be evaluated in other properties hereinafter.

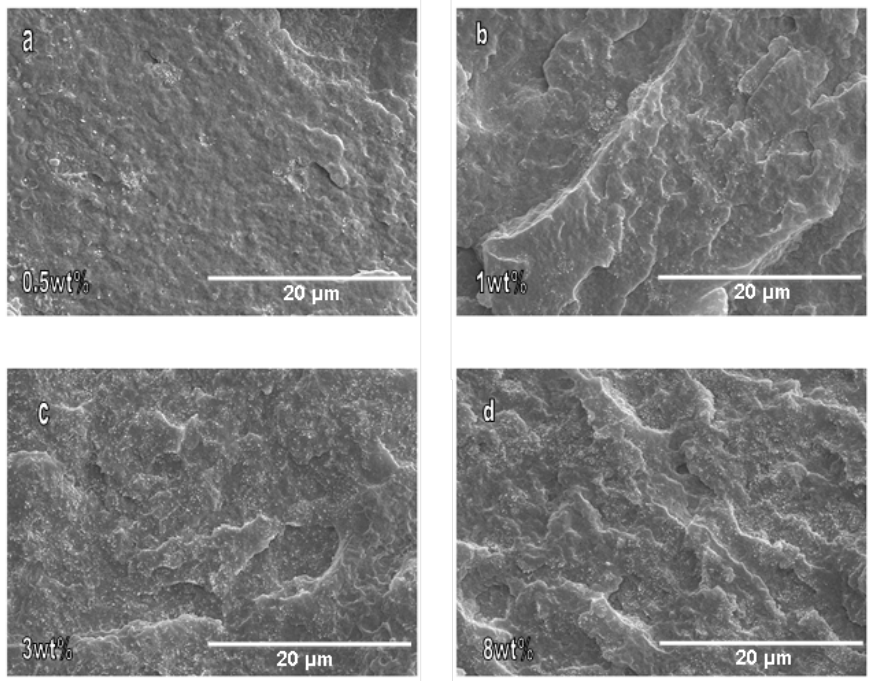

Figure 1 SEM micrographs of PA12/PA6/MWCNT composites. Legend inside shows the respective nanotube contents

5.3.2 Rheological measurements

The rheological data previously published [5] showed that there is a transition between liquid-like and solid-like behavior, above 0.5 wt.% CNT, in this system. This fact indicates that an interconnected structure of nanotubes is formed in the polymer matrix [26,27]. In the work cited in reference [5], a rheological threshold of $p_{c,G'} = 0.15$ wt.% and a electrical threshold of $p_c = 0.42$ wt.% were obtained.

Although the rheological threshold was detected at low CNT concentrations, it is possible that other physical properties are more related to the stiffness evolution of samples. For these reason, a more detailed study of this aspect was performed. Figure 2 represents storage modulus versus loss modulus. The slope of G' versus G'' decreases with increasing nanotubes content. The shift and the change in slope of the G' versus G'' curves indicate

that the microstructure of these composites changes significantly with addition of nanotubes. In this graph it can be observed too that PA12/PA6 blend presents a liquid like behavior (G''>G') in all frequency range. At contents 0.5 wt.% MWCNT (above rheological threshold) this behavior starts to change. The G'/G'' crossover points are collected in Table 1. In the Table is clear that the crossover points shift to higher frequencies as MWCNTs increase until a solid like behavior is obtained (G'>G'') for nanocomposite with 8 wt.% CNT in all frequency range. This behavior is also observed in Figure 2, all composites intersect in some point of G'=G'' line except the PA12/PA6/CNT composite with 8 wt.% of nanofiller. The increase in the elastic response with the MWCNT content indicates that the amount of interfaces between MWCNTs has increased, that is, a dense percolated network has been formed that causes a higher melt strength.

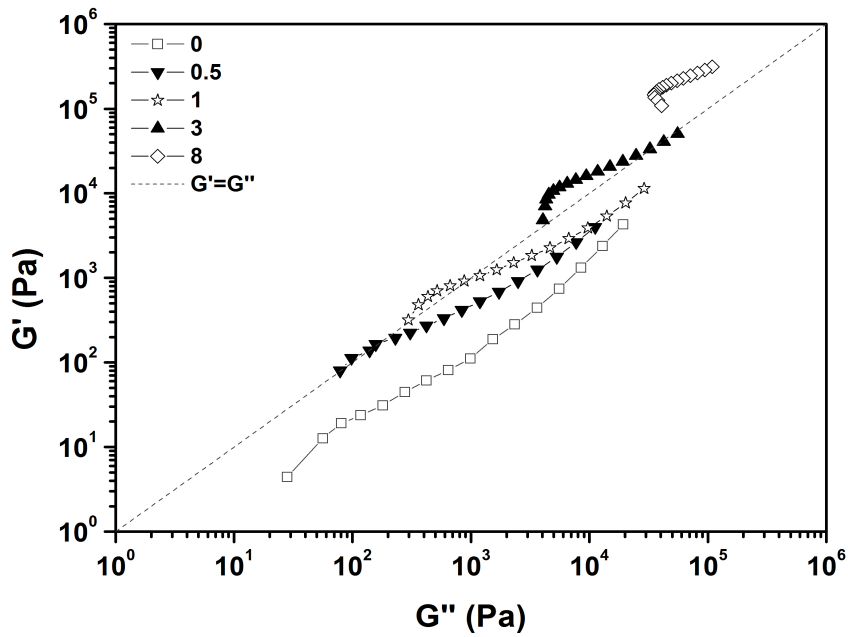

Figure 2 Storage modulus as function of loss modulus of PA12/PA6/MWCNT composites

In conclusion, taking into account the composites stiffness behavior observed in rheology, a CNT amount higher than electrical and rheological thresholds [5] could be necessary to

reach substantial increments in other properties of nanocomposites (as water uptake).

5.3.3 Effect of MWCNT contents on crystallization of polyamides

The nucleating effect of CNT in semicrystalline polymers is well known from literature. As macroscopic properties (conductivity, mechanical parameters or water uptake content) depend on the material crystallinity it is important to investigate the effect of CNT amount in the thermal behavior of polyamide blend.

5.3.3.1 Melting behavior and crystalline degree

Figure 3a shows the DSC curves obtained during the first heating of samples prepared with similar thermal history than the samples used for water uptake experiments, rheological tests and XRD measurements.

As can be observed, the pristine polyamides melt in different temperature ranges, showing well-defined melting peaks centered at 180.8 ± 0.2°C (PA12) and 223.0 ± 0.1°C (PA6) with a crystalline degree of 29,5 ± 0.7 % for PA12 and 29.0 ± 0.8 % for PA6. Besides, both polyamides display a cold crystallization peak probably due to the presence of metastable phase which reorganizes into other stable phase (α or γ, according to PA6 or PA12). In the thermograms of polyamide blend and CNT composites, this exotherm is only observed before the melting peak of PA12. Probably, recrystallization exists in PA6 but it is overlapped with the other thermal events. The exotherm is well defined in composites with low CNT contents. As nanotubes amount increases, the exothermal is more difficult to detect, for this reason, it was not taken into consideration for the crystallinity calculus from 1wt.% CNT.

The thermogram of 50/50 PA12/PA6 sample shows two separate melting peaks but centered at slightly lower temperatures than the pristine polyamides. When the CNTs are added, the effect obtained is different in PA12 than in PA6. DSC thermograms for the first scan show that while PA12 peak is practically unaffected, the PA6 melting peak widens at lower temperatures.

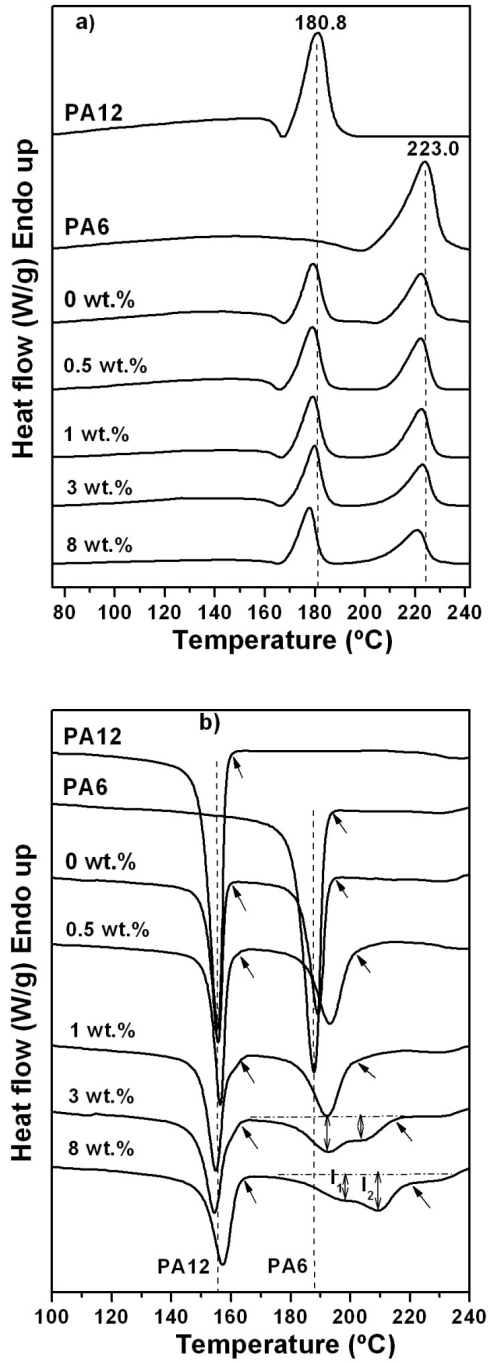

Figure 3 DSC thermograms of PA12/PA6/MWCNT a) first heating and b) cooling scans

The crystallinity degree of both polyamides was calculated from the area under melting peak obtained after deconvolution of peaks (Figure 6). The overall crystallinity of samples (Xc DSC) increases with 1 and 3 wt.% CNTs. This enhance is related with the PA12 crystallinity, which increases noticeable from 3 wt.% whereas the PA6 crystallinity remains practically constant. On the other hand, notwithstanding the PA6 crystallinity remains practically constant with the CNT increases, the widening of its melting peak, mentioned before, suggest a greater heterogeneity in the crystal population of Polyamide 6 as CNTs increasing [28].

The crystallinity changes in both polyamides can be explained if the composites morphology is considered. As discussed above, CNTs are included from a masterbatch in PA12 matrix with a lower viscosity than PA6. However, due to the rheological properties of polyamides and the lower interface energy between CNT and PA6, the nanotubes are preferably localized in the polyamides interface. After the electrical threshold ($p_{c'} = 0.42$ wt.%.), the CNT network is denser (as was previously commented in rheology section) and some nanotubes are present in both polyamides acting as nucleating agents [5]. For this, from the 1 wt.% CNTs, PA12 crystallinity increases significantly and the widening in the PA6 melting peak is more evident.

However in PA12/PA6/CNT composite with 8 wt.% CNT, the overall and single polyamide crystallinities were slightly reduced. Some researches pointed out that high content of nanotubes could retard the growth of crystals, due to the confinement effect imposed by the CNT network on mobility of polymer chains, and so, lower the crystallinity values [29-31].

To examine the crystalline state of CNT/PA12/PA6 composites, XRD tests were performed using samples with similar thermal history than DSC samples.

Figure 4 shows XRD patterns for the PA12/PA6 nanocomposites. The diffraction peaks at 2θ = 20.6° and 23.4° are assigned to (200) and (202) + (002) planes of the α crystalline phase, whereas the peaks at 21.6° are assigned to (200) and (001) planes of the γ phase [32, 19] for PA6 and at 21.7° to the (200) plane of the γ phase in the case of PA12 [33]. To estimate the sample crystallinity, a deconvolution procedure was applied on the patterns using the open-source software Fityk [34]. Each pattern was decomposed in an amorphous halo and the peaks, corresponding to α and γ phases, as described above.

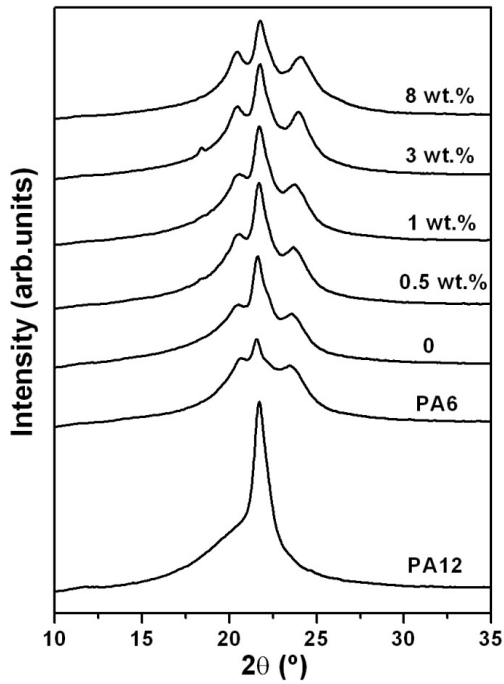

Figure 4 XRD patterns of polyamides, polyamide blend and their composites with different MWCNT contents

From the results obtained, the crystalline degree and the contribution of α and γ phases were calculated for each sample. As an example, Figure 5 displays the fitting performed for the pristine PA6 and PA12. The fitting of XRD patterns results in crystallinity values of 51.4 % for PA6 and 34.1 % for PA12. Besides, the PA6 pattern displays a little contribution of γ phase to its crystallinity. It was not detected in the DSC thermogram which displayed a single peak (corresponding with the melting of α phase). It is possible that the γ phase melt (around 118°C) was overlapped by the α phase melt or that it has recrystallized in other more stable phase (as α phase) during the DSC heating. The PA12 pattern displays only γ phase in agreement with the single peak detected by DSC. The discrepancies between both techniques are important in the crystallinity calculus of pristine PA6. In this case, it is clear that, DSC leads to an underestimation of PA6 crystallinity level (29% versus 51% measured by XRD). The fact that it does not happen in pristine PA12 (29.5% by DSC versus 34.1% by XRD), leads us to

believe that it could be related with hygroscopic capacity of PA6. This polyamide can absorb moisture during the time of DSC sample preparation [22] which is lost endothermically during the sample heating, shifting the baseline.

The comparison of overall crystallinity of samples obtained from DSC scans and the XRD patterns (see Figure 6) are in reasonable agreement. For both techniques, the crystallinity of composites increases as CNT amount increases, except for PA12/PA6/CNT composite with 8 wt.% nanofiller as noted above.

The discrepancies in crystallinity values between DSC and XRD tests for polyamides were previously examined by Khanna [22]. The different thermal events which occur during the heating scan of PA6 (lost moisture, subsequent melting and recrystallization of less stable phases, etc) handicap the placement of DSC baseline and, consequently, the measurement of melt enthalpy.

In spite of this, as concerns the effect of the addition of MWCNT in crystalline phases of polyamides, the data confirms that CNTs promote the formation of the α form crystals, making it the dominant phase (see Figure 4). The γ phase was also detected in the composites patterns, but it did not follow a clear upward trend as function of nanotubes content.

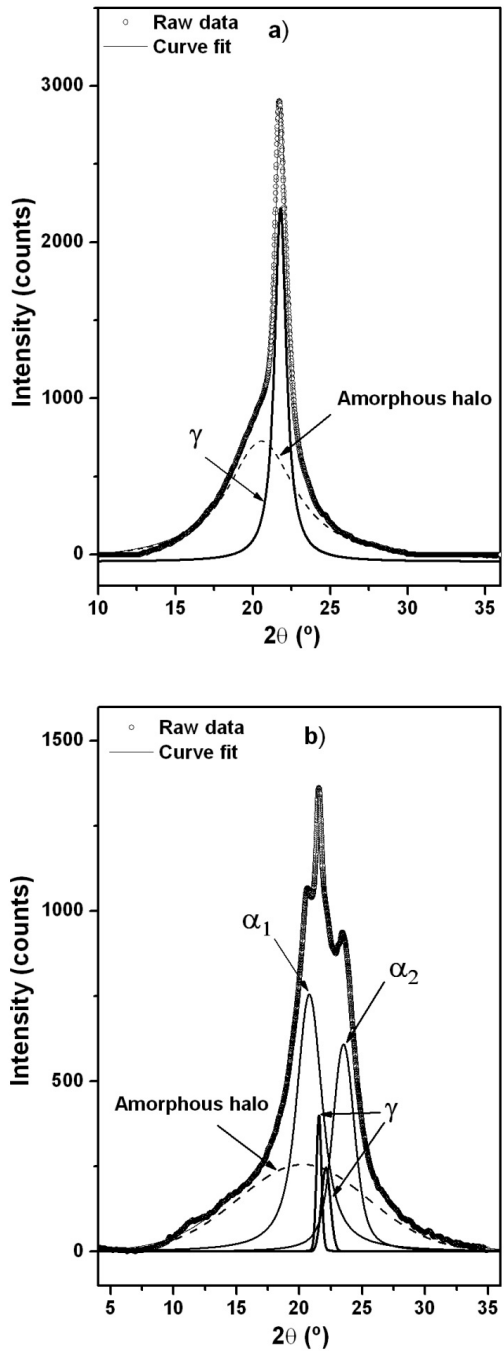

Figure 5 Deconvolution of XRD patterns with the software Fityk for: a) PA12 and b) PA6

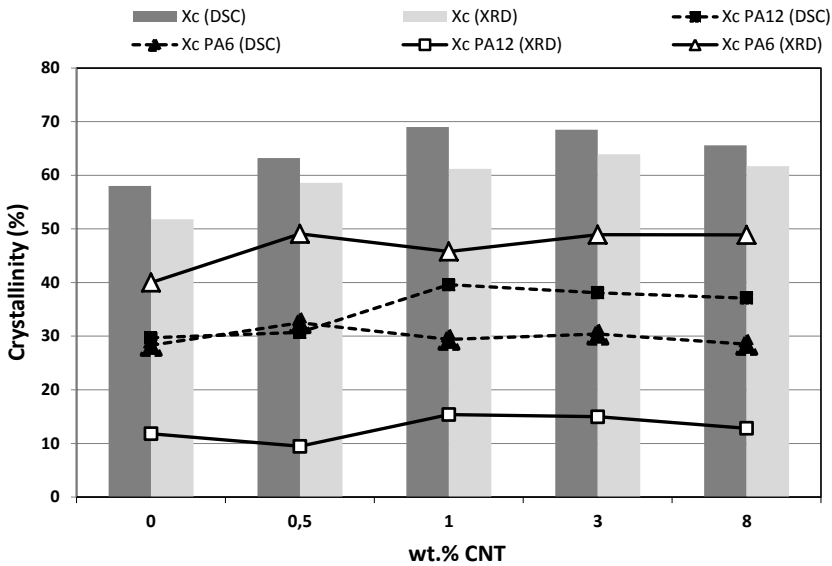

Figure 6 Crystallinity data obtained by XRD and DSC techniques and water uptake normalized at polyamide mass, as function of MWCNT content

It has been well-documented that for PA6 the α crystalline phase is thermodynamically stable and consists of sheets of hydrogen bonded chains formed between antiparallel chains. As the same way, the γ crystalline phase, predominant in pristine PA12, is metastable and consists of random hydrogen bonding between parallel chains [35]. On the assumption that all α form crystals belong to PA6 and all γ phase, to PA12, the contribution of each polyamide to overall crystallinity could be measured. Figure 6 plots the evolution of PA12 crystallinity (Xc PA12) and PA6 crystallinity (Xc PA6) calculated from the XRD data, together with the crystallinity of both polyamides measured by DSC. The Xc PA6 from the XRD data grows as CNT increases; meanwhile the PA6 contribution at DSC crystallinity did not follow the same trend. The evolution of the contributions Xc PA12 (XRD) and PA12 crystallinity by DSC is similar. But the main discrepancy is the fact that the contribution of PA12 is the highest in DSC crystallinity, while in XRD patterns, the main contribution to the overall crystallinity is due to PA6. It seems clear that the measurement by DSC overestimates the PA12 crystallinity in nanocomposites samples. Different melts and cold-crystallization events could be happening during the sample heating which are not considered in the enthalpy

calculus. On the other hand, the widening at lower temperatures of PA6 melting peak could be the cause of its crystallinity underestimation. Since, it increases the uncertainty in the placement of baseline.

5.3.3.2 Crystallization behavior

Figure 3b shows the crystallization exotherms of pristine polymers and nanocomposites. The nanotubes act as hetero-nucleating agents in both polyamides [36, 37]. The Tc and the onset temperature of crystallization (marked by arrows in the graph) are shifted toward higher temperatures in both polymers. The nucleating effect is more important in crystalline state of PA6. This fact is due to CNT migration from PA12 to PA6 during the nanocomposite extrusion, caused for a lower interfacial energy with PA6 than with PA12 [5], as can be mentioned before. Besides, PA6 displays a second crystallization peak/shoulder (centered at higher temperatures) clearly visible from 3 wt.% CNT. The relative intensity of the second crystallization peak increases as function of CNT amount. The splitting of the crystallization peak has been previously reported in other CNT/PA6 nanocomposites [38, 21]. Brosse et al [38] assigned the second crystallization peak to the trans-crystalline lamellae of PA6 on the nanotube surface, while the first one, to the crystalline lamellae which are not directly connected to nanotubes surface. In their work, the authors point out several factors as the origin of this phenomenon: the dispersion state of CNT into PA6 matrix, the existence of two crystalline phases or the existence of a unique phase with different lamellae morphologies. As was previously noted, the existence of γ phase in the crystalline state of PA6 cannot be excluded, even when the DSC thermograms obtained, in a subsequent heating (**supplementary material**) show a single melting peak corresponding to α phase melting. However, every facts point to the γ phase is minority in this case. For that, the splitting phenomena could be related with the CNT migration to PA6 (more important at higher CNT amount) and the morphology of CNT network, more stiffness at high nanotubes contents. This produces more interfaces between polyamide and nanotubes and, as consequence; more crystalline lamellae are nucleated on CNT surface, increasing the intensity of the second crystallization peak.

5.3.4 Effect of MWCNT contents on water uptake

The water uptake behavior is displayed in Figure 7 for the different nanocomposites and pristine polyamides. As shown in the

graph, all samples present a sigmoidal-shaped curve. In the first part of the curves (until about 25 hours), the water uptake is directly proportional to the time. This linearity allows the description of the sample behavior by means of a simple Fickian diffusion model. In this case, the diffusion coefficient and the equilibrium solvent uptake can be determined with the numerical solution of the approximated form of Fick's equation [39]:

$$\frac{M_t}{M_\infty} = 1 - \frac{8}{\pi^2} \sum_{m \to 0}^{\infty} \frac{1}{(2m+1)} \exp\left[\frac{D(2m+1)\pi^2 t}{l^2} \right] \qquad (3)$$

where M_t is the increase in mass at time t, M_∞ the increase in mass at infinite time (saturation state) and D is the diffusion coefficient through the thickness l of the material. Simplified solution of eq. (3) by Crank [40] showed that for the initial stage of the sorption process, that is, $Dt/l^2 << 0.05$ or $M_t/M_\infty < 0.6$, the following relation can be applied:

$$\frac{M_t}{M_\infty} = \left(\frac{16D}{\pi L^2} \right)^{1/2} \cdot t^{1/2} \qquad (4)$$

In this initial absorption phase, the diffusion profiles on the different sides of the sample do not overlap and develop independently. Thus, the diffusion coefficient of a polymer or nanocomposite can be determined from the best linear fitting of (M_t/M_∞) data versus $t^{1/2}$. The results obtained (D coefficient) together with normalized water uptake at saturation (i.e. ($mass_{water}$ / $mass_{dry\ polyamides}$) x100) are plotted in Figure 8. The diffusion coefficients are of same order of magnitude than those published in the literature for PA66 at high water activities and at room temperature [41]. As expected, PA6 water uptake at saturation is the highest one (7.6 %) and the diffusion rate of water molecules, faster than in the other samples. The opposite behavior is observed in the more hydrophobic polyamide 12, with an increase in mass of 1.4% at equilibrium and with a D coefficient about a half that for PA6. The PA12/PA6 blend shows an intermediate behavior, closer to the expected behavior predicted by the mixture rule. But when the nanotubes are included in polymer, the normalized water content at equilibrium, is slightly lower from 3 wt.% CNT. With less nanofiller amount, the water uptake at equilibrium is similar to the polyamides blend. Nevertheless, the reduction is important in comparison with pristine polyamide 6. This result is a clear

advantage in polyamide nanocomposites. Other researchers could not obtain similar improvements even adding up to 20 wt.% of nanotubes in PA6 matrix [19].

The diffusion of solvent molecules in CNT composites is also slower and, in consequence, the D values are lower with respect to the polyamides blend. Comparing the different nanocomposites, D remains constant up to 3 wt.% CNT and then, slightly decreases.

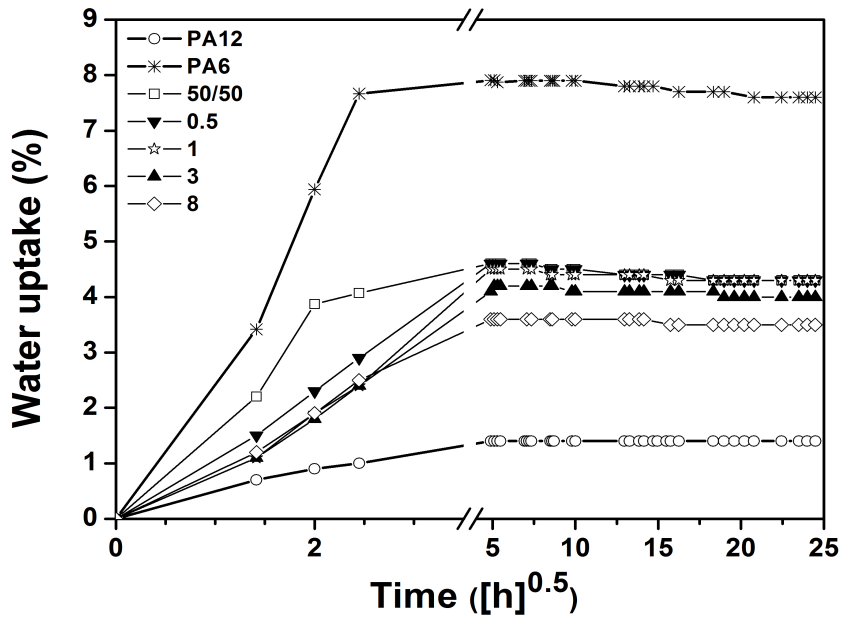

Figure 7 Water sorption behavior of polyamides, pristine blend and their MWCNT composites

In our case, the diminution of the water absorbed by polyamides is related with several factors. As it is known, the water is sorbed only in the amorphous phase of materials, because the crystalline part is inaccessible for water [42]. Thus, the crystallinity degree of nanocomposites is a key aspect. As discussed above, the overall crystallinity enhances as CNT increases except for the nanocomposite with 8 wt.% nanotubes. In this case, a denser network of CNTs (as was probed in rheological tests) could hinder the movement of water molecules through material, decreasing the diffusion coefficient and the water content at equilibrium. Besides, it should not be forgotten CNTs tend to move towards PA6, more

hygroscopic than PA12, reducing water absorption through its amorphous phase and, as a result, the overall water uptake of the nanocomposite.

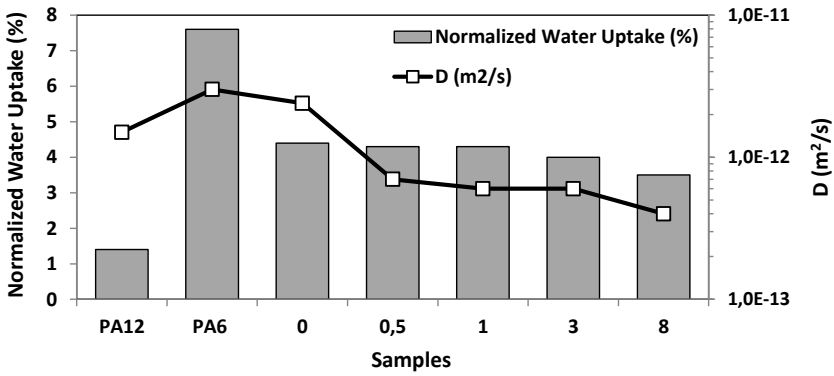

Figure 8 Normalized water uptake at saturation and diffusion coefficients of pristine polyamides, polyamides blend and MWCNT composites, measured at room temperature.

5.4. Conclusions

In this work, different MWCNT quantities were dispersed in an immiscible blend of 50/50 PA12/PA6. The mixing strategy followed to prepare the nanocomposites promoted a selective localization of CNT at the interphase between polyamides leading to a conductive segregated network with a low threshold. To explain the water uptake behavior of these nanocomposites, their morphology, their rheological properties and their crystalline state were assessed as function of the nanofiller content. The main conclusions are summarized below:

CNTs show an acceptable dispersion level into the polyamide blend, as was observed in SEM micrographs.

Rheological measurements exhibit important differences in stiffness of nanocomposites.

The total crystallinity of nanocomposites increases noticeable from 1 wt.% MWCNT. This enhancement is lower with 8 wt.% CNT associated with the restriction to mobility and diffusion of polymer chain segments caused by a denser conductive network. This

result is accordingly with the solid-like behavior observed in all frequency range for this composite.

By both DSC and WAXD, similar trend was obtained for the calculus of overall crystallinity but they differed in the measurements of the individual contribution of each polyamide to the overall crystallinity. The discrepancies can be explained for the uncertainty associated to the baseline placement in DSC experiments and to the amorphous halo in XRD tests.

The cooling thermograms obtained by DSC show that the nucleating effect of CNTs is more important in PA6 than in PA12. A second crystallization peak at higher temperatures was detected for PA6, related with the polyamide crystallization on nanotube surface

The water uptake experiments prove that the water uptake at saturation decreases and the diffusion of water molecules into the polymer matrix is slower in CNT nanocomposites than in PA6. These results are associated with the increase in crystallinity of polyamides and the migration of nanotubes to PA6 matrix in composites with high CNT amounts.

These positive outcomes show that the achievement of conductive segregated network morphology allowed the improvement in the water sorption behavior of PA/CNT composites. This is critical to achieve suitable properties in the new nanocomposites designed.

5.5. Supplementary information

DSC second heating of PA12/PA6/MWCNT composites at different MWCNT contents

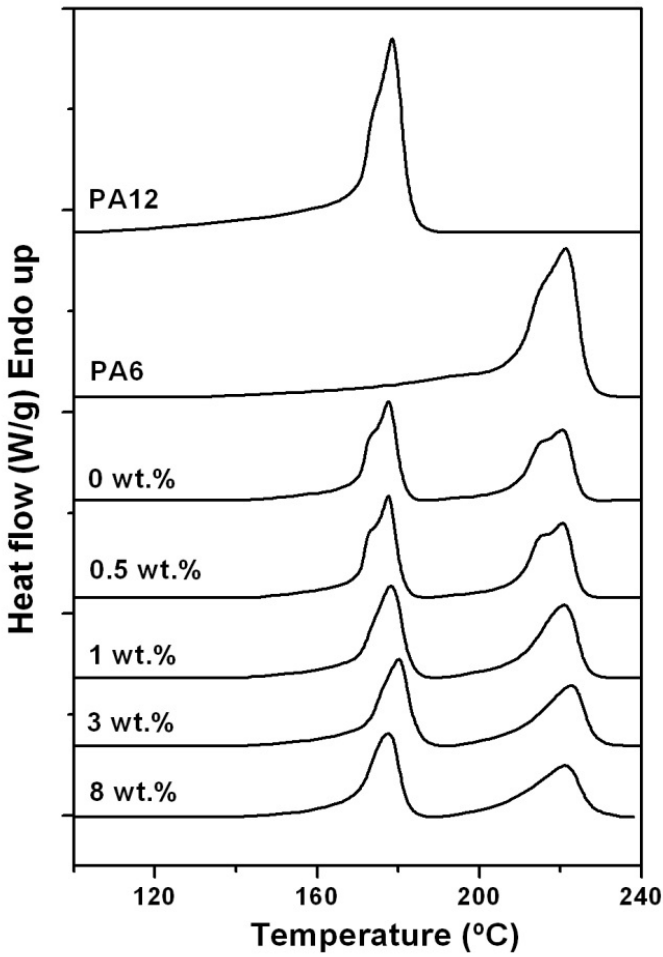

5.6. References

1. Dencheva N, Nunes T, Oliveira MJ, Denchev Z. Polymer, 46: 887 (2005)

2. Liu X-Q, Yang W, Xie B-H, Yang M-B**.** Materials and Design, 34:355 (2012)

3. Jogi BF, Bhattacharyya AR, Poyekar AV, Pötschke P, Simon GP, Kumar S., 55(2): 457-465 (2015)

4. Besco S, Lorenzetti A, Roso M, Modesti M. Polymers for Advanced Technologies, 22: 1518–1528 (2011)

5. Arboleda-Clemente L, Ares-Pernas A, Dopico S. Polymer Composites, 1–8. doi: 10.1002/pc (2015)

6. Launay A, Marco Y, Maitournam MH, Raoult I. Mechanics of Materials, 56: 1 (2013)

7. Reimschuessel HK. Journal of Polymer Science: Polymer Chemistry, 16: 1229 (1978)

8. Bretz PE, Hertzberg RW, Manson JA. Journal of Materials Science, 16: 2061 (1981)

9. Valentin D, Paray F, Guetta B. Journal of Materials Science, 22: 46 (1987)

10. Puffr R, Sebenda J. Journal of Polymer Science Part C: Polymer Symposia 16: 79 (1967)

11. Cohen MH, Turnbull D. Journal of Chemical Physics, 31(5): 1164 (1959)

12. Kumins CA, Kwei TK. Handbook of Diffusion in polymers: Free volume and other theories; Crank J, Park GS, Eds: p.108 (1968)

13. Moy P, Karasz FE. Polymer Engineering and Science, 20(4): 315 (1980)

14. Merdas I, Thominette F, Tcharkhtchi A, Verdu J. Composites Science and Technology, 62(4): 487 (2002)

15. Zimm BH, Lundberg JL. Journal of Physical Chemistry, 60(4): 425 (1956)

16. Fedors RF. Polymer, 20(9): 1087 (1979)

17. Sabard M, Gouanve F, Espuche E, Fulchiron R, Seytre G, Fillot L-A. Journal of Membrane Science, 415–416: 670 (2012)

18. Le Gac PY, Roux G, Davies P, Fayolle B, Verdu J. Polymer, 55(12): 2861 (2014)

19. Logakis E, Pandis C, Peoglos V, Pissis P, Stergiou C, Piontek J, Pötschke P, Micusik M, Omastova M. Journal of Polymer Science Part B: Polymer Physics, 47: 764 (2009)

20. Sengupta R, Ganguly A, Sabharwal S, Chaki TK, Bhowmic AK. Journal of Materials Science, 42: 923 (2007)

21. Phang IY, Ma J, Shen L, Liu T, Zhang W-D. Polymer International, 55: 71 (2006)

22. Khanna YP, Kuhn WP. Journal of Polymer Science Part B: Polymer Physics, 35: 2219 (1997)

23. Edith Turi A. Handbook of Thermal characterization of polymeric materials, Vol. 2, Polytechnic University Brooklyn, New York (1997)

24. Gogolewski S, Czerntawska K, Gastorek K. Colloid and Polymer Science, 258(10): 1130 (1980)

25. Pang H, Xu L, Yan D-X, Li Z-M. Progress in Polymer Science 39: 1908 (2014)

26. Pötschke P, Abdel-Goad M, Alig I, Dudkin S, Lellinger D. Polymer, 45: 8863 (2004)

27. Meincke O, Kaempfer D, Weickmann H, Friedrich C, Vathauer M, Holger W. Polymer, 45: 739 (2004)

28. Caamaño C, Grady B, Resasco DE. Carbon, 50: 3694 (2012)

29. Li J, Fang Z, Tong L, Gu A, Liu Fu. Journal of Polymer Science Part B: Polymer Physics, 44: 1499 (2006)

30. Xiang F, Shi Y, Li X, Huang T, Chen C, Peng Y, Wang Y. European Polymer Journal, 48: 350 (2012)

31. Ke K. Wen R, Wang Y, Yang W, Xie BH, Yang MB. Journal of Materials Science, 4: 1542 (2011)

32. Liu T, Phang IY, Shen L, Chow SY, Zhang W-D. Macromolecules, 37: 7214 (2004)

33. Dencheva N, Nunes TG, Oliveira MJ, Denchev Z. Journal of Polymer Science Part B: Polymer Physics, 43(24): 3720 (2005)

34. Wojdyr M. Journal of Applied Crystallography, 43(5): 1126 (2010)

35. Lincoln DM, Vaia RA, Wang Z-G, Hsiao BS. Polymer, 42: 1621 (2001)

36. Ryu J, Han M. Composites Science and Technology, 102: 169 (2014)

37. Jose MV, Steinert BW, Thomas V, Dean DR, Abdalla MA, Price G, Janowski GM. Polymer 48: 1096 (2007)

38. Brosse A-C, Tencé-Girault S, Piccione PM, Leibler L. Polymer 49: 4680 (2008)

39. Crank J, Park GS. Handbook of Diffusion in Polymers; J.Crank, G.S. Park Eds; Academic Press, New York (1968)

40. Crank J. Handbook of the Mathematics of Diffusion; Chapter 4, Clarendon, Oxford (1994)

41. Broudin M, Le Gac PY, Le Saux V, Champy C, Robert G, Charrier P, Marco Y. European Polymer Journal, 67: 326 (2005)

42. Kohan MI. Handbook of Nylon plastics handbook; Carl Hanser Eds, Munich (1995)

Capítulo 6

Improving thermal conductivity of polyamide 12/polyamide 6 composites with a segregated network of MWCNT

Página intencionadamente en blanco

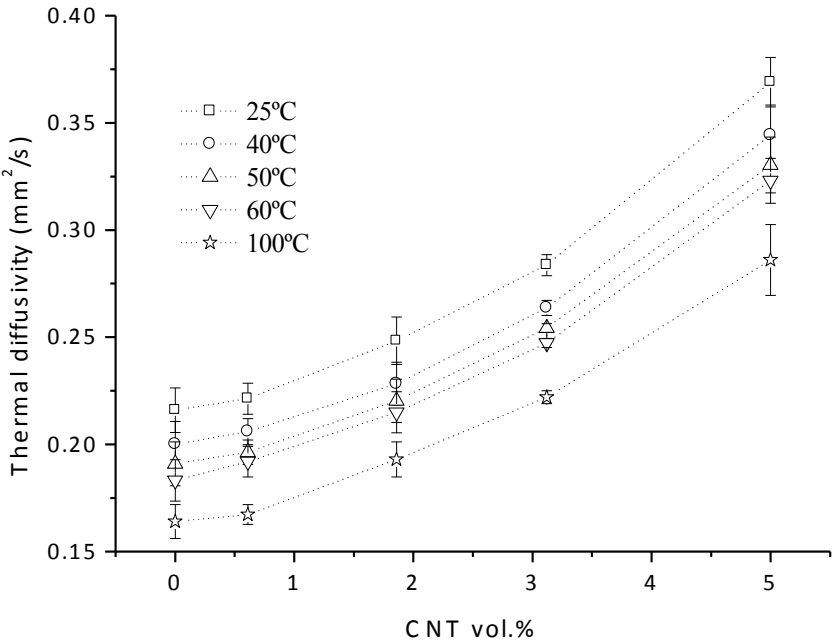

Estudio de la relación entre la condutividad térmica, la morfología y las propiedades reológicas. Efecto de la temperatura en el nivel de percolación y en la estructura de red conductora.

Este capítulo está basado en la siguiente publicación:

Laura Arboleda-Clemente, Xoán-Xosé García-Fonte, María-José Abad, Ana Ares-Pernas, Improving thermal conductivity of polyamide 12/polyamide 6 composites with a segregated network of MWCNT, enviado Journal of Materials Science, enero 2017

Página intencionadamente en blanco

6.1. Introduction

In the manufacturing of electrical and electronic devices, the use of polymers is widespread because these materials offer unique properties as good processability, light weight, low water absorption, high electrical resistivity, high voltage breakdown strength, corrosion resistance and most importantly, low cost, in comparison with other materials. By contrast, most polymers have a low thermal conductivity, not enough to dissipate heat rapidly which is critical to the performance, lifetime, and reliability of electronic devices. The thermal conductivity of polymers depends on many factors, such as their physico-chemical properties, crystallinity, morphology, processing conditions, etc. In general, the phonon scattering through numerous defects or at the interface between the crystalline and amorphous phases (in semicrystalline polymers) causes low values in thermal conductivity for traditional polymers. For this reason, the development of polymers with improved thermal conductivity is a topic of great interest [1-4].

The incorporation of conductive fillers, into a polymer matrix is a commonly used method to obtain materials with tailored and controlled thermal conductivity without compromising the processing ease of the polymer matrix [5-8]. Traditionally, graphite, carbon black, carbon fibers, ceramic or metallic particles were used as thermal conductive fillers. With the development of nanotechnology, numerous studies were focused on the use of conductive nanofillers, as carbon nanotubes (CNT), to improve the thermal conductivity of polymers [9].

CNTs exhibit a longitudinal thermal conductivity between 2000 and 6000 W/mK [9-11]. The great part of these values are based on theoretical simulations or indirect measurements due to the experimental difficulties associated with the measurements in nanoscale. Nevertheless, the most researchers agree that aspects as nanotube morphology, structural defects, functionalization or the presence of impurities affect to the thermal conductivity of nanotubes. Furthermore, the thermal conductivity of CNT polymer composites depends on structure formed during the processing step, the dispersion state of filler and on the interfacial thermal resistance (polymer-nanotube) [12-13] Due to all these reasons, thermal properties of CNT/polymer composites are lower than would be expected [14].

Localization of fillers into well-defined co-continuos region can be an option to enhance the thermal contact area between conductive particles of filler [15-16].

In our previous work, different quantities of multiwalled carbon nanotubes and an immiscible blend of polyamides, 50 vol.%/50 vol.%. Polyamide 12/polyamide 6 (PA12/PA6), were melt blending by extrusion to obtain conducting polymer composites. The mixing strategy followed, by using a PA12 masterbatch and an immiscible blend of polyamides, was suitable to form a segregated conductive network in the matrix with low CNT quantities. From electrical and rheological measurements, a low percolation threshold was determined, probably due to the high aspect ratio of the nanotubes, kept after the composite processing, and to the preferential localization of carbon nanotubes (CNTs) in the polyamides interfaces (the latter was confirmed by transmission electron microscopy) [17]. The water uptake at saturation of nanocomposites decreases respect to the pristine PA6 because of the diffusion of water molecules into the polymer matrix was slower. These results are associated with the increase in crystallinity of polyamides and the migration of nanotubes to PA6 matrix in nanocomposites with high CNT amounts [18].

In view of this outcome, it seems interesting to investigate the thermal conductivity of these CNT composites where nanofiller forms a segregated conductive network in the polyamide matrix. On the other hand, it is worthwhile to assess the effect of molding temperature in the CNT network structure, since if its structure was modified it could affect the nanocomposites properties. The rheology tests can be a useful tool for this aim.

So, in this manuscript, the thermal conductivity (TC) of the PA12/PA6/MWCNTs composites is studied and related with their rheological properties and their morphology. With the purpose to predict the thermal conductivity of these nanocomposites, several different models were evaluated and were compared with the experimental data. Besides, from a deeper rheological study, the effect of temperature in the percolation level and the conductive network structure is analyzed. The final target is to assess the impact of this variable in the network structure of nanocomposites and consequently, in their macroscopic properties as thermal conductivity.

6.2. Materials and methods

6.2.1 Materials and composite processing

A blend of Polyamide 12 (PA12 Grilamid supplied by EMS Grivory) and Polyamide 6 (PA6 Zytel supplied by DuPont) was

used in this study. PA6 has a density of 1.14 $g.cm^{-3}$, a melting temperature of 220 °C and a zero shear viscosity of 723.8 Pa.s measured at 235 °C. On the other hand, PA12 has a density of 1.01 $g.cm^{-3}$, a melting temperature of 180 °C and a zero shear viscosity 391.7 Pa.s measured at 235 °C. To prepare CNT composites, a masterbatch of MWCNT (NC7000, Nanocyl S.A, Sambrevile, Belgium) pre-dispersed at 15 wt.% in PA12 was used (Plasticyl PA1502, Nanocyl S.A, Sambrevile, Belgium). MWCNTs have an average diameter of 9.5 nm, a length of 1.5 ∓m, a carbon purity of 90% and a surface area of 250-300 $m^2.g^{-1}$, according to the supplier.

Sample Nomenclature	PA12 (wt.%)	PA6 (wt.%)	MWCNT(wt.%)	MWCNT(vol.%)
PA12	100	0	0	0
PA6	0	100	0	0
0	50	50	0	0
0.15	49.875	49.875	0.25	0.15
0.31	49.750	49.750	0.50	0.31
0.46	49.625	49.625	0.75	0.46
0.61	49.500	49.500	1.00	0.61
0.92	49.250	49.250	1.50	0.92
1.23	49.000	49.000	2.00	1.23
1.34	97.500	97.500	2.50	1.34
1.86	48.500	48.500	3.00	1.86
3.12	47.500	47.500	5.00	3.12
5	46.000	46.000	8.00	5.00

Table 1 Formulations of PA12/PA6/MWCNT nanocomposites

Composites of a 50/50 wt.%/wt.% PA12/PA6 blend and different MWCNT contents were prepared by diluting the masterbatch with the same PA12 used in the masterbatch (Table 1). Before extrusion, masterbatch and pristine polyamides were dried in an oven at 110 °C for 6 h. Then, the different composites were extruded using a co-rotating twin-screw extruder (Brabender

DSE 20) operating at 30 rpm, with a temperature profile between 220-235 °C. All the components were premixed by tumbling and then, fed simultaneously into the extruder. The extruded composites with the appropriate geometries for thermal and rheological tests were compression-molded at 245ºC applying a pressure of 30 bar for 5 min.

6.2.2 Characterization

The composites morphology was analyzed by transmission electron microscopy, an analytical TEM (JEOL JEM 1010) was used to investigate the CNT network formation in the different composites at nanoscale. Ultrathin sections of 70 nm were cut, at room temperature, from compression molded samples.

Viscoelastic characterization was performed by using a controlled strain rheometer (ARES, TA Instruments) with parallel-plate geometry (25 mm diameter, 1 mm gap) in the linear viscoelastic region (LVE) at various temperatures ranging from 235 to 255ºC. The rheological tests were performed in the linear viscoelastic region (LVE) where the modulus is independent of strain. LVE region was determined by a strain sweep test. Furthermore, frequency sweep measurements were set up in the frequency range from 10^{-1} to 10^{2} rad/s.

Thermal diffusivity of different CNT composites was measured by using the flash diffusivity technique with thermal analyzer (LFA 447 Nanoflash, Germany). For the measurements, round samples were compression-molded with 12.5 mm in diameter and 1 mm in thickness. The samples were sprayed with a coating of graphite on both sides before testing (for uniform thermal adsorption). Measurements were done at different temperatures ranging from 25 to 100ºC. The LFA 447 illumination is a Xenon flash lamp with a wavelength in broadband visible and near IR. Pulse corrected by Cowan model was used to analyze the data in analysis software. Finally, the thermal conductivities were derived from the following equation:

$$k = \alpha \ \rho \ c_p \qquad (1)$$

where k is the thermal conductivity, α is the thermal diffusivity, ρ is the density of sample, and c_p is the specific heat capacity. The nanocomposites density was calculated using the rule of mixtures, and their specific heat capacity c_p, by differential scanning calorimetry (DSC) using sapphire as standard.

6.2. Results and discussion

6.2.1 Morphological analysis

Fig. 1 shows the TEM micrograph of PA12/PA6 with 0.46 vol.% CNTs. As already seen in a previous work, the two polyamides are distributed in two different phases and CNTs are mainly placed in the interphase between polyamides. This preferential localization of carbon nanotubes (in the polyamides interphase) is the desired morphology to form a segregated network and to obtain low percolation thresholds [17]. Hence, the thermal conductivity is defined by composite morphology as well as, by the structure and properties of polymer and filler, the effect of this morphology in thermal properties of CNT composites will be evaluated hereinafter.

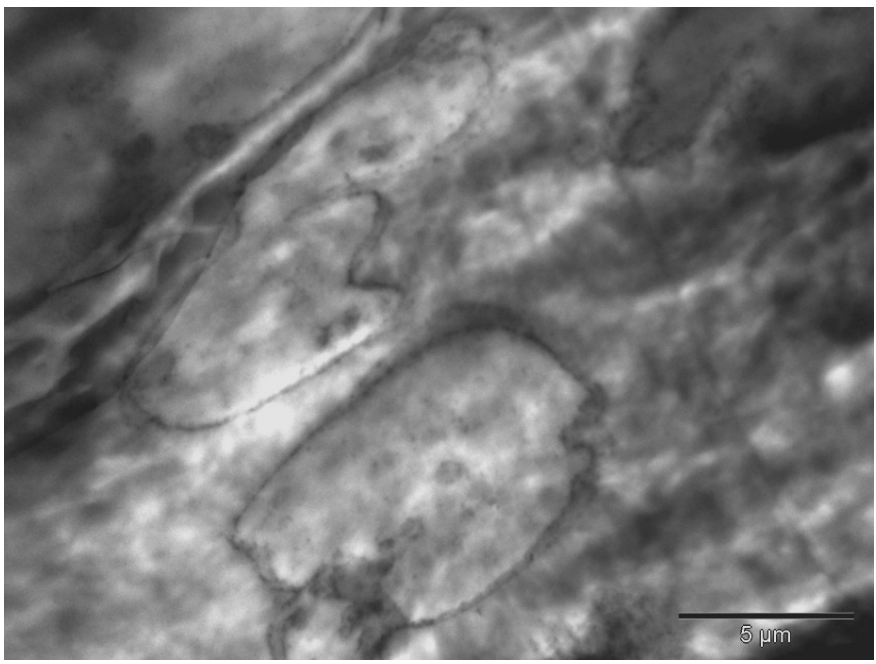

Figure 1 SEM micrographs of PA12/PA6/MWCNT composites; (a) 0.31 vol.% and 1.86 vol.%

6.2.2 Thermal conductivity

Fig. 2 and 3 show thermal diffusivity and thermal conductivity of nanocomposites respectively for several temperatures. It is clearly shown that, after adding CNTs, both properties enhanced in comparison with the polyamide blend, at any temperature. The

thermal diffusivity of unfilled polymer blend is comparable to values already published for different types of polyamides [4]. Increases of 41 % in thermal diffusivity and 78 % in thermal conductivity (Fig. 2 and 3), in comparison with the unfilled material, were observed for nanocomposites reinforced with 5 vol.% CNTs at 25ºC. The comparison of these values with the data previously published in other papers is difficult because of the different experimental techniques and matrices used for the TC measurements. Han et al. conducted a summary of thermal conductivities performances for CNT-based nanocomposites reported in the literature. They concluded that the greater part of k/k_P (TC composite/TC matrix) values are lower than 2 in nanocomposites with CNT volume fractions lower than 10 vol.% [9]. Our data are comparable and, in many cases, higher than ones previously published. The significant experimental error involved in thermal conductivity measurements is common in these tests. Difficulties in controlling the test conditions, such as the thermal contact resistance with the sample, lead to accuracy of thermal conductivity measurements typically in the range of 5-10%. In indirect methods that assess the thermal conductivity from the thermal diffusivity, experimental errors on density and heat capacity values also contribute to the experimental error in the thermal conductivity.

Fig. 2 and 3 show the temperature-dependent changes in thermal properties of PA12/PA6 nanocomposites. The reduction observed in thermal diffusivity with increasing temperature can be related with the softening of the polymer [19-20]. Whereas, the thermal conductivity rises lightly with temperature increases (Fig. 3).

To analyze if some mathematical model could predict the thermal behavior of nanocomposites, several of them were used to adjust thermal conductivity data measured at 25ºC. The Table 2 displays the mathematical equations of used models and Fig. 4 and 6, the fit of the experimental data. In the adjustments, a value of 2000 W/mK was used for the thermal conductivity of MWCNTs according to the literature data [9-11].

One of the simpler models the series model. It is based on the assumption that the heat flux is uniform and the temperature gradient is the weighted sum of the temperature gradients through the matrix and filler domains. Our experimental data (see Fig. 4), is closer to the prediction of the series model. This is most suitable for composites where the fillers are dispersed in a matrix and there is no percolation even at high volume fractions [4].

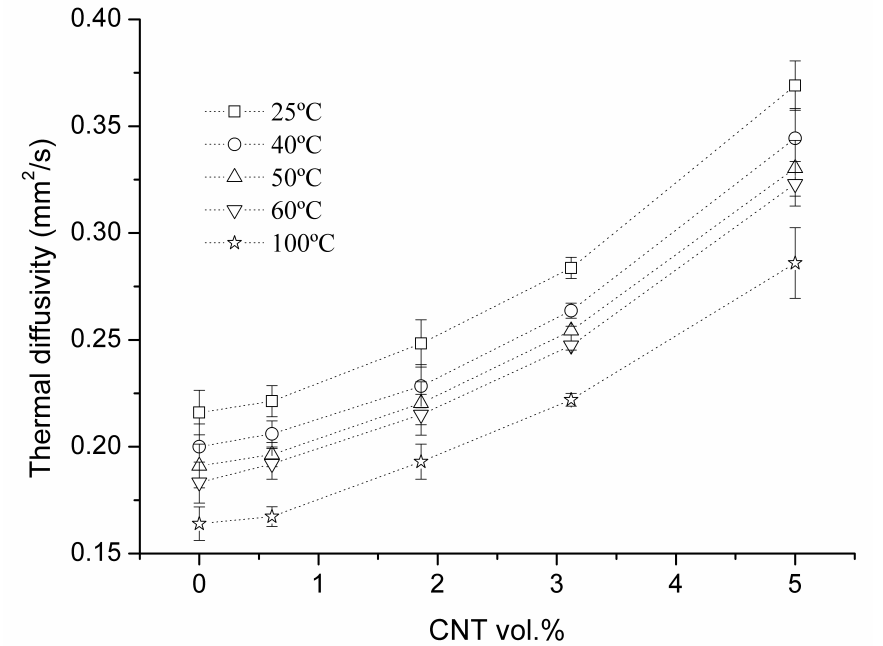

Figure 2 Thermal diffusivity of PA12/PA6/MWCNT composites vs. CNT loading at different temperatures.

A new approach to the TC behavior of nanocomposites was proposed by Maxwell-Garnett [4, 21] model. Nevertheless, the model fitting obtained similar results than the simple series model. Maxwell-Garnett model accepts that temperature experiences no discontinuity at the filler surface. This assumption works well on a macroscopic scale, but breaks down on much smaller characteristic length scales where the thermal energy carriers (electron or phonons) scatter at the interface.

Bruggeman model provides an extension of Maxwell model, where the interactions among the randomly distributed fillers are considered [22]. However, in view of Fig. 3, none of the models fit perfectly the thermal conductivity behavior. It may be due to none of these micromechanical models take into account the percolation phenomenon and the subsequent formation of a conductive network in the system from a critical amount of CNT (threshold).

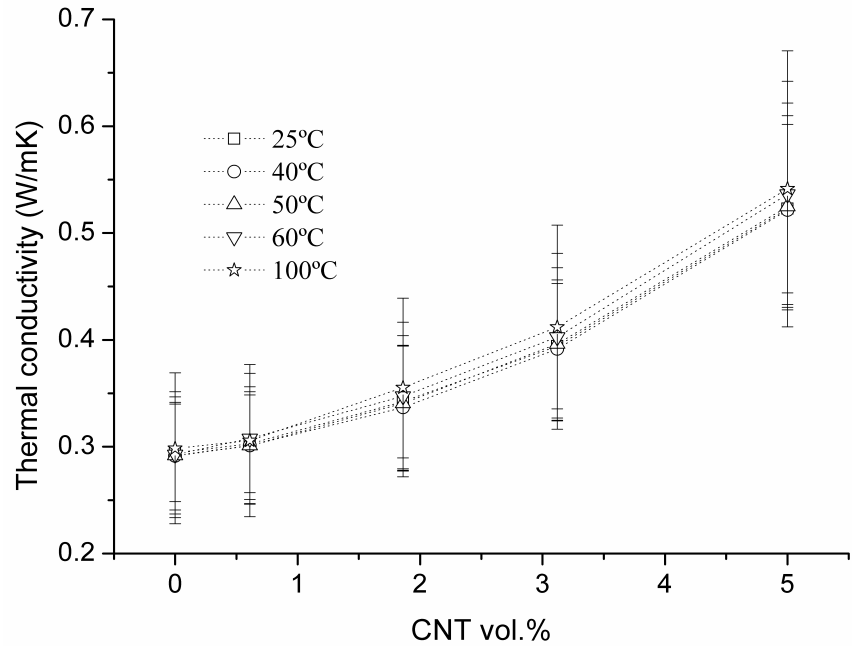

Figure 3 Thermal conductivity of PA12/PA6/MWCNT composites vs. CNT loading at different temperatures.

Unfortunately, the graphical representation of thermal conductivity data versus filler amount (Fig. 3) not show clearly, the threshold composition. The main reasons reported in literature in order to explain this lack of percolation threshold are the poor heat transfer between polymer and CNTs and the high thermal resistance between adjacent nanotubes. Nevertheless, there is still a debate whether, for these polymer composites, the thermal conductivity improvement should be described by means of percolation or by using effective medium approaches [23-24]. In the first case, as suggested Bonnet et al [25], thermal conductivity could be proper modeled by the data adjustment to the following equation:

$$\Delta k = k_0 \left[\frac{p - p_c}{1 - p_c} \right]^t \qquad (2)$$

where ϕ_c is the threshold composition. Since polyamides blend is not a thermal insulator, the contribution of the polyamides to the composite thermal conductivity is $k_p(1-p)$ whereas the difference $\Delta \mathrm{k} = k - k_p x(1-p)$ reflects the contribution arising from the

connected carbon nanotubes network. The evolution of ∆k with CNTs reduced volume fraction $(p - p_c)/(1 - p_c)$ is shown in Fig. 5. The solid line is the fit for $p \geq 0.15\ vol.\%$ with a $p_c = 0.09\ vol.\%$. The best fit for composites gives a prefactor $k_c = 6.78 \pm 0.18 W/mK$ and $t = 1.14\ (R^2 = 0.98)$. It must be pointed out a reduction of the exponent below 2, as discussed by Foygel et al [23].

The thermal conductivity prefactor k_0 should represent the thermal conductivity of the CNT network which is nearly three times lower than the 20-30 W/mK value measured on unaligned SWCNT buckypaper [26] and nearly 25 times greater than the thermal conductivity of PA12/PA6 blend. The goodness of lineal fit and the obtained results explain the reasonable use of percolation theory for describing the enhancement of thermal conductivity with CNTs increase in polyamide blend. This fact clearly suggests that above a certain critical content of carbon nanotubes ϕ_c, thermal conductivity is mainly controlled by CNTs network in this kind of systems. Besides, this critical composition is in line with the values of electrical threshold (p_c=0.258±0.001 vol.%) and rheological threshold (p_c=0.09±0.01 vol.%) previously calculated for these composites [17].

Since the critical composition or threshold is very low, the previous mathematical models which do not consider the effects of percolation phenomenon, only are valid for the lowest CNT compositions (see Fig. 4).

A different approach to the thermal conductivity behavior is the one proposed by Agari's model [27]. This empirical model, whose mathematical expression is displayed in Table 2, considers the dispersion state of filler and the matrix structure (or crystallinity) including two coefficients, C_1 and C_2. The first parameter, C_1, is related with the crystallinity and crystalline size of polymer and, the second one, C_2, with the ease in forming conductive paths. Although Agari corroborated the validity of his model in highly filled polymer composites with microparticles, others researchers have proved that Agari's model can fit reasonably well, the thermal conductivity data of nanocomposites [16]. Fig. 6 shows the adjustment of our experimental data to the Agari's model. The values of parameters obtained were C_1=0.96±0.02 and C_2=-1.3±0.1 (R=0.99).

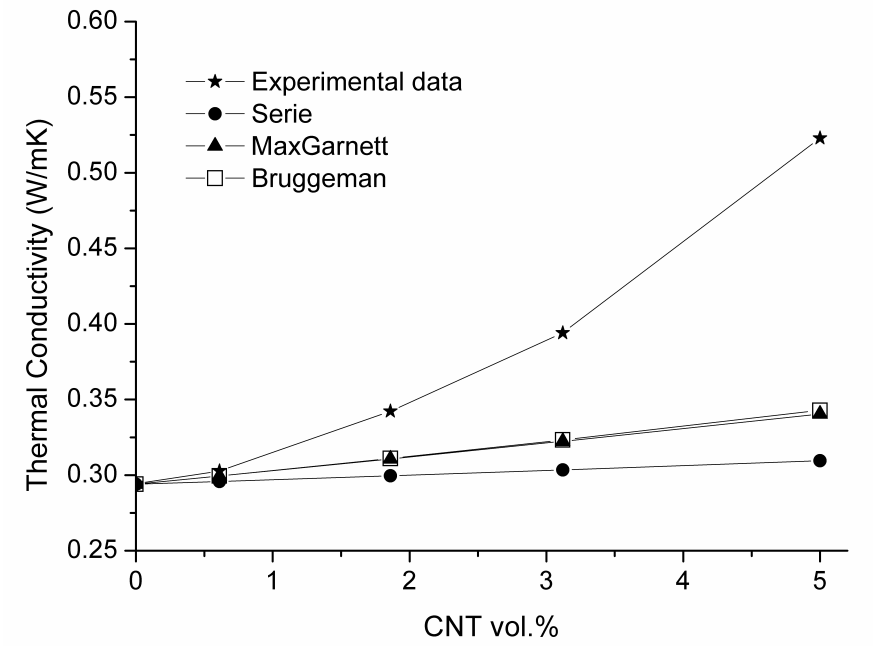

Figure 4 Thermal conductivity of PA12/PA6/MWCNT composites predicted by different models and compared with the experimental results measured at 25ºC

The value of C_1, closer to 1, suggests that the polyamides structure is not affected by the presence of nanotubes. Nevertheless, DSC and XRD data showed that polymer crystallinity increases when the nanotubes are added [18]. Probably, this change (a maximum increase around a 10%) was not enough to enhance the thermal conductivity. On the other hand, the value obtained for C_2 parameter (absolute value greater than 1) probes the ease of nanotubes in forming conductive paths in the matrix. This could be linked to the fact that the CNTs are preferably placed in the interface between polyamides, as was already proven [17].

Analytical models	Mathematical expression
SERIES	$k = \left[\frac{(1-p)}{k_P} + \frac{p}{k_f}\right]^{-1}$
MAXWELL-GARNET	$k = k_P\left(1 + \frac{3p(\delta-1)}{2+\delta-p(\delta-1)}\right)$ where $\delta = k_f/k_P$
BRUGGEMAN	$(1-p) = \frac{k_f - k}{k_f - k_p}\left(\frac{k_p}{k}\right)^{\frac{1}{3}}$
AGARI	$k = pC_2\, log k_f + (1-p) log(C_1 k_P)$

p:volume fraction of fillers

Table 2 Mathematical equations of used models

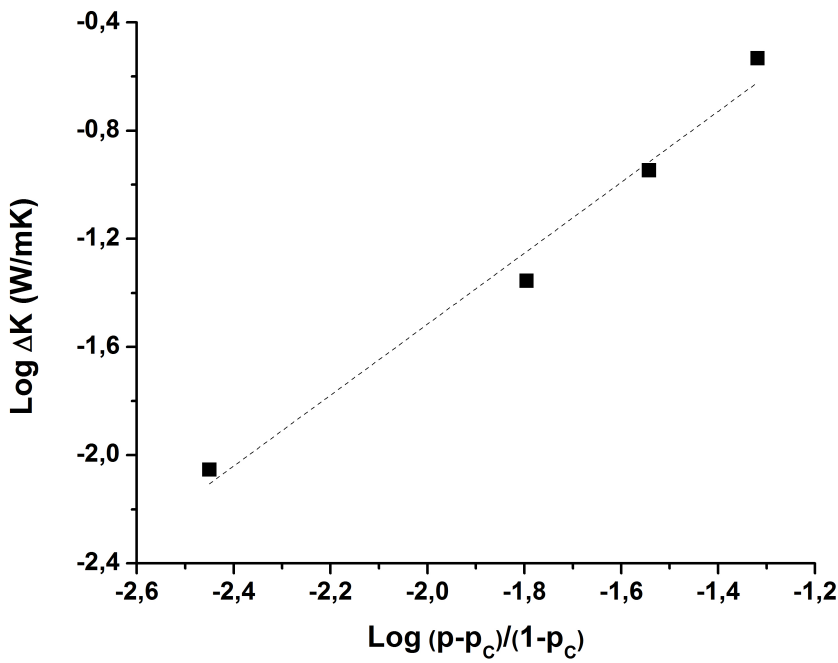

Figure 5 Thermal conductivity of CNT network ΔK contribution as function of reduced volume fraction of CNTs (log-log plot) and linear fit equation (2) for loadings $\phi \geq 0.15$ vol.%

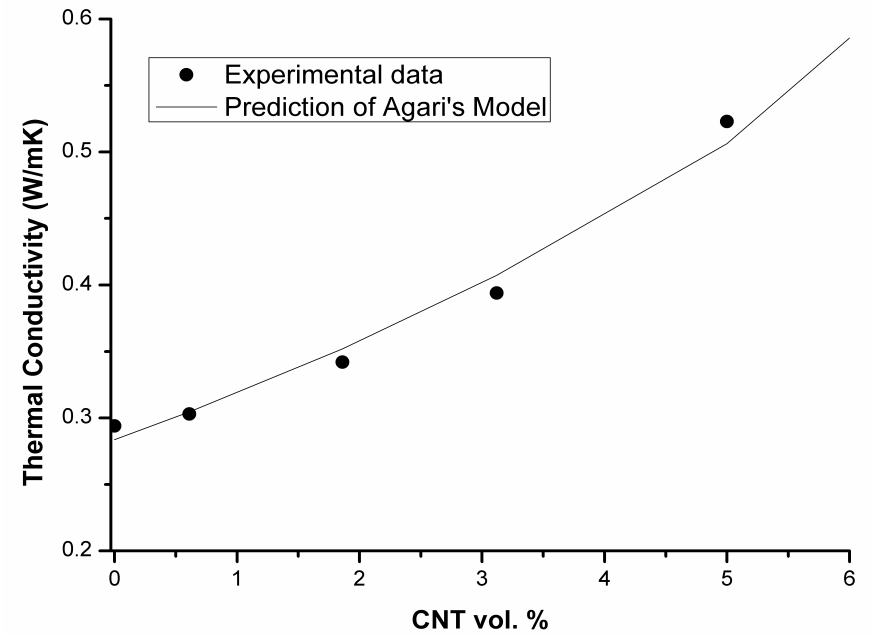

Figure 6 Thermal conductivity of PA12/PA6/MWCNT composites predicted by Agari's model and compared with the experimental results measured at 25ºC

6.3.3 Rheological properties

Since the thermal conductivity behavior of PA12/PA6/CNT composites can be explained using percolation theory, the percolation level reached by the CNT network should be considered to optimize the thermal conductivity values with the lowest filler amount. The percolation level and the conductive network structure are influenced by processing or molding temperature of materials, as was previously observed in other composites [28-29]. This aspect was carefully analyzed in PA12/PA6/CNT composites conducting rheological tests at different temperatures in the range between 235ºC and 255ºC. These temperatures were selected into the processing window of the nanocomposites. It is known that the changes observed in rheological properties near the percolation threshold of a filler network embedded in a viscoelastic liquid is equivalent to the so called "liquid-solid transition". This transition can be observed plotting different rheological parameters. One of these graphs, van Gurp-Palmen plots, are displayed in Fig. 7. In these graph, the phase angle, δ, is plotted against the absolute value of the complex

modulus, G*, for the a temperature of 235ºC. In these plot, it is possible to appreciate that the polymer chains corresponding to pristine PA12/PA6 blend are completely relaxed for a value or approximately 90º for δ in the low G* region. This indicates the dominant response of viscous flow in polyamides blend. On the other hand, the deviation of δ from 90º shows the elastic response of the nanocomposites, forming a percolated structure in the melt sample. As it is shown in Fig. 7 the value of δ begins to decrease with CNTs increasing. To help obtain a clearer representation of the data, Fig. 8 just displays the rheological curves for a set of nanocomposites at different test temperatures. Similar trend was obtained in the tests performed at 245 and 255ºC.

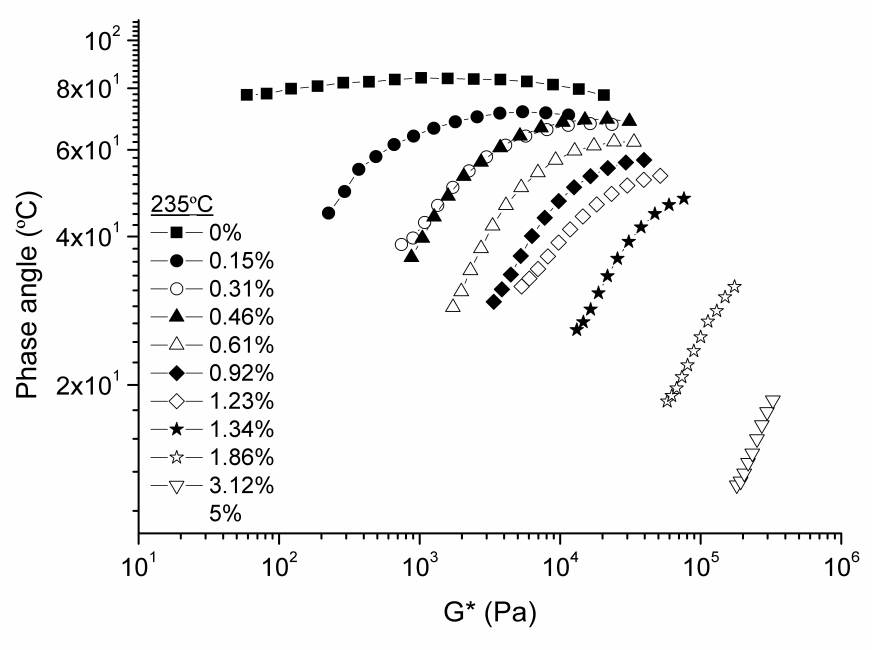

Figure 7 Van-Gurp Palmen plot of PA12/PA6/MWCNT composites at 235ºC

The appearance of a maximum in δ at some intermediate value of G*, suggesting a liquid-solid transition, was observed in the rheological tests performed at the three temperatures. The value agrees with a previous study which concluded that from 0.15 vol.% CNT the nanocomposites are rheologically percolated (see Fig. 7) [17]. Moreover, when the test temperature increases, a

displacement of this maximum to high values of G* is observed. This means that for the same CNT composite, as test temperature increases, the solid-like behavior is more pronounced. The crossover points (Table 3) calculated from graphical representation of moduli against frequency (some of these graphs were previously published in ref. [17]), proves this fact. From these data, the liquid-like behavior for pristine polyamide blend was confirmed for the three test temperatures. Besides, the crossover points were clearly shifted to higher frequencies as MWCNTs amount increased until a solid-like behavior, in all frequency range, is obtained (G'>G''). The improvement of the elastic response in CNT composites with high filler contents, indicates that the number of interfaces between CNTs has increased, that is, a denser percolated network was formed and it causes a high melt strength.

	ω_C / G_C (rad.s^{-1} / Pa)		
SAMPLE	**235ºC**	**245ºC**	**255ºC**
0	G''>G'	G''>G'	G''>G'
0.31	0.2 / 131	0.6 / 245	0,8 / 318
0.61	1.1 / 950	1.6 / 669	1,7 / 932
1.86	47 / 35880	G'>G''	G'>G''
5	G'>G''	G'>G''	G'>G''

Table 3 Crossover points of different PA12/PA6/MWCNT composites

If the rheological data obtained at different temperatures are compared, it can be observed that the transition to solid-like behavior occurs with low CNT amount at the highest temperatures (with 1.86 vol.% CNT at 245 ºC and 255ºC against 5 vol.% CNT at 235ºC), according to the trend observed in Fig. 8.

With the rheology results in mind, it seems that an increase in molding temperature leads lower viscosity values of polymer matrix, which could facilitate nanofiller dispersion resulting in a better formation of CNT network [30]. Pötschke and co-workers [31] proposed that the density of the networks changes with temperature due to the reduced particle-particle distance and enhanced interactions among CNTs in a lower viscosity matrix.

A denser CNT network could improve the conductive paths into the nanocomposite and consequently, enhance their thermal conductivity.

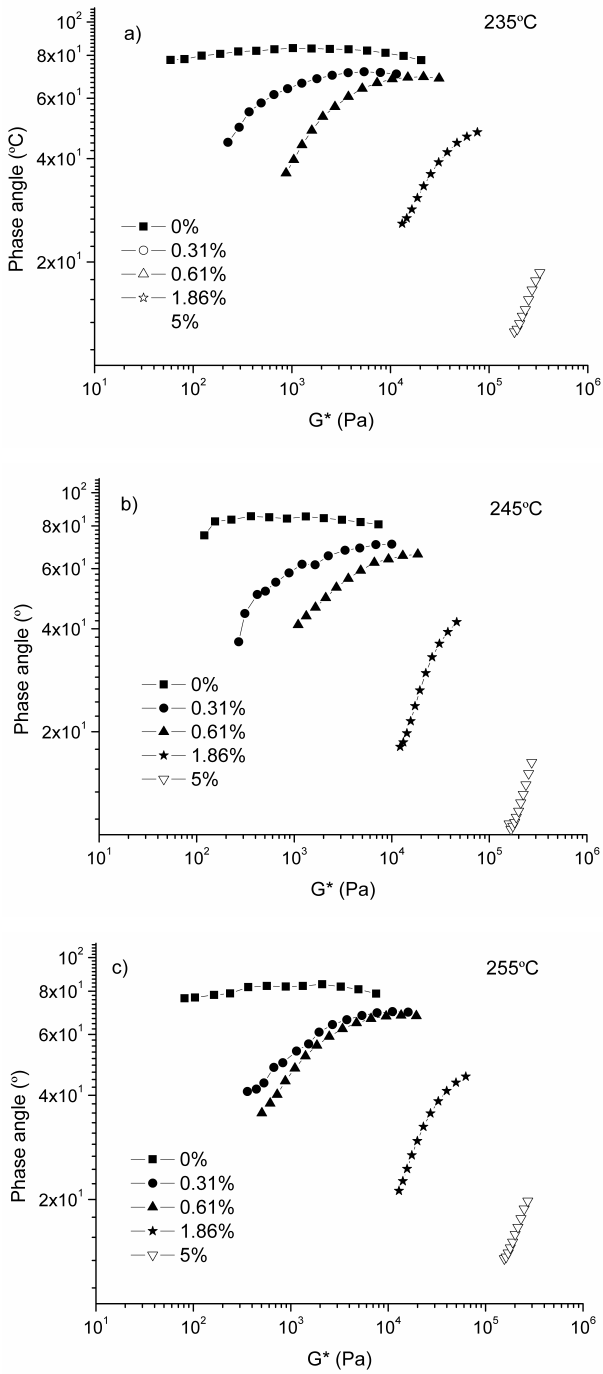

Figure 8 Van-GurpPalmen plot of PA12/PA6/MWCNT composites at different temperatures (a) 235ºC; (b) 245ºC and (c) 255ºC

6.3. Conclusions

The thermal conductivity of PA12/PA6/CNT composites was measured and was related with CNT amount, the composite morphology and the structure of conductive network. The main conclusions are summarized as follows:

-CNT incorporation produces significant increment in thermal diffusivity and thermal conductivity of PA12/PA6 blend (increases of 41 % in thermal diffusivity and 78 % in thermal conductivity at 25ºC with 5 vol.% CNT).

-The thermal diffusivity is temperature-dependent and it decreases as temperature increases due to the softening of polymeric matrix. On the contrary, the thermal conductivity of nanocomposites remained practically constant or increases slightly in the temperature range of the experiments.

-The comparison of the thermal data with theoretical and empirical models reveals that the classic approaches to the thermal conductivity behavior are not valid to predict the thermal properties of PA12/PA6/CNT composites since they do not take into account the contribution of the conductive network formed into the matrix. This contribution to thermal transport was proved by the data adjustment to the equation proposed by Bonnet. The threshold composition calculated (ϕ_c=0.09±0.01 vol.%) is in line with the values of electrical threshold and rheological threshold previously calculated for these composites.

-The empirical model proposed by Agari is able to predict accurately the thermal conductivity behavior of nanocomposites at 25°C. The parameters obtained from the data adjustment, suggest that the polyamides structure is not affected by the CNTs and the nanofillers can easily form conductive paths in the PA12/PA6 matrix.

-Finally, the rheological properties of nanocomposites measured at different temperatures, show that the transition to solid-like behavior occurs with lower CNT amount as molding temperature increases. It likely to be due to the lower viscosity of polymer matrix, which facilitates nanofiller dispersion causing the formation of denser CNT network and consequently, rising the number of conductive paths.

6.4. References

1. Moore AL, Shi L. Materials Today, 17: 163 (2014)
2. Tong XC, *Advanced materials for thermal management of electronic packaging*. Springer; New York (2011)
3. Huang XY, Jiang PK and Tanaka T. IEEE Electrical Insulation Magazine, 27: 8 (2011)
4. Chen H, Ginzburg V, Yang J, Yang Y, Liu W, Huang Y, Du L and Chen B. Progress in Polymer Science, 59: 41 (2016)
5. Kumar SK and Krishnamoorti R. Annual Review of Chemical and Biomolecular Engineering, 1: 37 (2010)
6. Winey KI, Vaia RA. MRS Bulletin, 32: 314 (2007)
7. Balazs AC, Emrick T, Rusell TP. Science, 314: 1107 (2006)
8. Tjong SC. Polymer Composites with carbonaceous nanofillers: properties and applications, Wiley-VCH; Weinheim (2012)
9. Han Z, Fina A. Progress in Polymer Science, 36: 914 (2011)
10. Kim P, Shi L, Majumdar A, McEuen PL. Physical Review Letters, 87: 215502 (2001)
11. Samani MK, Khosravian N, Chen GCK, Shakerzadeh M, Baillargeat D, Tay BK, International Journal of Thermal Science, 62: 40 (2012)
12. Kuriger RJ, Alam MK, Anderson DP and Jacobsen RL. Composites: Part A, 33: 53 (2002)
13. Gojny FH, Wichmann MHG, Fiedler B, Kinloch IA, Bauhofer W, Windle AH, Schulte K. Polymer, 47: 2036 (2006)
14. Chen T, Weng GJ and Liu WCJ. Applied Physics, 97: 104312 (2005)
15. Cao JP, Zhao X, Zhao J, Zha J-W, Hu G-H, Dang Z-M, ACS Applied Materials and Interfaces, 5 (15): 6915 (2013)
16. Cao J-P, Zhao J, Zhao X, You F, Yu H, Hu G-H, Dang Z-M, Composites Science and Technology, 89: 142 (2013)
17. Arboleda-Clemente L, Ares-Pernas A, García X, Dopico S and Abad MJ, Polymer Composites, doi:10.1002/pc (2015)
18. Arboleda- Clemente L, A. Ares-Pernas A, García-Fonte X, Abad MJ. Journal of Materials Science, 51: 8674 (2016)
19. Weidenfeller B, Hofer M, Schilling FR. Composites, Part A: 35: 423 (2004)
20. Weidenfeller B, Anhalt M, Kirchberg S. Journal of Applied Physics, 112: 093513 (2012)
21. Sharma J, Chand N, Bapat MN. Results in Physics, 2: 26 (2012)

22. Kim YS, Cho BJ, Sohn D-S, Park JM. Journal of Nuclear Materials, 466: 576 (2015)

23.Foygel M, Morris RD, Anez D, French S, Sololev VL, Physical Review B, 71: 104201 (2005)

24. Shenogina N, Shenogin LX and Keblinski P. Applied Physics Letters, 87: 133106 (2005)

25. Bonnet P, Sireude B, Garnier B, Chauvet O. Applied Physics Lett*ers*, 91: 201910 (2007)

26. Burton DJ, Glasgow DG, Lake ML, Kwag C, Finegan JC. Proceedings of the 46th International SAMPE Symposium and Exhibition, Long Beach, CA, 46: 647 (2001)

27. Agari Y, Ueda A, Tanaka M, Nagai S. Journal of Applied Polymer Science, 40 (5-6): 929 (1990)

28. Yuan L, Wu D, Zhang M, Zhou W, Lin D. Industrial and Engineering Chemistry Research, 50 (24): 14186 (2011)

29. Pöstchke P, Abdel-Goad M, Alig I, Dudkin S, Lellinger D. Polymer, 45 (26): 8863 (2004)

30. Krause B, Pöstchke P, Häußler L. Composites Science and Technology, 69 (10): 1505 (2009)

31. Pöstchke P, Fornes TD, Paul DR. Polymer, 43: 3247 (2002)

Financiación Recibida

Página intencionadamente en blanco

Los autores agradecen la financiación al MINECO-FEDER (proyecto de investigación IPT-420000-2010-004) y a la Xunta de Galicia-FEDER (Programa de Consolidación y estructuración de unidades de investigación competitivas (CN2011/008 and GRC 2014/036).

Laura Arboleda agradece el apoyo financiero del Ministerio de Educación con el programa "Becas para la movilidad de estudiantes para estancias de formación doctoral en Universidades y Consolidación de Programas de Doctorado con Mención de Excelencia".

Además, este trabajo ha sido financiado por FEDER a través del COMPETE Program y por la Fundación Portuguesa para la Ciencia y la Tecnología (FCT) dentro del Proyecto PEST-C/FIS/UI607/2011 y del proyecto PTDC/CTM-NAN/112574/2009. Pedro Costa y Armando Ferreira también agradecen a la FCT por las becas SFRH/BD/64267/2009 y SFRH/BD/69796/2010, respectivamente. Los autores también agradecen la financiación de "Matepro –Optimizing Materials and Processes", ref. NORTE-07-0124-FEDER-000037", co-fundado por el "Programa Operacional Regional do Norte" (ON.2 – O Novo Norte), bajo el "Quadro de Referência Estratégico Nacional" (QREN), a través de "Fundo Europeu de Desenvolvimento Regional" (FEDER). Tamnbién se agradece la financiación de COST Action MP1003, 2010 'European Scientific Network for Artificial Muscles' y MP0902 "Composites of Inorganic Nanotubes and Polymers, COINAPO".

Página intencionadamente en blanco

Conclusiones

Página intencionadamente en blanco

Durante el desarrollo del trabajo de tesis, se han diseñado y caracterizado nuevos materiales compuestos poliméricos conductores utilizando nanotubos de carbono y diferentes mezclas de poliamidas como matriz. Los nanocompuestos fueron procesados mediante mezclado en fundido puesto que es la técnica más fácilmente escalable a procesos de transformación industriales. Los resultados obtenidos en el estudio pueden ser resumidos en las siguientes conclusiones:

- El estudio de las propiedades piezoeléctricas de los compuestos poliamida 66 / poliamida 6 / MWCNT con diferentes ratios entre poliamidas, distinto contenido de nanotubos y de masterbatch utilizada, mostraron que la combinación de 75/25 PA66/PA6 y un 3% en peso de nanotubos predispersos en PA66, obtuvo un valor de Gauge Factor de 6. Esto indica que podría ser un material adecuado para la fabricación de sensores piezoeléctricos.

- El análisis realizado en profundidad del estado de dispersión y la morfología obtenida en nanocompuestos poliamida 66 / poliamida 6 con un 3% en peso de CNT, mostró que la conductividad eléctrica es más alta en aquellos compuestos donde se utilizó la masterbatch más fluída (la de poliamida 6). Las mejores propiedades eléctricas se obtuvieron con un ratio PA66/PA6 de 50/50 gracias a que los aglomerados de nanotubos se distribuían uniformemente, en una matriz con morfología co-continua. Estos composites serían apropiados para otro tipo de aplicaciones donde el requerimiento más importante fuese el de la conductividad eléctrica.

- Utilizando una mezcla inmiscible de poliamidas como matriz, en proporción 50/50 (PA12 / PA 6) se obtuvieron nanocompuestos con un bajo umbral de percolación eléctrica, 0,26% en volumen de CNT. Los análisis morfológicos demostraron la formación de una red conductora segregada donde los nanotubos se localizan preferentemente en la interfase entre las dos poliamidas. Para favorecer la aparición de esta morfología, los nanotubos utilizados estaban previamente dispersos en la PA12, más fluída, con menor punto de fusión que la PA6, pero con mayor energía interfacial con los nanotubos. La morfología de red segregada permite obtener composites conductores con una pequeña proporción de nanotubos lo que va a favorecer el proceso industrial, tanto desde el punto de vista de facilidad del procesado como desde el punto de vista económico.

- Se observó también que los nanocompuestos PA12/PA6/MWCNT con morfología de red segregada, absorben menor contenido en agua con respecto a la PA6. Este efecto se relaciona con un aumento en la cristalinidad de las poliamidas debido a la presencia de los nanotubos y a la migración de los CNT hacia la PA6 en los nanocompuestos con mayor contenido de nanorelleno. La mejora en la absorción de agua en composites con poliamidas es crítica para obtener estabilidad en las propiedades mecánicas de los nuevos nanocompuestos y mitiga, por tanto, uno de los grandes inconvenientes de estas matrices con importantes aplicaciones en automoción.

- Finalmente, la inclusión de los nanotubos y la morfología de red segregada obtenida en los nanocompuestos PA12/PA6/MWCNT permitió obtener además compuestos con conductividad térmica mejorada con respecto a la PA6. La mejora en esta propiedad es crítica en aquellas aplicaciones donde el compuesto sirva para mejorar el rendimiento, la vida útil y la fiabilidad de dispositivos electrónicos.

Anexos

Página intencionadamente en blanco

Anexo I: Contribuciones a congresos

Esta tesis ha dado lugar a distintas contribuciones a congresos que se detallan a continuación:

- Autores: L. Arboleda-Clemente, M.J. Abad, A. Ares, A.Lasagabaster
Título: "Dispersion versus distribution: critical balance to achieve conducting composites"
Tipo de participación: Póster
Congreso: EUPOC 2015 Conducting Polymeric Materials
Publicación: Book of Abstracts: EUPOC 2015 Conducting Polymeric Materials
Lugar de celebración: Gargnano, Lago di Garda (Italia) Fecha: 24-28 Mayo 2015

Premio al Mejor Póster por su calidad científica, otorgado por la editorial Wiley.

- Autores: A. Ares, M.J. Abad, L. Arboleda-Clemente, Rosa Bellas
Título: "Rheological monitoring of polyamide66/polyamide6/multiwalled carbon nanotubes composites"
Tipo de participación: Póster
Congreso: EUPOC 2015 Conducting Polymeric Materials
Publicación: Book of Abstracts: EUPOC 2015 Conducting Polymeric Materials
Lugar de celebración: Gargnano, Lago di Garda (Italia) Fecha: 24-28 Mayo 2015

- Autores: L. Arboleda-Clemente, A. Ares, X. García, M.J. Abad
Título: "Incremento de la conductividad eléctrica y térmica en compositesPA12/PA6/CNT"
Tipo de participación: Comunicación oral
Congreso: XXXV Reunión Bienal de la Real Sociedad Española de Química
Publicación: Book of Abstracts: ISBN 978-84-606-9786-2
Lugar de celebración: A Coruña (España) Fecha: 19-23 Julio 2015

- Autores: A. Ares, L. Arboleda-Clemente, Xoán García, M.J. Abad

Título: “Enhanced termal conductivity of rheologically percolated polyamide 12/polyamide 6/multiwalled carbon nanotubes composites”

Tipo de participación: Póster

Congreso: IBEREO 2015 Conference

Publicación: Proceedings (ISBN: 978-989-26-1056-6)

Lugar de celebración: Coimbra (Portugal) Fecha: 07-09 Septiembre 2015

Anexo II: Portadas artículos

Página intencionadamente en blanco

J Polym Res (2013) 20:326
DOI 10.1007/s10965-013-0326-y

ORIGINAL PAPER

Piezoresistive response of carbon nanotubes-polyamides composites processed by extrusion

L. Arboleda · A. Ares · M. J. Abad · A. Ferreira · P. Costa · S. Lanceros-Mendez

Received: 6 September 2013 / Accepted: 14 November 2013 / Published online: 30 November 2013

Abstract The piezoresistive response of carbon nanotube (CNT)-polyamide composites processed by extrusion has been investigated as a function of CNT amount, polyamide 66 (PA66) / polyamide 6 (PA6) ratio, within the matrix and the masterbatch used to incorporate the CNT into the composite (PA66 masterbatch or PA6 masterbatch). The dispersion level of CNT in PA66/PA6 matrix was evaluated and related with the thermal, electrical and electromechanical properties. It is concluded that the inclusion of the CNT in the PA6 masterbatch helps to improve dispersion leading to larger values of the electrical conductivity in the composites prepared with larger PA66 content. On the other hand, the Gauge Factor (GF), which provides the sensitivity of a piezoresistive sensor, is larger for composites prepared from the PA66 masterbatch. The increase of PA66 content improving also the electromechanical response and GF reaches values up to 6. This fact demonstrates the suitability of the materials for sensor applications produced in an up-scaled production way.

Keywords Piezoresistive · Gauge factor · Carbon nanotubes composites · Polyamides

Introduction

Most polymers are known for their excellent insulating properties. Nevertheless increasing number of applications demand from these materials dissipative or conductive characteristics. In this way, intrinsic conductive polymers and conductive composites based on conductive fillers such as carbon nanotubes (CNTs) and polymer matrices have been developed as functional components in the manufacture of sensors, microelectrodes, electromagnetic shielding, electroconductive rubbers and electrostatically paintable materials, among others [1].

Enhanced conductivity in polymers can be thus achieved either using inherently conductive polymers or adding electrical conductive fillers to the polymer matrix. Polyaniline, polypyrrole or polythiophene are, among others, inherently conductive polymers due to their conjugated π-electron system [2]. With these materials, transparent electrical conductive polymer films have been achieved, which are widely used, for example, in organic solar cells [3]. The main drawbacks of these materials are their high prices, the difficulties in melt compounding due to nonmeltability combined with thermal degradation, and their poor long-term stability.

In a second approach, electrical conductive fillers are incorporated in the polymer matrix. Above certain filler content, the electrical percolation threshold is achieved at which the conductive filler particles form electrical pathways through the polymer matrix. As conductive fillers, metal powders and carbon based additives are quite commonly used in industry [4].

Within this family, carbon nanotubes (CNTs) are known to produce composites with superior electrical and mechanical properties when compared to other carbon allotropes such as carbon black (CB) or carbon nanofibers (CNF) [5]. Strong increases in electrical conductivity and mechanical properties can be obtained in polymer nanocomposites with CNT concentrations below 5 wt.% [6–8].

Electrical, thermal and mechanical properties of the composites are affected both by the characteristics of the CNT and also by the processing technique used to prepare the polymer

L. Arboleda · A. Ares · M. J. Abad (✉)
Grupo de Polímeros, University of A Coruña, CIT- Campus de Esteiro, 15403 Ferrol, Spain
e-mail: mjabad@udc.es

A. Ferreira · P. Costa · S. Lanceros-Mendez
Center/Department of Physics, University of Minho, Campus de Gualtar, 4710-057 Braga, Portugal

Página intencionadamente en blanco

Synthetic Metals 221 (2016) 134–141

Contents lists available at ScienceDirect

Synthetic Metals

journal homepage: www.elsevier.com/locate/synmet

Influence of polyamide ratio on the CNT dispersion in polyamide 66/6 blends by dilution of PA66 or PA6-MWCNT masterbatches

Laura Arboleda-Clemente, Ana Ares-Pernas, Xoán García, Sonia Dopico, María José Abad*

Grupo de Polímeros, Centro de Investigacións Tecnolóxicas, Universidade da Coruña, Campus de Ferrol, 15471 Ferrol, Spain

ARTICLE INFO

Article history:
Received 20 June 2016
Received in revised form 22 July 2016
Accepted 27 July 2016
Available online 3 September 2016

Keywords:
Carbon nanotubes
Rheology
Polyamide
Electrical properties
Polymer blends

ABSTRACT

Nanocomposites with 3 wt.% multi-walled carbon nanotubes (MWCNTs) are produced by melt dilution technique using two commercial masterbatches where MWCNTs are pre-dispersed in PA66 and PA6. As polymer matrix, two blends (polyamide 66 (PA66)/polyamide 6 (PA6)) are assessed with different PA66/PA6 ratio (25/75 and 50/50). The influence of both masterbatch and polyamide ratio on microstructure of CNT composites and the relations between microstructure and physical properties (dielectrical properties, crystallinity and rheology) are analysed.

Though all nanocomposites are rheologically percolated, those prepared from PA6 masterbatch show higher stiffness. The highest conductivity value corresponds to the nanocomposites with 50/50 PA66/PA6 ratio, possibly because the nanotubes form well-distributed big agglomerates in co-continuous blend morphology. Comparing the different masterbatches, the best electrical results are obtained with PA6 masterbatch, probably due to the fact that its lower melt-viscosity encourages CNT dispersion during extrusion and subsequent re-agglomeration during compression moulding.

1. Introduction

Dispersing conductive fillers, as carbon nanotubes (CNT), in a polymeric matrix is a relatively simple route to develop new electrically conductive polymer composites (CPCs). The targets to obtain are easy processing, low cost and obviously, tunable electrical properties. The final properties of CPCs depend on both material composition and morphology obtained. If the CPC matrix is a blend of two immiscible polymers, the material morphology is given by the polymer composition as well as the rheological properties of polymers and the processing variables [1]. The addition of carbon nanotubes can also alter the morphology of immiscible blends. Recent researches [2] have proved that the nanoparticles addition can change the blend morphology in three important aspects: reduction of the domain size of the dispersed phase (compatibilizer effect), change sea-island into co-continuous morphology and phase inversion. These ones are related with changes in the viscosity ratios due to the selective distribution of nanoparticles in one polymer or another. All these variables directly affect the final properties of composites, specifically the electrical properties [3]. Since there are no general rules, which are able to predict the macroscopic behaviour, it is necessary a study of each conductive nanocomposite.

CNT dispersion in the polymer matrix seems to be a key factor to obtain the desirable final properties. This one influences greatly viscoelastic properties of CNT composites [4–6] and for this reason, nanofiller dispersion level can be evaluated from rheological studies [7–13]. To obtain high electrical conductivity, an initial dispersion of nanotubes in polymer matrix during mixing process is required. However, according to previous literature [14–16], reaggregation of well-dispersed nanotubes encourages their interconnectivity reducing the distance between the tubes to the tunnelling range and, as consequence, decreasing the filler amount required for electrical percolation. Both dispersion and re-aggregation of CNTs are controlled by diffusion mechanisms, which are related to attractive forces between polymer chains and nanotubes, as well as external forces applied during the melt-blending. Initially, the polymer chains infiltrate into the primary agglomerates, removing the CNT on their surface and reducing their size or dissolving them. This process depends on the melt viscosity of the polymer resin and the interfacial energy between CNTs and matrix. Then, the wetted CNTs are distributed within the polymer matrix. The mixing parameters applied (shear strain and mixing time), establish the degree of nanofiller dispersion [17].

The study of CPCs obtained from CNTs and polyamide blends with different viscosities are particularly interesting and novel

* Corresponding author.
E-mail address: mjabad@udc.es (M.J. Abad).

http://dx.doi.org/10.1016/j.synthmet.2016.07.030
0379-6779/

Página intencionadamente en blanco

Segregated Conductive Network of MWCNT in PA12/PA6 Composites: Electrical and Rheological Behavior

Laura Arboleda-Clemente, Ana Ares-Pernas, Xoán García, Sonia Dopico, María José Abad
Grupo de Polímeros, Centro de Investigacións Tecnolóxicas, Universidade da Coruña, Campus de Ferrol, 15471 Ferrol, Spain

In the present study, different quantities of multiwalled carbon nanotubes and an immiscible blend of polyamides, 50 vol%/50 vol%. Polyamide 12/polyamide 6 (PA12/PA6), are melt blending by extrusion to obtain conducting polymer composites. The rheological and electrical properties of nanocomposites are evaluated as function of nanofiller content. Both rheological and electrical percolation thresholds are calculated by graphical methods and fitting the experimental data to the well-known power-law expression. The low percolation thresholds are probably due to the high aspect ratio of the nanotubes, kept after the composite proccessing and to the preferential localization of carbon nanotubes (CNTs) in the polyamides interface. This latter is predicted by the wetting parameter and finally confirmed by TEM micrographs. The mixing strategy followed, by using a PA12 masterbatch and an immiscible blend of polyamides, seems suitable to form a segregated conductive network in the matrix with low CNT quantities. POLYM. COMPOS., 00:000–000, 2015. © 2015 Society of Plastics Engineers

INTRODUCTION

The dispersion of conductive fillers (such as carbon nanotubes) (CNTs) in a polymer matrix or a polymer blend can result in electrically conductive polymer composites (CPCs) [1–5]. In CPC achievement, the use of melt mixing technologies (extrusion and injection molding) is a great advantage for industrial end applications. Besides, the use of polyamide 12/polyamide 6 (PA12/PA6) blends, both commodity polymers in the industry, could be able to overcome some of PA 6 drawbacks, such as high sensitivity to notch propagation under impact test in particular at subzero temperatures, high moisture sorption, and poor dimensional stability.

General speaking, the properties of CNT composites (such as electrical conductivity) are related with both material composition and morphology reached during their processing. In detail, electrical conductivity depends on the formation of a three dimensional conductive network into the insulating polymer above a critical filler concentration, called percolation threshold (p_c) [6, 7]. As conductive fillers, carbon nanotubes (CNT) have exceptional electrical properties and high aspect ratio ($L/D \approx 1000$) allowing to get typical p_c values in the range 1–3 wt% [6]. Moreover, for immiscible polymer blends (such as polyamide 12/polyamide 6 blend in our case) the nanocomposite morphology is not only governed by thermodynamics and/or kinetic effects but also, by the viscosity ratio of polymers [8]. In theory, a morphology where CNTs migrate at the interfaces between the polymers (instead of randomly distributed in the immiscible polymer blend) would enable the formation of a segregated structure with a lower percolation threshold [9].

The percolation threshold of nanocomposites can be investigated by means of electrical conductivity measurements as well as by the evaluation of their rheological behavior. These techniques together provide insight into the nanoscale structure and organization of the MWCNTs in polymeric matrices [6, 7, 10].

Thus, the principal aim of this work is to design new CNT nanocomposites with electrical conductivity and a low percolation threshold, using an immiscible blend of polyamides as matrix. The percolation threshold p_c will be determined through rheological tests and alternating current (ac) measurements, to discuss in detail the frequency dependence of conductivity. Furthermore, light microscopy (LM) and transmission electronic microscopy (TEM) were used to investigate the nanocomposites morphology and CNT localization in polymer matrix, finding out that this is a key aspect to explain the macroscopic properties of nanocomposites.

EXPERIMENTAL

Materials

A blend of polyamide 12 (PA12 Grilamid supplied by EMS Grivory) and polyamide 6 (PA6 Zytel supplied by DuPont) was used in this study. PA6 has a density of 1.14 g cm^{-3}, a melting temperature of 220°C and a zero shear viscosity of 723.8 Pa s measured at 235°C. On the

Correspondence to: M. José Abad (E-mail: mjabad@udc.es)
DOI 10.1002/pc.23865
Published online in Wiley Online Library (wileyonlinelibrary.com).

Página intencionadamente en blanco

J Mater Sci (2016) 51:8674–8686

Water sorption of PA12/PA6/MWCNT composites with a segregated conductive network: structure–property relationships

Laura Arboleda-Clemente[1], Ana Ares-Pernas[1], Xoán-Xosé García-Fonte[1], and María-José Abad[1,*]

[1] *Grupo de Polímeros, Centro de Investigacións Tecnolóxicas, Universidade da Coruña, Campus de Ferrol, 15471 Ferrol, Spain*

Received: 30 March 2016
Accepted: 8 June 2016
Published online: 16 June 2016

ABSTRACT

The structure–properties relationships of a polyamide 12 (PA12)/polyamide 6 (PA6) blend containing multiwalled carbon nanotubes have been investigated as a function of nanofiller amount. The influence of the filler content in the water diffusion behavior of the immiscible PA12/PA6 blend is studied. An acceptable dispersion level of nanotubes in polymer matrix is observed by scanning electron microscopy. The water uptake at saturation, normalized to the polyamide mass, decreases, and the diffusion rate is slower in CNT composites. The enhancement is in line with the increase in stiffness measured in rheological tests. This behavior is related with the rise in the overall crystallinity of the polymer matrix and the selective migration of CNT towards PA6 (more hygroscopic than PA12). These findings display a substantial improvement in respect to the water uptake behavior of pristine PA6 and PA6/CNT composites, expanding the potential applications of composites.

Introduction

In order to reduce CO_2 emission and fuel consumption, the automotive industry wishes to reduce the mass of vehicles. Polyamide composites reinforced with fillers, such as carbon nanotubes, are suitable substitutes of metals in automotive parts. They combine an affordable price and a reasonable stiffness due to the complex shapes allowed by the injection molding process. The blend of polyamides with other polymers has been extensively studied [1–3] but the scientific literature about blending of nylons themselves is still quite limited [4, 5]. The use of polyamide 12/polyamide 6 (PA12/PA6) blends, both commodity polymers in the industry, could be able to overcome some of PA6 drawbacks, such as high sensitivity to notch propagation under impact test in particular at subzero temperatures, high moisture sorption, and poor dimensional stability. These polyamides are nowadays increasingly used for structural applications such as engine mounts or clutch pedals which are submitted to complex cyclic movements. Furthermore, important variations of the temperature and relative humidity can be induced by the service conditions (underbonnet temperature and

Address correspondence to E-mail: mjabad@udc.es

DOI 10.1007/s10853-016-0127-x